ARMY RESEARCH LABORATORY

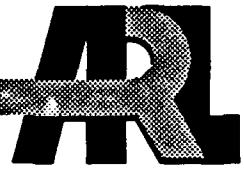

Theoretical Modeling of the Interior Ballistics of the Electrothermal Gun

Paul S. Gough

ARL-CR-47 July 1993

prepared by

Paul Gough Associates, Inc.
1048 South Street
Portsmouth, New Hampshire 03801

under contract

DAAA15-88-D-0013

DISCLAIMER NOTICE

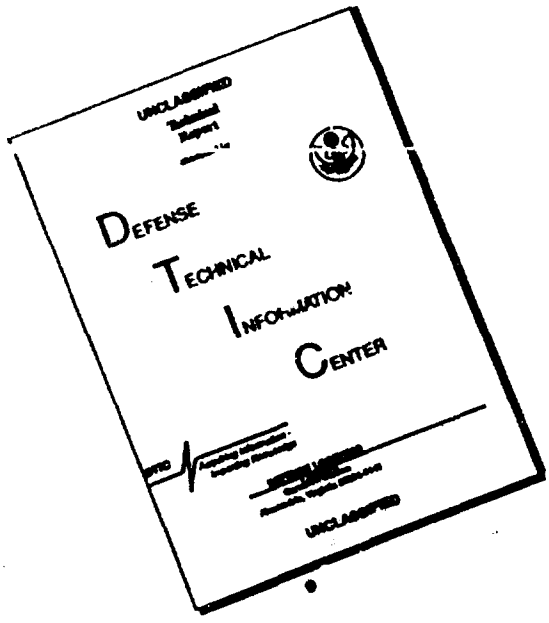

THIS DOCUMENT IS BEST QUALITY AVAILABLE. THE COPY FURNISHED TO DTIC CONTAINED A SIGNIFICANT NUMBER OF PAGES WHICH DO NOT REPRODUCE LEGIBLY.

NOTICES

Destroy this report when it is no longer needed. DO NOT return it to the originator.

Additional copies of this report may be obtained from the National Technical Information Service, U.S. Department of Commerce, 5285 Port Royal Road, Springfield, VA 22161.

The findings of this report are not to be construed as an official Department of the Army position, unless so designated by other authorized documents.

The use of trade names or manufacturers' names in this report does not constitute indorsement of any commercial product.

REPORT DOCUMENTATION PAGE

Form Approved
OMB No. 0704-0188

1. AGENCY USE ONLY (Leave blank)	2. REPORT DATE	3. REPORT TYPE AND DATES COVERED
	July 1993	Final, Jan 90 - Aug 90

4. TITLE AND SUBTITLE
Theoretical Modeling of the Interior Ballistics of the Electrothermal Gun

5. FUNDING NUMBERS
C: DAAA15-88-D-0013

6. AUTHOR(S)
Paul S. Gough

7. PERFORMING ORGANIZATION NAME(S) AND ADDRESS(ES)
Paul Gough Associates, Inc.
1048 South Street
Portsmouth, NH 03801

8. PERFORMING ORGANIZATION REPORT NUMBER

9. SPONSORING/MONITORING AGENCY NAME(S) AND ADDRESS(ES)
U.S. Army Research Laboratory
ATTN: AMSRL-OP-CI-B (Tech Lib)
Aberdeen Proving Ground, MD 21005-5066

10. SPONSORING/MONITORING AGENCY REPORT NUMBER
ARL-CR-47

11. SUPPLEMENTARY NOTES
The Contracting Officer's Representative for this report is Ms. Gloria P. Wren, U.S. Army Research Laboratory, ATTN: AMSRL-WT-PA, Aberdeen Proving Ground, MD 21005-5066.

12a. DISTRIBUTION/AVAILABILITY STATEMENT
Approved for public release; distribution is unlimited.

12b. DISTRIBUTION CODE

13. ABSTRACT *(Maximum 200 words)*

A lumped parameter model is described in which the working fluid is assumed to decompose at a finite rate. The model is used to explore the sensitivity of maximum pressure and muzzle velocity to the failure of the rate of decomposition to keep pace with the rate of injection of energy. The influence of initial ullage as a desensitizing parameter is discussed, as is the use of the model as a means of determining the rate of decomposition given the history of plasma flux and chamber pressure.

Second, modifications to the XNOVAKTC Code (XKTC), a one-dimensional two-phase model of solid propellant gun interior ballistics, are described to represent a class of ETG devices in which a central ullage port is initially present. The code is used to explore further the ballistic consequences of nonuniform mixing.

Finally, we present the formulation of a two-dimensional model of the ETG which is intended to address those processes which are outside the scope of the two simpler models.

14. SUBJECT TERMS	15. NUMBER OF PAGES
interior ballistics, models, electrothermal gun	137
	16. PRICE CODE

17. SECURITY CLASSIFICATION OF REPORT	18. SECURITY CLASSIFICATION OF THIS PAGE	19. SECURITY CLASSIFICATION OF ABSTRACT	20. LIMITATION OF ABSTRACT
UNCLASSIFIED	UNCLASSIFIED	UNCLASSIFIED	SAR

INTENTIONALLY LEFT BLANK.

ACKNOWLEDGMENTS

The author expresses his gratitude to Dr. John Powell and Mr. William Oberle of the U.S. Army Research Laboratory for their helpful advice during the performance of the present effort.

The author also wishes to acknowledge some useful criticisms of an interim version of the lumped parameter model which were prepared by Dr. Martin Summerfield of the Princeton Combustion Research Laboratory.

Technical cognizance for the subject contract was provided by Dr. G. E. Keller and Ms. Gloria P. Wren of the U.S. Army Research Laboratory.

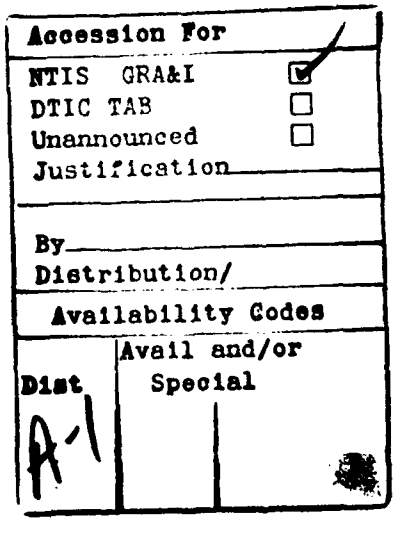

INTENTIONALLY LEFT BLANK.

TABLE OF CONTENTS

INTENTIONALLY LEFT BLANK.

LIST OF FIGURES

INTENTIONALLY LEFT BLANK.

LIST OF TABLES

1.0 INTRODUCTION

The Electrothermal Gun (ETG) offers a way to circumvent a fundamental performance limitation associated with conventional chemical propulsion. Since the specific chemical energy of conventional propellants is limited, increases in total propulsive energy are accompanied by a concomitant increase in the total mass of the propellant. As the propellant is required to follow the projectile, a fraction of the total energy is necessarily stored as kinetic energy of the moving propellant. This kinetic energy represents a loss of efficiency which is proportional to C/M, the ratio of the mass of the propellant to that of the projectile. For conventional ammunition in which the muzzle velocity is approximately 1 km/s, the value of C/M is about 0.25 and the kinetic energy loss is not large. However, for hypervelocity weapons operating at muzzle velocities of the order of 3 km/s, the value of C/M can be significantly greater than 1 at which point the kinetic energy losses can begin to dominate: a regime of diminishing returns is entered as the chemical energy is expended primarily to accelerate the propellant itself rather than the projectile.

The ETG uses an intensely heated plasma which is injected into a working fluid to create a pressurized gas which in turn propels the projectile. The basic configuration is illustrated in Figure 1.1. The review by Juhasz et al [1] may be consulted for a discussion of the various types of configurations presently under consideration; these include examples in which the working fluid is either inert or reactive. As shown in Figure 1.2, the working fluid may have a central cavity and the reactive examples may utilize either monopropellants or bipropellants. Since the plasma is created by an external supply of electrical energy, it is possible, in principle, to achieve an arbitrarily high energy density in the heated working fluid. Accordingly, the C/M constraint associated with conventional chemical propulsion is removed. However, a new constraint appears in connection with the thermal response of the tube. It is necessary that the heat capacity of the working fluid be sufficiently high as to moderate the temperature of working fluid so that the heat transfer to the gun tube is not excessive. Since the heat capacity is obviously proportional to the total mass of the heated fluid, it is clear that this thermal constraint is in effect a C/M constraint similar to that associated with the kinetic energy loss. However, the ETG admits the use of working fluids having much larger specific heat capacities than those of chemical propellants. It is this additional degree of freedom of design which preserves the apparent propulsive advantage attached to the use of an external supply of energy. Otherwise, keeping the heat transfer to the tube comparable to that obtained with conventional propellants would require a mass of working fluid which diluted the plasma energy to a value comparable to that of the conventional propellant itself, at which point the conventional level of kinetic energy loss would be experienced.

---

1. *Juhasz. A., Jamison, K., White, Y. and Wren, G. "Introduction to Electrothermal Gun Propulsion" Proceedings of the 25th Jannaf Combustion Meeting* *1988*

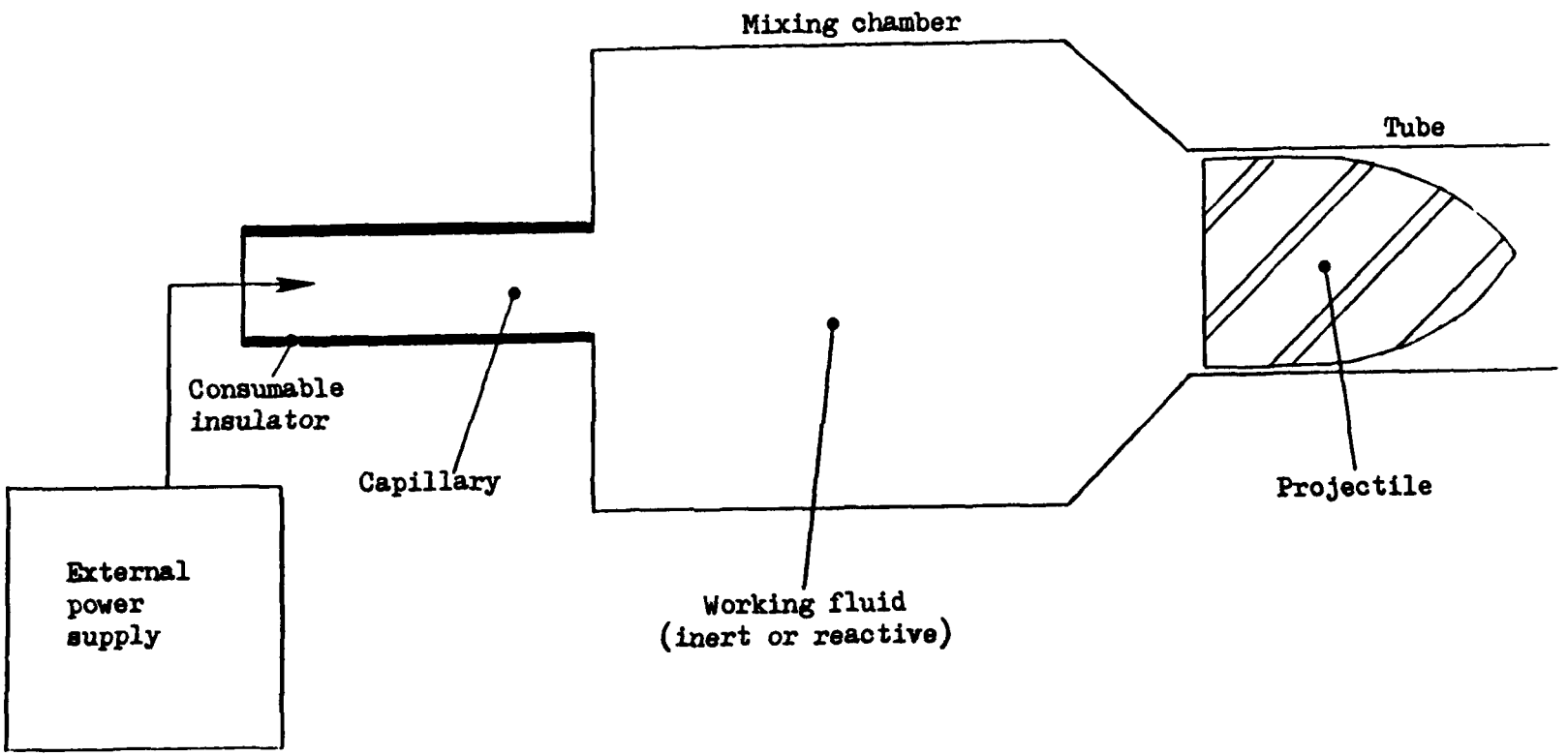

Figure 1.1 Components of the Electrothermal Gun (ETG)

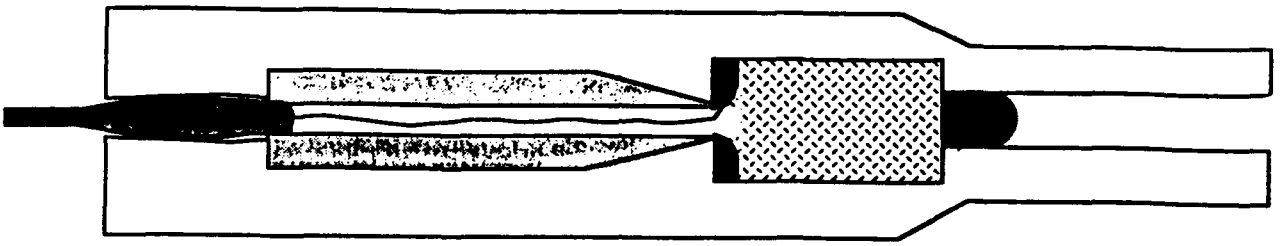

(a) Single Fluid, Homogeneous

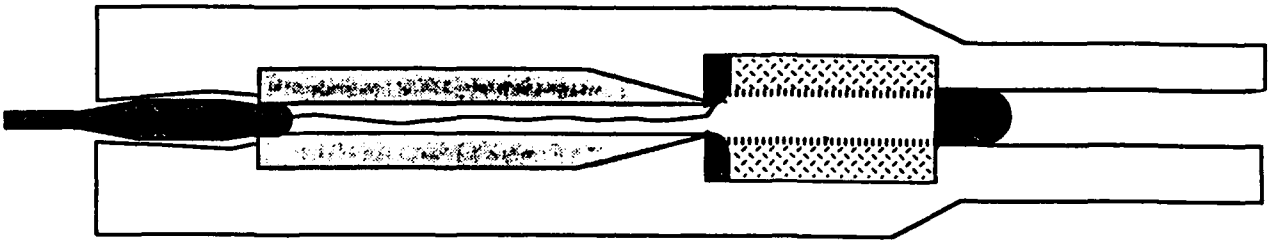

(b) Single Fluid, with Cavity

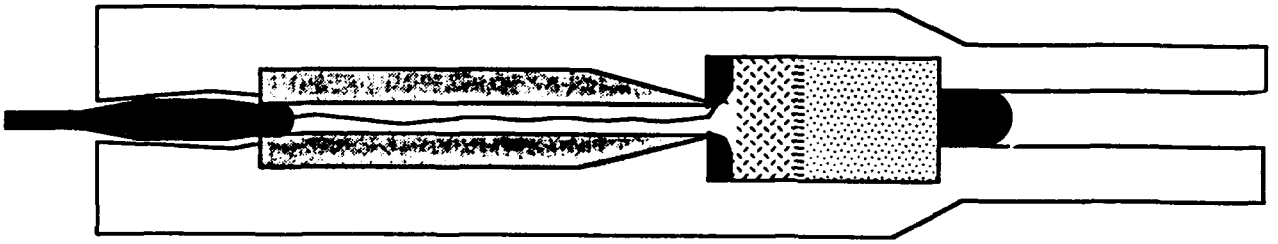

(c) Bipropellant, no Cavity

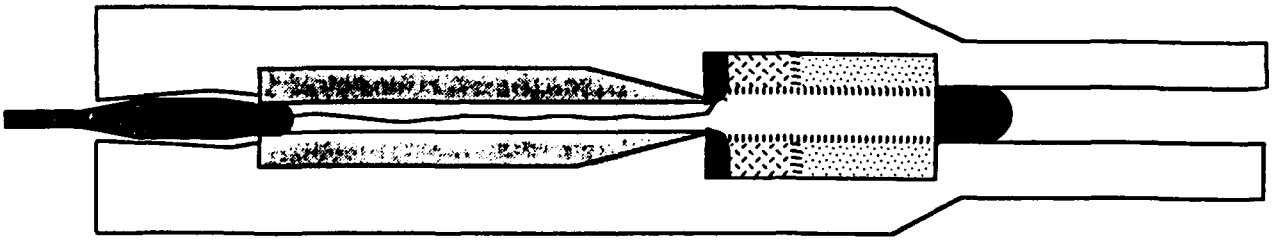

(d) Bipropellant, with Cavity

Figure 1.2 Types of ETG Configurations

The preceding discussion has been based on an implicit assumption, namely that the plasma energy is uniformly distributed throughout the working fluid. In fact, this is not likely to be true. Thus one must ask to what extent are the ballistic performance and the rate of heat transfer to the tube affected by the details of the mixing process. It may be anticipated that propulsion will be affected less strongly by the details of mixing than will the heat transfer. Since the spacemean pressure is essentially proportional to the total energy within the mixing chamber, the overall rate of pressurization is not expected to depend strongly on the rate of mixing. Such dependence as arises will stem from non-idealities in the equation of state, the influence of the effective C/M on the pressure gradient in the gun tube, and on transient wave phenomena. However, the mixing process will be of paramount importance in regard to the distribution of temperature and therefore the heat transfer to the tube. Poor mixing will produce intensely heated gas but at the same time will preserve a region of relatively cool fluid. Heat transfer to the tube may be either reduced or increased by poor mixing depending on whether or not the cool fluid acts as an insulating layer near the tube wall.

In Chapters 2.0 and 3.0 of this report we focus attention on the ballistic consequences of the rate of mixing insofar as this topic can be addressed in terms of lumped parameter and one-dimensional continuum models. Meaningful analysis of the implications of the mixing rate on the heat transfer to the tube requires a two-dimensional model. Chapter 4.0 presents the formulation of such a model.

The results presented in Chapters 2.0 and 3.0 are all based on the assumption that the rate of injection of the plasma, and its energy content, are predetermined. Only the state of the mixture of the plasma and the working fluid is modeled explicitly. The approach is therefore similar in spirit to that described by Oberle [2] who used the lumped parameter interior ballistics code IBHVG2 [3] to model the response of the working fluid to

---

2. *Oberle, W. "Electrothermal Guns -- A Theoretical Investigation of Factors for Optimal Performance" Ballistic Research Laboratory Report BRL-TR-2999* *1989*

3. *Anderson, R.D. and Fickie, K.D. "IBHVG2 - A User's Guide" BRL Technical Report BRL-TR-2829 Ballistic Research Laboratory, Aberdeen Proving Ground, MD* *1987*

the addition of the plasma. Models which address specifically the formation of the plasma have been advanced by Powell and Zielinski [4], Tidman et al [5], Loeb and Kaplan [6] and by Chryssomallis et al [7].

Chapter 2.0 contains a complete discussion of the lumped parameter model developed under the present contract task. The model is encoded as a program referred to as LUMPET. Appendix A contains a listing of the code together with a complete description of the input files. Sample data bases and solutions are presented in Appendices C and D. In addition to the discussion of the model, Chapter 2.0 presents a number of numerical results. The model is used first to predict the influence of the rate of mixing on the interior ballistics for a nominal ETG configuration. Second, the code is applied in an inverse mode to deduce the rate of mixing, or decomposition of the working fluid, when both the plasma flux and the gun pressure history are given. The first set of results shows relatively little sensitivity of the interior ballistics to the rate of mixing. Not surprisingly, the second set of results make it clear that very accurate experimental data will be required if the code is to be used in an inverse mode to determine the rate of mixing with any degree of precision.

To clarify further the dependence of pressure on the extent of decomposition of the working fluid we provide a short computer code referred to as PMAP. The code is described in Section 2.3 and a listing, together with a description of input, is given in Appendix B.

The discussion of Chapter 3.0 provides only a brief summary of the one-dimensional model. Reference is made to independent documentation of the relevant code, referred to as XNOVAKTC or, more briefly, as XKTC [8]. Chapter 3.0 only presents those model details which are particular to the representation of the ETG and which were encoded as part of the present contract task. The revised version of XKTC is used to assess the influence of the rate of mixing from a one-dimensional perspective which allows

---

4. *Powell, J.D. and Zielinski, A.E. "Analysis of the Plasma Discharge in an Electrothermal Gun" Proceedings of the 26th Jannaf Combustion Meeting* *1989*

5. *Tidman, D.A., Thio, Y.C., Goldstein, S.A. and Spicer, D.S. "High Velocity Electrothermal Mass Launchers" GT Devices Technical Note Number GTD 86-7* *1986*

6. *Loeb, A. and Kaplan, Z. "A Theoretical Model for the Physical Processes in the Confined High Pressure Discharges of Electrothermal Launchers" IEEE Trans. Magn. MAG-25, 342* *1989*

7. *Chryssomallis, G.S., Marinos, C.D., Ricci, R.S. and Cook, D.C. "Combustion Augmented Plasma Gun" in Technology Efforts in ET Gun Propulsion, edited by A. A. Juhasz vol. 1* *1988*

8. *Gough, P.S. "The XNOVAKTC Code" PGA-TR-86-1 Final Report, Task Order II, Contract DAAK11-85-D-0002* *1986*

spatial non-uniformity. We study the same ETG configuration as in Chapter 2.0. The results confirm those of Chapter 2.0 in the sense that only modest sensitivity is seen for the sample problem under consideration. A sample XKTC data base is presented in Appendix E.

In Chapter 4.0 we present the details of a two-dimensional model of the ETG. The discussion includes a statement of the principal governing equations and of the intended method of solution. However, the relevant coding and the determination of numerical solutions is outside the scope of the present task and will be presented in a subsequent report.

2.0 LUMPED PARAMETER MODEL

This chapter has three sections. In Section 2.1 we present the details of a lumped parameter model of the interior ballistics of the ETG. In Section 2.2 we present some numerical results which illustrate the dependence of the interior ballistics on the rate of mixing of the plasma with the working fluid. In Section 2.3 we consider the use of the model as a means of determining the rate of mixing when the pressure history of the gun is given in addition to a characterization of the plasma flux. As we shall see in Section 2.2, the interior ballistics of the ETG are only weakly dependent on the rate of mixing. This is a desirable result from the point of view of the gun designer since it implies that pressurization is dominated by the rate of addition of plasma. On the other hand, it implies that the determination of the rate of mixing from the pressure history will require relatively precise data. We explore this latter point in some detail in Section 2.3.

2.1 GOVERNING EQUATIONS

We assume that we have a mixing chamber where volume, prior to motion of the projectile, is V_o. The chamber contains a total mass C of working fluid and an initial mass m_o of gas. The density of the unmixed portion of the working fluid is $\rho_p(p)$, a function of the pressure, p. At any time t, a fraction $\alpha(t)$ of the working fluid has been vaporized and mixed uniformly with the injected plasma. While we neglect the time delay associated with the mechanical process of mixing each element of vaporized working fluid with the mixture of gases already present, we do consider the possibility that the approach to chemical equilibrium requires a period of time which is not negligible from an interior ballistic perspective. Accordingly, the mixture of gases is formally decomposed into an intermediate species S_I, whose mass fraction is Y, and a final species S_F, whose mass fraction is obviously 1 - Y. At any given time, the total mass of plasma in the mixing chamber is $m_i(t)$ and the energy of the plasma is $E_i(t)$.

As noted previously, we assume that $m_i(t)$ and $E_i(t)$ are furnished as tabular data; the plasma flux is not modeled directly. In subsequent subsections we discuss the equations of motion of the projectile, the relations governing the pressure gradient, the equations of state of the unvaporized working fluid and, finally, the equations which govern the mixture of gases.

Motion of the Projectile

The projectile has mass M, displacement x_p and velocity v_p. Its motion is resisted by two forces, the first is due to the engraving band and is represented by a pressure p_{res} while the second is due to the compression of air in front of the projectile and is represented by p_{air}. The equation of motion of the projectile is

$$\frac{dv_p}{dt} = \frac{g_o A_b}{M} (p_{base} - p_{res} - p_{air}) \quad , \tag{2.1}$$

where A_b is the bore area and p_{base} is the pressure at the base of the projectile. We assume that $p_{res} = p_{res}(x_p)$ and that the functional dependence is characterized by a table of values. The value of p_{air} is assumed to follow from the jump conditions for a shock wave in which the gas ahead of the shock is at rest while the gas behind the shock has a velocity equal to that of the projectile. It follows that [9]

$$p_{air} = p_a\left\{(1 + \mu_a^2)\left[\frac{v_p + [v_p^2 + 4(1 - \mu_a^2)^2 c_a^2}{2(1 - \mu_a^2)c_a}\right]^{1/2} - \mu_a^2\right\} \quad , \quad (2.2)$$

where $\mu_a^2 = (\gamma_a - 1)/(\gamma_a + 1)$ and γ_a is the ratio of specific heats of the air in the barrel. We also have c_a, the speed of sound in the unshocked air and p_a is the pressure. The user of the code has the option of including the effect of the air shock or of neglecting it. The properties of the air are assumed to be characterized by the values $\gamma_a = 1.4$, $p_a = 0.101$ MPa and $c_a = 343.2$ m/s.

Pressure Gradient Relations

The equation of motion of the projectile involves the base pressure p_{base}. The balance equations which describe the thermodynamic state of the mixture will be predicated on the spacemean pressure, p. Moreover, it is of interest to the charge designer to know the breech pressure, p_{br}, since this is expected to be the highest pressure in the gun. The model admits two different sets of analytical relations between these values of pressure. The first set is referred to as the Lagrange relations [10] while the second set is referred to as the Chambrage relations [11]. The first set is very familiar to interior ballisticians and takes no account of the variations in cross-sectional area of the chamber. The second set reflects the non-uniform area of the chamber. Relations of the second type appear to have

---

9. *Courant, R. and Friedrichs, K.O. "Supersonic Flow and Shock Waves" Interscience, New York* *1948*

10. *Corner, J. "Theory of the Interior Ballistics of Guns" Wiley, New York* *1950*

11. *Robbins, F.W., Anderson, R.D. and Gough, P.S. "Continued Studies of the Development of a Modified Pressure Gradient Equation for Lumped-Parameter Interior Ballistic Codes" Ballistic Research Laboratory Technical Report* *Undated*

been reported first by Vinti [12]. Similar results have been obtained more recently by Morrison and Wren [13] and cast into a more general format by Robbins et al [11].

Both the Lagrange and the Chambrage relations are based on the assumption that the flow is homogeneous. However, in the present application we cannot assume that the unvaporized working fluid is necessarily at rest. Nor can we assume that it moves with the same velocity as the mixture of gases. We therefore introduce a parameter $\beta(t)$, referred to as the Lagrange coupling coefficient, which reflects the degree to which the unvaporized working fluid moves with the gases. If $\beta = 0$, the unvaporized working fluid is assumed to be at rest. If $\beta = 1$, the working fluid moves with the gases. The value of β is required to be specified by the user of the code. In Section 2.3 we discuss the experimental determination of $\beta(t)$ from an inverse analysis of the observed interior ballistic behavior.

Lagrange Relations

Let K be defined as

$$K = \frac{C(\alpha + \beta(1 - \alpha)) + m_i + m_o}{M} \quad . \tag{2.3}$$

The value of the breech pressure and the base pressure are related to the spacemean pressure according to

$$P_{base} = \frac{1}{1 + K/3} P \quad , \tag{2.4}$$

$$P_{br} = \frac{1 + K/2}{1 + K/3} P \quad . \tag{2.5}$$

In addition, we have the following expression for the kinetic energy of the unvaporized working fluid and the mixture of gases,

$$E_{kin} = \frac{KM}{6g_o} v_p^2 \quad . \tag{2.6}$$

---

12. *Vinti, J.P. "The Equations of Interior Ballistics" Ballistic Research Laboratory Report 307* *1942*

13. *Morrison, W.F. and Wren, G.P. "A Lumped Parameter Description of Liquid Injection in a Regenerative Liquid Propellant Gun" Proceedings of the 23rd Jannaf Combustion Meeting* *1988*

Chambrage Relations

Again, with K as defined by Equation 2.3 we have the following relations between the various values of pressure,

$$p_{base} = \frac{p + k_1}{k_2} \quad , \tag{2.7}$$

$$p_{br} = \frac{k_3}{k_2} p + \frac{k_3 k_1}{k_2} + k_4 \quad . \tag{2.8}$$

The kinetic energy is given by

$$E_{kin} = \frac{KM}{2g_o} A_b^2 \frac{J_4(z_p)}{V^3(z_p)} v_p^2 \quad , \tag{2.9}$$

where z_p is the distance from the breech face to the base of the projectile and we introduce the following expressions.

$$V(z) = \int_o^z A(z)dz \quad , \tag{2.10}$$

$$J_1(z) = \int_o^z \frac{V(z)}{A(z)} dz \quad , \tag{2.11}$$

$$J_2(z) = V^2(z)/A^2(z) \quad , \tag{2.12}$$

$$J_3(z) = \int_o^z A(z)J_1(z)dz \quad , \tag{2.13}$$

$$J_4(z) = \int_o^z A(z)J_2(z)dz \quad , \tag{2.14}$$

$$a_1(t) = \frac{KMA_b}{g_o V^2(z_p)} \left[\frac{A_b v_p^2}{V(z_p)} + \frac{g_o A_b}{M} (p_{res} + p_{air}) \right] \quad , \tag{2.15}$$

$$a_2(t) = - \frac{KA_b^2}{V^2(z_p)} \quad , \tag{2.16}$$

$$b(t) = - \frac{KM}{2g_o} \frac{A_b^2 v_p^2}{V^3(z_p)} \quad , \tag{2.17}$$

$$k_1 = a_1 J_1 + bJ_2 - \frac{a_1 J_3}{V(z_p)} - \frac{bJ_4}{V(z_p)} \quad , \tag{2.18}$$

$$k_2 = 1 - a_2 J_1 + \frac{a_2 J_3}{V(z_p)} \quad , \tag{2.19}$$

$$k_3 = 1 - a_2 J_1 \quad , \tag{2.20}$$

$$k_4 = - a_1 J_1 - bJ_2 \quad . \tag{2.21}$$

Equation of State of Unvaporized Working Fluid

Assuming that the bulk modulus, K_p, of the unvaporized working fluid is at most a linear function of pressure

$$K_p = K_1 + K_2(p - p_o) \quad , \tag{2.22}$$

we have the equation of state in the form,

$$\rho(p) = \begin{cases} \rho_{p_o}(1 + (p - p_o)/K_1) & \text{if } K_2 = 0 \quad , \\ \rho_{p_o}(1 + \dfrac{K_2}{K_1}(p - p_o))^{1/K_2} & \text{if } K_2 \neq 0 \quad , \end{cases} \tag{2.23}$$

where $\rho_{p_o} = \rho_p(p_o)$. Corresponding to this equation of state we have the following expression for the energy per unit mass stored by the compressed fluid,

$$e_p(p) = \begin{cases} -\dfrac{(p - p_o)}{\rho_p(p)} + \dfrac{K_1}{\rho_{p_o}} \ln\left[1 + \dfrac{p - p_o}{K_1}\right] & \text{if } K_2 = 0 \text{ or } 1, \\ -\dfrac{(p - p_o)}{\rho_p(p)} + \dfrac{K_1 + K_2(p - p_o)}{(K_2 - 1)\rho_p(p)} - \dfrac{K_1}{(K_2 - 1)\rho_{p_o}} & \text{if } K_2 \neq 0 \text{ and } K_2 \neq 1. \end{cases} \tag{2.24}$$

Equations for the Mixture of Plasma and Unvaporized Working Fluid

At any given time the mixture of plasma and vaporized working fluid occupy the instantaneous volume

$$V = V_o + x_p A_b - (1 - \alpha)\frac{C}{\rho_p} \quad . \tag{2.25}$$

The density of the mixture is

$$\rho = \frac{m_i + m_o + \alpha C}{V} \quad , \tag{2.26}$$

where ρ is understood to be a spacemean value like the pressure p.

We may write a balance equation for the intermediate species S_I in the form

$$\frac{d}{dt}(\rho Y V) = C\frac{d\alpha}{dt} - VAT^n(Y\rho)^\nu \exp\left[-\frac{E_A}{R_u T}\right] \quad . \tag{2.27}$$

Evidently, the first term on the right hand side of Equation 2.27 represents production of S_I via decomposition of the working fluid while the second term represents depletion according to an Arrhenius reaction law. The reaction term introduces A, the pre-exponential factor; n, the temperature exponent; ν, the reaction order; E_A, the activation energy; and R_u, the universal gas constant. Using the balance of mass for the mixture as a whole, Equation 2.27 can be recast into the computational form

$$\frac{dY}{dt} = \frac{(1 - Y)}{\rho V} C\frac{d\alpha}{dt} - \frac{Y}{\rho V}\frac{dm_i}{dt} - \frac{1}{\rho} AT^n(Y\rho)^\nu \exp\left[-\frac{E_A}{R_u T}\right] \quad . \tag{2.28}$$

The specific heats, covolume and molecular weight of the mixture can be written as follows

$$c_v = Yc_{v_I} + (1 - Y)c_{v_F} \quad , \tag{2.29}$$

$$c_p = Yc_{p_I} + (1 - Y)c_{p_F} \quad , \tag{2.30}$$

$$b = Yb_I + (1 - Y)b_F \quad , \tag{2.31}$$

$$M_w = \frac{1}{\frac{Y}{M_{w_I}} + \frac{(1 - Y)}{M_{w_F}}} \quad . \tag{2.32}$$

Here c_v and c_p are respectively the specific heats at constant volume and constant pressure, b is the covolume and M_w is the molecular weight. We have used subscripts I and F to denote properties of S_I and S_F respectively. It should be noted that we neglect the influence of m_o, the mass of gas initially present. The properties of S_F are understood to reflect the mixture of plasma and working fluid at chemical equilibrium.

We assume that the spacemean properties satisfy the covolume equation of state in the form

$$p = \frac{(\gamma - 1)e_{eff}}{\frac{1}{\rho} - b} \quad , \tag{2.33}$$

where e_{eff} is the effective internal energy whose determination we now discuss.

We may write a global energy balance for the mixture as follows

$$\begin{aligned}[m_i + m_o + \alpha C][(1 - Y)(e_F + H_F) + Y(e_I + H_I)] + (1 - \alpha)Ce_p(p) \\ + \frac{M}{2g_o} v_p^2 + E_{kin} + W_f + Q_w + (1 - \alpha)CH_o \\ = E_o + E_i + Ce_p(p_o) + CH_o + (m_i + m_o)[(1 - Y)H_F + YH_I] \quad .\end{aligned} \tag{2.34}$$

Here e_F and H_F are the thermal energy and the heat of formation of the final products S_F, and e_I and H_I are the corresponding properties of the intermediate products. The second term on the left hand side is the energy stored in the unvaporized working fluid. The third term is the kinetic energy of the projectile and the fourth is the kinetic energy of the mixture of gases and the unvaporized working fluid. The fifth term is the work done against the forces resisting the motion of the projectile,

$$W_f = \int_o^{x_p} A_b(p_{res} + p_{air})dz \quad . \tag{2.35}$$

The sixth term Q_w represents the heat lost to the tube and is presently set equal to zero. The last term on the left hand side represents the heat of formation of the unvaporized working fluid. The terms on the right hand side correspond respectively to the initial energy of the gas in the combustion chamber, the energy added by the plasma, the energy of compression of the working fluid at the initial conditions, the heat of formation of the working fluid and finally, a heat of formation term consistent with our neglect of the detailed influence of the initial mass of gas and the mass of the plasma.

We introduce

$$Q_H = H_I - H_F \quad , \tag{2.36}$$

$$Q_v = H_I - H_o \quad , \tag{2.37}$$

and we write

$$e_I = C_{v_I} T \quad , \tag{2.38}$$

where T is the temperature of the mixture. Then we solve for e_F in the form

$$e_F = \left\{ E_i + \phi\alpha C(Q_H - Q_v) - \alpha C Y Q_H - \frac{M v_p^2}{2 g_o} - E_{kin} - W_f - Q_w + E_o + C e_p (p_o) \right.$$
$$\left. - (m_i + m_o + \alpha C) Y C_{v_I} T - (1 - \alpha) C e_p \right\} / [(m_i + m_o + \alpha C)(1 - Y)] \quad . \tag{2.39}$$

In Equation 2.39 we have introduced a coefficient ϕ whose value depends on the convention adopted in the determination of the thermodynamic properties.

The model admits two distinct conventions. The first is referred to as the constant thermochemistry option and takes the properties of S_F to be fixed at all times. In this case, $\phi = 1$, and the effective ground state for the internal energy is that defined by the heat of formation of the unvaporized working fluid. Thus Q_v is to be interpreted as the heat required to vaporize a unit mass of working fluid and Q_H is to be interpreted as the heat released per unit of mass transformed from S_I to S_F. The effective internal energy e_{eff} as required by Equation 2.33 is taken to be equal to e_F as defined in Equation 2.39. In the second convention, referred to as the variable thermochemistry option, we set the value of $\phi = 0$. In this case

the effective ground state is that of the final products following heating by the plasma. The properties of the mixture are assumed to have been characterized by a series of runs using the BLAKE Code as described by Oberle [2]. A table of values is presumed to be given in which the effective thermal energy, e_{eff}, and the values of $\gamma = c_p/c_v$, b, M_w and Q_H are specified for a series of values of energy added per unit mass. These correspond to the thermodynamic equilibrium of the mixture and accordingly discount the energy associated with vaporization of the working fluid and reaction of any intermediate products. In this case Q_H is interpreted to be the difference in heat of formation of the intermediate and final products and is positive if the transformation of S_I into S_F is exothermic. The value of e_F determined by Equation 2.39 is used to determine e_{eff} and the other variables by linear interpolation of the tabulated BLAKE Code results.

Solution of the Governing Equations

The model consists of a number of algebraic equations and a total of four differential equations, two for the equations of motion of the projectile, one for the work done against the forces resisting projectile motion and one for the rate of change of the mass fraction of the intermediate species. The differential equations are solved using a standard fourth order Runge-Kutta algorithm [14] with a fixed time step.

Several of the algebraic relations are non-linear. The solution of the energy equation is accomplished by means of Newton's method with the pressure as the independent variable. If a chemical reaction is considered, a solution by Newton's method is also required in order to determine the temperature. The model is encoded into a Fortran program referred to as LUMPET. Appendix A contains a listing of the code together with a discussion of the input data. Sample solutions are presented in Appendices C and D. These pertain to the discussion of Sections 2.2 and 2.3 respectively.

In its normal mode of operation the code accepts a tabular description of the time dependence of $\alpha(t)$, $m_i(t)$ and $E_i(t)$. From these inputs, together with a characterization of the thermodynamic properties of the mixture, the interior ballistic history is computed. In a second mode the user may specify a constant value of breech pressure together with a total value of plasma mass and energy. The code will then determine the histories α, m_i and E_i to provide the desired constant pressure up to the point at which the plasma supply is exhausted. The rate of decomposition is taken to be strictly proportional to the plasma energy flux. A midpoint search is used to determine the value of E_i at each time step.

In a third mode of operation the code accepts a tabular description of the observed pressure history in the gun together with the details of $m_i(t)$ and $E_i(t)$. This is referred to as the inverse mode and the code proceeds to deduce $\alpha(t)$ and, if both breech and base pressure are given, $\beta(t)$ as well. We provide further details of this mode of operation and the method of solution in Section 2.3.

---

14. Ralston, A. "A First Course in Numerical Analysis" McGraw-Hill 1965

2.2 Ballistic Implications of Rate of Mixing

In the present section we illustrate the use of the lumped parameter model to probe the sensitivity of the interior ballistics of the ETG to the rate of decomposition of the working fluid. We recall that the model assumes the working fluid to be mixed with the ambient as soon as it decomposes. Thus the discussion of this section, and the next, may be viewed as addressing either the rate of decomposition or the rate of mixing since there is no difference between the two. The study is similar to that reported in a previous paper [15] in which a rudimentary version of the present model was employed. The numerical results presented here differ from those of Reference 15 due to revisions to the model and certain minor differences in the data bases.

We first discuss the influence of the rate of sensitivity in general analytical terms by focussing on the implications of the equation of state. We then discuss the data bases and the numerical results.

Dependence of Pressure on α

The influence of the rate of mixing can be anticipated from an examination of Equation 2.33 which we repeat as

$$p = \frac{(\gamma - 1)e_{eff}(e_F)}{\frac{1}{\rho} - b} \quad .$$

As discussed in the previous section, we admit two conventions with respect to the representation of the thermochemical properties of the mixture of plasma and vaporized working fluid, namely a constant thermochemistry option and a variable thermochemistry option. In the latter, the effective energy, e_{eff}, and the values of γ and b are functions of e_F, which is seen to be a strong function of α through the denominator of Equation 2.39. In the former case, however, we have γ and b constant and $e_{eff} = e_F$. We therefore confine our discussion for the moment to the former case and make the simplifying assumption that Q_H, Q_v, W_f, Q_w, E_o, e_p, m_i, m_o and Y are all zero. That is to say, we assume the working fluid to be inert and the losses associated with work against friction, heat loss to the tube and compression of the unvaporized working fluid to be negligible. We also neglect the mass of the plasma and the influence of the initial ambient. With these assumptions, Equations 2.26 and 2.39 show that

$$e_{eff} = e_F = \frac{E_i - \frac{Mv_p^2}{2g_o} - E_{kin}}{\alpha C} \quad . \qquad (2.40)$$

---

15. *Gough, P.S. "Influence on Interior Ballistics of Electrothermal Gun of Rate of Mixing of Plasma with Working Fluid" Proceedings of the 26th Jannaf Combustion Meeting 1989*

We use the simple Lagrange relation for the kinetic energy E_{kin} as given in Equation 2.6 whereupon 2.33 and 2.40 give the result

$$p = \frac{(\gamma - 1)\left[E_i - \frac{Mv_p^2}{2g_o}\left(1 + \frac{C}{3M}(\alpha + \beta(1 - \alpha))\right)\right]}{V_o + x_p A_b - \frac{C}{\rho_p} + \alpha C\left(\frac{1}{\rho_p} - b\right)} \quad . \tag{2.41}$$

In this simplified situation we have the following conclusions. First, p is completely insensitive to α in the special case when $\beta = 1$ and $1/\rho_p = b$. Second, p will be only weakly sensitive to α in the more general situation defined by the pair of inequalities.

$$\left.\begin{aligned} &C/M \ll 1 \quad , \\ &V_o - \frac{C}{\rho_p} + x_p A_b \gg \alpha C\left(\frac{1}{\rho_p} - b\right) \quad . \end{aligned}\right\} \tag{2.42}$$

From an examination of the second inequality it is apparent that the presence of initial ullage, $V_o > C/\rho_p$, may be expected to desensitize the ETG interior ballistics to the rate of mixing. In general, configurations having a low C/M and low initial loading density of the working fluid will be expected to exhibit less sensitivity to the rate of decomposition than configurations with large values of C/M and high loading densities. Of course, all this discussion is predicated on the assumption that the thermochemical properties are constant. As we shall see in the numerical results which follow, the variation in properties with variations in the energy density e_F may exert a dominant role as regards the sensitivity of the interior ballistics to the rate of mixing.

Data Bases

The central gun parameters are based on those used in an earlier study by Oberle [2] and are summarized in Tables 2.1 and 2.2. With the exception of the plasma mass, which has been arbitrarily set equal to 1 g, and the recognition of the compressibility of the working fluid, the data of Table 2.1 are as in the study by Oberle [2] and correspond to the case with water as the working fluid. We note the variation in the effective energy as a fraction of the input electrical energy as the energy density is varied. At low energies and at high energies the fraction of energy available to do work is reduced. For values of the input energy above the range of Table 2.2, a linear extrapolation is used to get the effective energy. Table 2.2 differs from the data of Oberle only in that a set of values is presented for the case when the input energy is zero. As in the previous study [15], we use the Lagrange pressure gradient relations. The code listing of the nominal input data is presented in Appendix C together with the complete solution.

In addition to this nominal configuration which corresponds to an initial loading density of 46%, we consider values of the chamber volume equal to 74.6, 56.0 and 49.8 cm^3 corresponding to initial loading densities of 60, 80 and 90% respectively. These allow us to probe the influence of initial ullage on the ballistic sensitivity to the rate of mixing. In order to assess the influence of the rate of mixing for each loading density we proceed as follows. First, we determine the rate of plasma addition to achieve a constant breech pressure of 435 MPa, until depletion of the supply, on the assumption that the rate of mixing $\alpha(t)$ is proportional to $E_i(t)$. Thus $\alpha(t)$ becomes equal to one at the instant that the supply of plasma is depleted. The plasma is supplied over an interval of approximately 1 ms at a more or less constant rate. The rate of delivery for each of the four loading densities is summarized in Table 2.3. The history of $E_i(t)$ so determined is used to perform runs in which the rate of mixing differs from the rate of plasma addition by a constant factor. Results are obtained using the thermochemistry defined by Table 2.2 and with values $\beta = 1$ and 0 to assess the influence of the mobility of the unvaporized working fluid. Results are also obtained with the thermochemistry frozen at the 10 kJ/g values of Table 2.2 and with $\beta = 0$. These results permit an assessment of the importance of variations in composition and also provide a basis for comparison with the one-dimensional results discussed in Chapter 3.0 since the latter are performed subject to the assumptions of stationary working fluid and constant mixture properties.

Numerical Results

Tables 2.4 and 2.5 present the influence of rate of mixing on maximum breech pressure and muzzle velocity for variable thermochemistry and mobile working fluid. It will be noted that the maximum value of breech pressure differs slightly from the target value of 435 MPa when $\dot{\alpha} = \dot{E}_i$ for each of the initial loading densities. This is a consequence of the tabular representation of the ideal history of E_i and could be removed by using greater resolution in the tabular data. However, for our purposes, it is the variation with respect to $\dot{\alpha}/\dot{E}_i$ which is of interest. The same tabular data are used for all values of $\dot{\alpha}/\dot{E}_i$ at a fixed loading density and the slight departure from nominal at $\dot{\alpha}/\dot{E}_i = 1$ is not important.

We see that the maximum pressure is relatively insensitive to a lagging of the mixing process. Maximum pressure is reduced by only about 10% when $\dot{\alpha}/\dot{E}_i = 0.1$ for all loading densities. We note that when $\dot{\alpha}/\dot{E}_i = 1$, the data of Table 2.2 imply that the effective energy will be optimal. When $\dot{\alpha}/\dot{E}_i = 0.1$ the effective energy is a smaller fraction of the input and pressurization is not as intense. On the other hand, the maximum pressure is much more sensitive to an accelerated rate of mixing with $\dot{\alpha}/\dot{E}_i > 1$. We see that in the limit when the working fluid is assumed to be entirely vaporized and mixed at the initial instant the pressure is increased relative to the ideal or proportional case. The low initial energy density results in low initial pressure, as is the case for $\dot{\alpha}/\dot{E}_i = 0.1$. The loss of effective energy is more extreme at low energy density than at high energy density as may be seen from the data of Table 2.2. The difference between the cases $\dot{\alpha}/\dot{E}_i = 0.1$ and $\dot{\alpha}/\dot{E}_i = \infty$ stems from the fact that in the latter one

Table 2.1 Parameters Used for Nominal Data Base (after Oberle [2]).

Chamber Volume	97.108 cm^3
Projectile Travel	145 cm
Bore Diameter	14 mm
Projectile Mass	18 g
Plasma Energy	447.8 kJ
Plasma Mass	1 g
Working Fluid	44.78 g of H_2O
Density	1 g/cm^3
Bulk Modulus	5000 MPa
Derivative of Bulk Modulus with respect to pressure	8.

Table 2.2 Thermochemistry of Working Fluid as a Function of Electrical Energy Added (after Oberle [2]).

Electrical Energy Input (kJ/g)	Effective Energy (kJ/g)	Gamma (-)	Covolume (cm^3/g)	Molecular Weight (g/mol)	Eff En./El. En. (-)
0.0	0.00	1.9414	-1.834	18.015	0.000
3.0	0.44	1.9414	-1.834	18.015	0.147
4.0	1.63	1.4000	-0.342	18.014	0.408
5.0	2.86	1.2987	0.082	18.014	0.572
6.0	4.08	1.2557	0.283	18.001	0.680
7.0	5.24	1.2323	0.404	17.967	0.749
8.0	6.32	1.2182	0.488	17.896	0.790
9.0	7.31	1.2093	0.554	17.783	0.812
10.0	8.23	1.2035	0.609	17.633	0.823
11.0	9.07	1.1998	0.659	17.450	0.825
12.0	9.85	1.1975	0.705	17.242	0.821
13.0	10.59	1.1962	0.748	17.015	0.815
14.0	11.29	1.1958	0.788	16.775	0.806
15.0	11.95	1.1959	0.826	16.526	0.797
16.0	12.59	1.1964	0.863	16.272	0.787
17.0	13.21	1.1973	0.898	16.015	0.777
18.0	13.81	1.1985	0.931	15.757	0.767
19.0	14.40	1.1998	0.964	15.501	0.758
20.0	14.97	1.2014	0.995	15.248	0.749
21.0	15.55	1.2030	1.025	14.998	0.740
22.0	16.11	1.2048	1.054	14.753	0.732
23.0	16.68	1.2066	1.082	14.512	0.725

Table 2.3 History of Plasma Flux to Achieve Constant Breech Pressure of 435 MPa

Time (msec)	Fraction of Energy Delivered to Mixing Chamber (-)			
	Percent Initial Loading Density (%)			
	46	60	80	90
0.0000	0.2779	0.1642	0.0701	0.0387
0.0500	0.2798	0.1660	0.0720	0.0406
0.1000	0.2854	0.1716	0.0776	0.0462
0.1500	0.2947	0.1810	0.0870	0.0556
0.2000	0.3078	0.1941	0.1001	0.0688
0.2500	0.3246	0.2110	0.1171	0.0858
0.3000	0.3452	0.2316	0.1378	0.1065
0.3500	0.3695	0.2560	0.1622	0.1310
0.4000	0.3976	0.2842	0.1904	0.1592
0.4500	0.4294	0.3161	0.2224	0.1912
0.5000	0.4650	0.3517	0.2581	0.2269
0.5500	0.5043	0.3912	0.2976	0.2665
0.6000	0.5472	0.4343	0.3408	0.3098
0.6500	0.5941	0.4811	0.3878	0.3568
0.7000	0.6445	0.5317	0.4385	0.4075
0.7500	0.6987	0.5861	0.4930	0.4620
0.8000	0.7567	0.6442	0.5512	0.5203
0.8500	0.8184	0.7059	0.6132	0.5823
0.9000	0.8837	0.7715	0.6788	0.6479
0.9500	0.9526	0.8407	0.7482	0.7174
1.0000	1.0000	0.9136	0.8213	0.7905
1.0500	1.0000	0.9902	0.8981	0.8673
1.1000	1.0000	1.0000	0.9785	0.9479
1.1500	1.0000	1.0000	1.0000	1.0000

Table 2.4 Effect on Maximum Breech Pressure of Mixing Rate of Plasma with Working Fluid. Thermochemistry as in Table 2.2. Unmixed working fluid moves.

Percent Initial Loading Density (%)	Pressure (MPa)					$P_\infty/P_{0.1}$(-)
	Rate of Mixing / Rate of Plasma Injection (-)					
	0.1	0.5	1.0	2.0	∞	
46	407.4	434.3	435.7	492.7	601.9	1.477
60	410.8	434.9	436.1	505.6	668.5	1.627
80	409.6	434.7	437.4	511.9	656.4	1.603
90	408.1	434.4	438.7	511.7	629.3	1.542

Table 2.5 Effect on Muzzle Velocity of Mixing Rate of Plasma with Working Fluid. Thermochemistry as in Table 2.2. Unmixed working fluid moves.

Percent Initial Loading Density (%)	Muzzle Velocity (m/s)				
	Rate of Mixing / Rate of Plasma Injection (-)				
	0.1	0.5	1.0	2.0	∞
46	1943.3	2058.6	2069.8	2064.7	2168.6
60	1992.9	2096.6	2105.2	2099.6	2245.4
80	2029.2	2124.2	2130.1	2122.1	2229.1
90	2037.8	2132.1	2137.4	2126.8	2191.7

achieves the condition of high effective energy at the time when the plasma supply is completed. When this occurs in the case of instantaneous mixing one has the projectile travel reduced by comparison with the case of proportional mixing; the free volume is reduced and the pressure then becomes excessive.

Accordingly, for the case studied here, namely that of water as the working fluid, a slow rate of mixing has only a weak effect on ballistics stemming from an inefficient use of the plasma energy to create propulsive gas. A rapid rate of mixing, however, has a stronger effect and is more dangerous since it results in increased pressure. Of course, the slow rate of mixing would imply higher mixture temperatures with the possibility of greater heating of the tube. We also note that the sensitivity to the rate of mixing as represented by the effect on maximum pressure is surprisingly indifferent to the initial loading density.

In Tables 2.6 and 2.7 we probe the influence of the mobility of the unvaporized working fluid. All input data are as for the corresponding results in Tables 2.4 and 2.5 except that now $\beta = 0$ so that the unvaporized working fluid is stationary. This implies that the ratios of p, p_{base} and p_{br} which were fixed in the previous set of results with $\beta = 1$, will now vary with $\alpha(t)$. The rate of plasma addition will be unchanged. Initially, therefore, the spacemean pressures will be the same for corresponding cases. However, the values of p_{br} will differ, the values in Table 2.6 being lower than those of Table 2.4 as may be seen from Equations 2.4 and 2.5. In general, the trends with respect to mixing rate are similar for the cases $\beta = 0$ and $\beta = 1$. However, with $\beta = 0$ the sensitivity is greater as evidenced by the ratios of pressure for the extremes. Again, sensitivity is remarkably indifferent to the value of the loading density.

Finally, in Tables 2.8 and 2.9 we examine the influence of the variations in thermochemistry implicit in the preceding results. The results in Tables 2.8 and 2.9 take the properties of the mixture to be fixed at the 10 kJ/g values of Table 2.2 and the unvaporized working fluid is assumed to be stationary, $\beta = 0$. Sensitivity of the maximum pressure to the rate of mixing is reduced as evidenced by the ratios for the extreme cases. For lagging mixing rates there is virtually no sensitivity of the maximum pressure since this is achieved at the initial instant. For the accelerated mixing rates one has a relative initial lag of projectile motion due to the increased pressure gradient. As in Tables 2.4 and 2.6 this results in a lower free volume when the plasma injection is complete, and hence higher pressure. We note in Tables 2.7 and 2.9 the relatively high velocities which occur for the lagging mixing rates. These reflect reduced pressure gradients when $\beta = 0$.

The results of Table 2.8 are consistent with the analysis presented in the preamble to this section. Here, with constant thermochemical properties, the presence of initial ullage, or low loading density, acts to desensitize the ETG to the variations in the rate of mixing. This is the case even though $\beta = 0$ and C/M = 2.5, a relatively large number. We may contrast these results with those of Table 2.6, also based on $\beta = 0$, where we see much greater sensitivity to the rate of mixing for all values of the initial loading density. Accordingly, we may conclude that the dominant influence in respect to the sensitivity exhibited in Table 2.6 stems from

Table 2.6 Effect on Maximum Breech Pressure of Mixing Rate of Plasma with Working Fluid. Thermochemistry as in Table 2.2. Unmixed working fluid stationary.

Percent Initial Loading Density (%)	Pressure (MPa)					$P_\infty/P_{0.1}$(-)
	Rate of Mixing / Rate of Plasma Injection (-)					
	0.1	0.5	1.0	2.0	∞	
46	297.0	365.2	388.7	461.8	601.9	2.027
60	297.1	358.7	376.8	446.4	668.5	2.250
80	301.0	353.8	365.7	429.9	656.4	2.181
90	306.5	353.0	361.9	424.5	629.3	2.053

Table 2.7 Effect on Muzzle Velocity of Mixing Rate of Plasma with Working Fluid. Thermochemistry as in Table 2.2. Unmixed working fluid stationary.

Percent Initial Loading Density (%)	Muzzle Velocity (m/s)				
	Rate of Mixing / Rate of Plasma Injection (-)				
	0.1	0.5	1.0	2.0	∞
46	2349.8	2282.8	2122.8	2041.1	2168.6
60	2356.7	2296.2	2153.2	2048.6	2245.4
80	2354.6	2294.7	2163.9	2041.1	2229.1
90	2355.3	2296.8	2167.3	2037.0	2191.7

Table 2.8 Effect on Maximum Breech Pressure of Mixing Rate of Plasma with Working Fluid. Thermochemistry fixed at 10 kJ/g values of Table 2.2. Unmixed working fluid stationary.

Percent Initial Loading Density (%)	Pressure (MPa)					$P_\infty/P_{0.1}$(-)
	Rate of Mixing / Rate of Plasma Injection (-)					
	0.1	0.5	1.0	2.0	∞	
46	382.4	386.5	388.1	412.1	454.0	1.187
60	379.8	378.7	376.1	391.3	472.4	1.244
80	376.4	371.2	364.5	375.5	502.0	1.334
90	373.7	367.6	360.1	371.7	526.6	1.409

Table 2.9 Effect on Muzzle Velocity of Mixing Rate of Plasma with Working Fluid. Thermochemistry fixed at 10 kJ/g values of Table 2.2. Unmixed working fluid stationary.

Percent Initial Loading Density (%)	Muzzle Velocity (m/s)				
	Rate of Mixing / Rate of Plasma Injection (-)				
	0.1	0.5	1.0	2.0	∞
46	2513.7	2304.0	2096.6	2023.6	2051.0
60	2486.1	2309.3	2124.7	2037.2	2106.4
80	2463.9	2302.1	2134.4	2036.3	2181.0
90	2466.2	2304.2	2138.2	2035.7	2222.3

the dependence of the thermochemical properties on the input energy density, e_F. This underscores the importance of a proper representation of the variation in composition of the mixture in any future theoretical modeling of the ETG.

We conclude this section with the following observation. The ballistic sensitivity to the rate of decomposition exhibited by the present calculations is encouraging from the standpoint of the safety of the ETG. However, it is also evident that reliable modeling will require information about the actual mixing rates since there is a significant difference between predictions based on the two simplest hypotheses, namely homogeneous mixing and proportional mixing.

2.3 Inverse Analysis to Determine Rate of Decomposition of Working Fluid

As mentioned in Section 2.1, the LUMPET code contains an option to determine the rate of decomposition of the working fluid when the pressure history of the gun is provided as an input. We have also mentioned previously that since the pressure is not strongly influenced by the rate of decomposition, we must expect the accuracy of the inverse solution to depend strongly on the precision of the data which characterize the plasma flux, the pressure history and the thermochemistry.

To explore further the influence of the extent of decomposition on the pressure achieved for a given supply of energy to the working fluid in a known volume, we have written a short code referred to as PMAP. We first discuss this code and present some numerical results which illustrate some of the difficulties associated with the inverse analysis. Subsequently, we discuss further the inverse analysis and present some numerical results for a nominal problem.

The PMAP Code

We assume that we are given a total mass of working fluid C in a volume V. The total energy available to heat the vaporized fraction of the working fluid is E. It follows from Equation 2.37 that

$$p = \frac{(\gamma - 1)e_{eff}(E/C\alpha)}{\frac{1}{\rho} - b} \quad . \tag{2.43}$$

We neglect the initial ambient and the mass of the plasma so that

$$\rho = \frac{\alpha C}{V - (1 - \alpha)C/\rho_p} \quad , \tag{2.44}$$

and, while we do not consider the influence of the energy of compression stored in the unvaporized working fluid, we do allow ρ_p to be a function of pressure in accordance with Equation 2.23. We substitute 2.44 into 2.43 and write the resulting equation for p in the form

$$p = \frac{(\gamma - 1)e_{eff}(E/\alpha C)}{\frac{1}{\alpha}\frac{V}{C} - \frac{1 - \alpha}{\alpha\rho_p} - b} \quad . \tag{2.45}$$

In the previous section we considered the case when the thermochemistry is constant so that $e_{eff} = E/\alpha C$ and the values of γ and b do not depend on $E/\alpha C$. Here we focus on the case when the thermochemistry is variable.

The PMAP Code accepts a set of values of E/C and C/V, values of K_1 and K_2 to support the equation of state $\rho_p - \rho_p(p)$, and a table of values of thermochemical data in the form presented in Table 2.2. The code then determines $p(\alpha)$ for $0.025 \leq \alpha \leq 1$ for each pair of values of E/C and C/V. Thus we can assess the dependence of pressure on the fraction of the working fluid which has decomposed for a variety of values of energy density and loading density. A listing of the code and a detailed description of the input files are given in Appendix B.

Tables 2.10, 2.11 and 2.12 present code output for values of E/C = 1000, 5000 and 10000 J/g respectively. The working fluid is taken to be water with K_1 and K_2 as in Table 2.1 and thermochemical properties as in Table 2.2. The values of C/V in each table range from 0.05, typical of muzzle exit conditions, to 0.5, typical of the initial or early time conditions. Each column presents the dependence of pressure on α for a fixed combination of E/C and C/V.

An inspection of the columns reveals three features which are of significance in respect to the inverse analysis. First, except for E/C = 10000 J/g and C/V < 0.3, each column shows at least one maximum of pressure as a function of α. Second, some columns, those corresponding to the lower values of E/C and the larger values of C/V, exhibit two maxima. Third, several columns exhibit extended regions where the pressure depends very weakly on α.

These observations have the following implications for the inverse analysis. First, the data used to characterize the pressure history will, as already anticipated, have to be very precise if gross errors in the determination of α are to be avoided. Indeed, it is conceivable that if a phase error were present in respect to the characterizations of pressure and plasma flux, say one lagging the other by 0.1 ms, conditions could easily arise in which no value of α could be found to match the stated values of energy and pressure. Second, the inversion algorithm must deal with the possibility of multiple roots. It is also possible for those roots to be quite close together with the result that a bifurcation occurs during the time dependent inversion process. Such a condition will arise when the conditions are close to a local maximum of pressure with respect to α. Accordingly, a principle of continuity may not suffice to determine the correct root. Further difficulties in selecting the proper root can stem from experimental noise which may temporarily scatter the solution into an inappropriate branch.

It is emphasized that the problems associated with the multiplicity of roots are a consequence of the dependence of the thermochemical properties on the energy density. It is obvious from an examination of the equation of state that a unique solution for α exists if the thermochemical properties are constant. However, the difficulties associated with the insensitivity of pressure to α will remain.

Inverse Analysis

We consider two possible modes with respect to the inverse analysis. In both cases we assume that the breech pressure history is given. In the first mode we assume that β is specified as a fixed value in the input data.

Table 2.10 Pressure as a function of fraction of working fluid converted to vapor (α) and ratio of mass of working fluid to chamber volume (C/V). Ratio of available energy to mass of working fluid (E/C) is 1000 J/g.

	Pressure (MPa)					
	C/V (g/cm^3)					
α (-)	.050	.100	.200	.300	.400	.500
.0250	7.2	15.1	34.0	58.2	90.0	133.4
.0500	7.9	16.7	37.6	64.3	99.3	147.1
.0750	8.4	17.6	39.5	67.4	103.7	152.6
.1000	8.8	18.5	41.4	70.2	107.6	157.4
.1250	9.0	19.0	42.3	71.6	109.0	158.4
.1500	9.2	19.2	42.6	71.6	108.4	156.2
.1750	9.1	19.1	42.2	70.6	106.0	151.2
.2000	8.9	18.6	40.8	67.6	100.6	141.9
.2250	9.0	18.8	40.8	66.8	98.0	136.0
.2500	8.4	17.5	37.5	60.9	88.2	120.6
.2750	10.1	20.6	43.4	68.7	96.8	128.0
.3000	9.7	19.7	40.6	62.8	86.3	111.4
.3250	7.8	15.7	31.8	48.2	65.0	82.1
.3500	6.9	13.8	27.6	41.5	55.3	69.0
.3750	6.9	13.7	27.3	40.6	53.7	66.7
.4000	6.9	13.6	26.9	39.8	52.3	64.5
.4250	6.8	13.5	26.5	39.0	50.9	62.4
.4500	6.8	13.4	26.2	38.2	49.7	60.5
.4750	6.8	13.3	25.8	37.5	48.4	58.7
.5000	6.8	13.3	25.5	36.8	47.3	57.0
.5250	6.7	13.2	25.1	36.1	46.1	55.4
.5500	6.7	13.1	24.8	35.4	45.1	53.9
.5750	6.7	13.0	24.5	34.8	44.1	52.4
.6000	6.7	12.9	24.2	34.2	43.1	51.1
.6250	6.6	12.8	23.9	33.6	42.2	49.8
.6500	6.6	12.7	23.6	33.0	41.3	48.5
.6750	6.6	12.7	23.3	32.5	40.4	47.4
.7000	6.6	12.6	23.1	32.0	39.6	46.2
.7250	6.6	12.5	22.8	31.5	38.8	45.2
.7500	6.5	12.4	22.5	31.0	38.1	44.1
.7750	6.5	12.3	22.3	30.5	37.3	43.2
.8000	6.5	12.3	22.0	30.0	36.6	42.2
.8250	6.5	12.2	21.8	29.6	36.0	41.3
.8500	6.4	12.1	21.5	29.1	35.3	40.5
.8750	6.4	12.0	21.3	28.7	34.7	39.7
.9000	6.4	12.0	21.1	28.3	34.1	38.9
.9250	6.4	11.9	20.9	27.9	33.5	38.1
.9500	6.4	11.8	20.6	27.5	32.9	37.4
.9750	6.3	11.7	20.4	27.1	32.4	36.7
1.0000	6.3	11.7	20.2	26.7	31.9	36.0

Table 2.11 Pressure as a function of fraction of working fluid converted to vapor (α) and ratio of mass of working fluid to chamber volume (C/V). Ratio of available energy to mass of working fluid (E/C) is 5000 J/g.

	Pressure (MPa)					
	C/V (g/cm^3)					
α (-)	.050	.100	.200	.300	.400	.500
.0250	32.0	67.4	150.9	256.0	390.4	565.7
.0500	32.9	69.5	155.6	264.0	402.8	584.1
.0750	33.9	71.5	160.2	272.0	415.3	602.7
.1000	34.9	73.6	164.9	280.1	427.8	621.4
.1250	35.9	75.6	169.6	288.1	440.4	640.2
.1500	36.8	77.7	174.3	296.2	453.1	659.3
.1750	37.8	79.8	179.0	304.3	465.8	678.4
.2000	38.8	81.9	183.7	312.5	478.6	697.8
.2250	39.5	83.3	186.9	317.8	486.7	709.5
.2500	39.7	83.6	187.2	317.7	485.3	705.2
.2750	40.0	84.2	188.2	318.6	485.2	702.6
.3000	40.4	85.0	189.4	319.9	485.6	700.6
.3250	40.8	85.8	190.8	321.3	486.2	698.7
.3500	41.2	86.6	192.3	322.9	487.0	697.1
.3750	41.7	87.5	193.6	324.2	487.3	694.8
.4000	42.1	88.2	194.9	325.4	487.4	692.1
.4250	42.5	89.0	196.1	326.4	487.2	688.9
.4500	42.9	89.8	197.2	327.2	486.7	685.3
.4750	43.3	90.4	198.1	327.7	485.6	680.8
.5000	43.6	91.0	198.8	327.8	484.0	675.7
.5250	43.9	91.4	199.2	327.5	481.7	669.5
.5500	44.1	91.8	199.4	326.7	478.7	662.5
.5750	44.3	92.1	199.5	325.7	475.5	655.0
.6000	44.5	92.3	199.4	324.4	471.6	646.7
.6250	44.6	92.4	198.9	322.5	467.1	637.7
.6500	44.8	92.6	198.6	320.7	462.4	628.2
.6750	44.8	92.6	197.9	318.3	457.0	617.8
.7000	44.8	92.4	196.8	315.4	450.9	606.7
.7250	44.8	92.2	195.8	312.5	444.8	595.4
.7500	44.9	92.2	194.8	309.6	438.4	583.8
.7750	44.8	91.9	193.5	306.1	431.4	571.3
.8000	44.7	91.4	191.7	302.0	423.6	558.2
.8250	44.5	90.8	189.6	297.4	415.3	544.6
.8500	44.4	90.6	188.3	293.8	408.0	531.8
.8750	44.5	90.4	186.9	290.0	400.4	518.7
.9000	44.4	90.0	185.0	285.6	392.1	505.0
.9250	44.1	89.3	182.7	280.6	383.1	490.6
.9500	43.8	88.4	180.1	275.1	373.6	475.8
.9750	43.4	87.4	177.0	269.1	363.6	460.7
1.0000	42.9	86.1	173.7	262.7	353.3	445.4

Table 2.12 Pressure as a function of fraction of working fluid converted to vapor (α) and ratio of mass of working fluid to chamber volume (C/V). Ratio of available energy to mass of working fluid (E/C) is 10000 J/g.

	Pressure (MPa)					
	C/V (-)					
α (-)	.050	.100	.200	.300	.400	.500
.0250	62.9	132.6	295.8	498.3	752.4	1075.0
.0500	63.9	134.7	300.5	506.6	765.6	1095.3
.0750	64.9	136.7	305.3	515.0	778.9	1115.8
.1000	65.9	138.8	310.1	523.4	792.3	1136.4
.1250	66.8	140.9	314.8	531.8	805.8	1157.4
.1500	67.8	143.0	319.6	540.2	819.4	1178.5
.1750	68.8	145.1	324.4	548.7	833.0	1199.8
.2000	69.8	147.2	329.2	557.2	846.8	1221.4
.2250	70.7	149.3	334.1	565.7	860.7	1243.3
.2500	71.7	151.3	338.9	574.3	874.6	1265.3
.2750	72.7	153.4	343.7	582.9	888.7	1287.7
.3000	73.7	155.5	348.6	591.6	902.8	1310.3
.3250	74.7	157.6	353.4	600.3	917.1	1333.2
.3500	75.6	159.7	358.3	609.0	931.5	1356.3
.3750	76.6	161.8	363.2	617.7	946.0	1379.7
.4000	77.6	163.9	368.1	626.5	960.5	1403.5
.4250	78.6	166.0	373.0	635.4	975.2	1427.5
.4500	79.0	166.8	374.4	637.3	977.4	1429.2
.4750	79.1	166.9	374.1	635.5	972.5	1418.2
.5000	79.3	167.2	374.0	634.0	967.8	1407.4
.5250	79.6	167.6	374.3	633.1	964.0	1397.8
.5500	79.9	168.1	374.7	632.4	960.3	1388.1
.5750	80.2	168.7	375.1	631.8	956.9	1378.8
.6000	80.6	169.3	375.7	631.2	953.5	1369.6
.6250	80.9	169.9	376.3	630.7	950.1	1360.3
.6500	81.3	170.6	377.0	630.3	946.7	1350.9
.6750	81.8	171.3	377.7	629.9	943.5	1341.7
.7000	82.2	172.0	378.4	629.6	940.3	1332.7
.7250	82.6	172.6	379.1	629.1	936.9	1323.2
.7500	83.0	173.3	379.5	628.3	932.9	1313.2
.7750	83.3	173.9	380.0	627.5	929.0	1303.2
.8000	83.7	174.5	380.5	626.5	924.8	1292.8
.8250	84.1	175.1	380.8	625.5	920.6	1282.4
.8500	84.5	175.6	381.2	624.5	916.2	1271.9
.8750	84.8	176.2	381.5	623.3	911.7	1261.1
.9000	85.2	176.7	381.7	622.0	907.1	1250.4
.9250	85.5	177.2	381.8	620.4	902.1	1239.1
.9500	85.8	177.6	381.8	618.7	896.7	1227.4
.9750	86.1	178.0	381.6	616.8	891.3	1215.7
1.0000	86.4	178.3	381.4	614.8	885.7	1204.0

In the second mode we do not specify β. Instead, the base pressure history is assumed to be given. The value of β is then permitted to vary with time and is deduced from the pressure gradient relations of Section 2.1. If the Lagrange relations are used we have

$$\beta = \frac{2M\left(\frac{p_{br}}{p_{base}} - 1\right) - C\alpha - m_i - m_o}{C(1 - \alpha)} \quad , \tag{2.46}$$

and, if the chambrage relations are used we have

$$\beta = \frac{M\left[\frac{p_{br} - p_{base}}{-a_2^* J_1 p_{base} - a_1^* J_1 - b^* J_2}\right] - \alpha C - m_i - m_o}{C(1 - \alpha)} \quad . \tag{2.47}$$

In Equation 2.47 we have $a_1^* = a_1/K$, $a_2^* = a_2/K$ and $b^* = b/K$ where a_1, a_2 and b are defined by Equations 2.15 - 2.17.

Since it is possible that $p_{br}(t)$ and $p_{base}(t)$ may contain experimental noise we provide an option to smooth the histories using a high frequency numerical filter developed by Shuman [16]. The filter consists of replacing the array f_j by $\tilde{f}_j$ where

$$\tilde{f}_j = f_j + \frac{w}{2}(f_{j+1} + f_{j-1} - 2f_j), \qquad 1 < j < N \quad , \tag{2.48}$$

and $\tilde{f}_1 = f_1$, $\tilde{f}_N = f_N$ where N is the total number of data. As recommended by Shuman, three consecutive passes are required with w taking the following successive complex values

$$w_1 = 0.49965 \quad , \tag{2.49}$$

$$w_2 = -0.22227 + 0.64240i \quad , \tag{2.50}$$

$$w_3 = -0.22227 - 0.64240i \quad . \tag{2.51}$$

---

16. *Shuman, F.G. "Numerical Methods in Weather Predictions: II Smoothing and Filtering" Monthly Weather Review November 1957*

The values of $\alpha(t)$ are determined from the pressure histories as follows. Depending on the mode, β is either given as a fixed input or is determined from the values of p_{br} and p_{base}. A trial value is selected for α and the solution is advanced to the required time level. The appropriate pressure gradient relations are used to convert the input value of breech pressure to a corresponding value of spacemean pressure, p_{exp}. The computed value of the spacemean pressure, $p(\alpha)$, is compared with the value corresponding to the input breech pressure. The value of α is then modified according to a numerical representation of Newton's method (Regula Falsi) in which the derivative is computed numerically from the values on successive steps. The test function is taken to be

$$f(\alpha) = \frac{p(\alpha)}{p_{exp}} - 1 \quad . \tag{2.52}$$

On the first iteration the derivative $f(\alpha)$ is not defined and we simply increase α by 0.01. Iteration continues until $|f(\alpha)|$ is less than some user defined tolerance, typically 10^{-4}.

At this point the root so determined may or may not be accepted. The user has the option of specifying a number of lagging values to which a linear regression line may be fitted. A total of 10 values has been found appropriate. If the regression line is not specified because the user did not request it or because the solution has not yet advanced sufficiently in time to establish the required number of values, the first root is accepted provided that it is larger than that at the previous time step. If it is less than the previous value, a series of searches for a larger root is conducted with the initial value being increased by 0.01 at the beginning of each search. The search is terminated as soon as a root is found which is larger than that at the previous time.

In general this approach is insufficient since noisy data may create conditions in which the solution for $\alpha(t)$ is not monotonic. The requirement of monotonicity may push the solution to an incorrectly large value. When the regression line is available a search for a larger root is conducted according to the preceding criteria. However, the regression line defines an expected value and either the smaller or the larger root will be accepted according to whichever is closer to the expected value and provided that the trend of the regression line is positive. If the trend of the regression line is negative, the larger root is accepted.

We note that the search for a second root is only conducted if the first root is less than the value at the previous step, whether or not the regression line is determined. We also tested an alternative, somewhat more complicated, scheme in which a search was also made for a smaller root if the first value of α was larger than the value at the previous step, the choice of the the two roots, if indeed a second root could be found, being made according to the previously described criteria. No significant differences were found for the trial problem considered here and so the simpler method is to be preferred on the basis of computational efficiency.

The trial value at each step is taken to be the value at the previous time step unless the regression line is defined in which case we use the expected value. The slope and intercept of the regression line are determined in accordance with the standard formulas [17].

Data Base and Numerical Results

We demonstrate the inverse analysis by reference to a nominal problem for which the principal data are summarized in Table 2.13. We see that the system parameters are quite different from those of Section 2.2. The value of C/M is 2.625 and the value of E/C = 4762 J/g. The thermochemical properties of the working fluid are described by Table 2.2. The Lagrange gradient relations are used. The value of β is 1. We note that the rate of decomposition of the working fluid is exactly one half of the rate of energy flux. The complete input and nominal solution for this problem are given in Appendix D. It should be noted that muzzle exit occurs at about 3.0 ms at which time the value of α is 0.75. Thus the working fluid does not decompose completely.

The computed histories of breech and base pressure are used in a variety of ways to construct input data to the LUMPET Code run in the inverse mode. Since both pressure histories are available the value of β will be determined as part of the inverse analysis. All the inverse analyses use a regression line based on 10 values.

The direct solution creates a table of values of pressure for which the time interval is 0.01 ms. The pressures are printed to two decimal places of accuracy. This complete table of data is used as input to determine the inverse solution represented in Table 2.14. We see that the value of β is determined almost exactly. Even with two decimal places of accuracy to describe the pressure, however, the value of α is reproduced with an accuracy no better than 2.0%. We note that the error is largest at intermediate times and in fact is relatively low as the projectile nears the muzzle.

In Table 2.15 we explore the consequences of a slightly less precise representation of the pressure histories. We enter them to one decimal place of accuracy. Since the breech pressure has a maximum value of 492 MPa and is still equal to 56 MPa at the muzzle, this level of accuracy is still beyond anything we are liable to obtain experimentally. We see that small errors now appear in the values of β, although these are for the most part less than 1%. The values of α are determined with an overall accuracy which is not much worse than that of the previous case, typically 2 - 3%. However, large errors occur near the muzzle, of the order of 10%. It is interesting that the inversion algorithm stabilizes itself: an error of 6.0% is followed by one of 0.9% and an error of 10.1% is followed by one of 0.8%. We also note the non-monotonic behavior of α towards the end of the calculation.

---

17. Hoel, P.G. "Introduction to Mathematical Statistics" John Wiley and Sons 1966

Table 2.13 Parameters Used for Inversion Study

Chamber Volume	444.6 cm^3
Projectile Travel	400.0 cm
Bore Diameter	4.0 cm
Projectile Mass	160 g
Plasma Energy *	2000000 J
Plasma Mass	0.0 g
Working Fluid **	420 g of H_2O
Density	1 g/cm^3
Bulk Modulus	5000 MPa
Derivative of Bulk Modulus with respect to Pressure	8.

* Plasma energy delivered at constant rate for 2 ms.
** Working fluid decomposes at constant rate for 4 ms.

Table 2.14 Inverse Solution for $\alpha(t)$ and $\beta(t)$. Breech and base pressure given at every time step to two decimal places of accuracy.

Time (msec)	α(-) Exact	α(-) Calculated	α(-) % Error	β(-) Exact	β(-) Calculated	β(-) % Error
0.2	0.050	0.050	0.0	1.000	1.000	0.0
0.4	0.100	0.101	1.0	1.000	1.000	0.0
0.6	0.150	0.151	0.7	1.000	1.000	0.0
0.8	0.200	0.203	1.5	1.000	1.000	0.0
1.0	0.250	0.253	1.2	1.000	1.000	0.0
1.2	0.300	0.304	1.3	1.000	1.000	0.0
1.4	0.350	0.354	1.1	1.000	1.000	0.0
1.6	0.400	0.406	1.5	1.000	1.000	0.0
1.8	0.450	0.458	1.8	1.000	1.000	0.0
2.0	0.500	0.509	1.8	1.000	1.000	0.0
2.2	0.550	0.557	1.3	1.000	1.000	0.0
2.4	0.600	0.601	0.2	1.000	1.000	0.0
2.6	0.650	0.652	0.3	1.000	1.000	0.0
2.8	0.700	0.699	0.1	1.000	1.000	0.0
3.0	0.750	0.752	0.3	1.000	1.001	0.1

Table 2.15 Inverse Solution for $\alpha(t)$ and $\beta(t)$. Breech and base pressure given at every time step to one decimal place of accuracy.

Time (msec)	$\alpha(-)$ Exact	$\alpha(-)$ Calculated	$\alpha(-)$ % Error	$\beta(-)$ Exact	$\beta(-)$ Calculated	$\beta(-)$ % Error
0.2	0.050	0.051	2.0	1.000	1.000	0.0
0.4	0.100	0.102	2.0	1.000	0.999	0.1
0.6	0.150	0.153	2.0	1.000	1.001	0.1
0.8	0.200	0.205	2.5	1.000	1.000	0.0
1.0	0.250	0.256	2.4	1.000	1.001	0.1
1.2	0.300	0.307	2.3	1.000	0.999	0.1
1.4	0.350	0.359	2.6	1.000	1.001	0.1
1.6	0.400	0.411	2.8	1.000	0.998	0.2
1.8	0.450	0.464	3.1	1.000	1.001	0.1
2.0	0.500	0.517	3.4	1.000	1.003	0.3
2.2	0.550	0.565	2.7	1.000	0.995	0.5
2.4	0.600	0.636	6.0	1.000	1.003	0.3
2.6	0.650	0.656	0.9	1.000	0.994	0.6
2.8	0.700	0.771	10.1	1.000	1.008	0.8
3.0	0.750	0.756	0.8	1.000	0.989	1.1

Table 2.16 Inverse Solution for $\alpha(t)$ and $\beta(t)$. Breech and base pressure given at every time step to zero decimal places of accuracy.

Time (msec)	$\alpha(-)$ Exact	$\alpha(-)$ Calculated	$\alpha(-)$ % Error	$\beta(-)$ Exact	$\beta(-)$ Calculated	$\beta(-)$ % Error
0.2	0.050	0.050	0.0	1.000	0.990	0.1
0.4	0.100	0.100	0.0	1.000	1.003	0.3
0.6	0.150	0.149	0.1	1.000	0.996	0.4
0.8	0.200	0.209	4.5	1.000	0.995	0.5
1.0	0.250	0.272	8.8	1.000	0.994	0.6
1.2	0.300	0.352	17.3	1.000	0.999	0.1
1.4	0.350	0.427	22.0	1.000	1.008	0.8
1.6	0.400	0.504	26.0	1.000	0.976	2.4
1.8	0.450	0.611	13.5	1.000	0.985	1.5
2.0	0.500	0.684	36.8	1.000	1.035	3.5
2.2	0.550	0.710	29.0	1.000	1.036	3.6
2.4	0.600	0.719	19.8	1.000	1.056	5.6
2.6	0.650	0.948	45.8	1.000	0.731	26.9
2.8	0.700	0.909	29.9	1.000	0.982	1.8
3.0	0.750	0.893	19.1	1.000	0.965	3.5

We carry the loss of accuracy one step further in Table 2.16 in which the pressures are characterized with zero decimal places. Now, even the values of β become subject to large sporadic errors. At 2.6 ms the error in β is 26.9%. Not surprisingly, this is accompanied by a very large error in α, namely 45.8%. We see that the error in α degrades rather quickly after 1.0 ms, being typically 20% and never less than 10%. Better results can be obtained if the pressure histories are smoothed using the algorithm described by Equations 2.48 - 2.51. Table 2.17 presents the results of such a calculation. We note that the initial results are less accurate than those of Table 2.16 due to the smearing of information. But the later results are in general better, the largest error in α being 23.2% while that for β is 5.8%.

Finally, in Table 2.18 we present the results of an inversion based on a subset of the complete pressure history. We only use every fifth datum from the pressure tables. Two decimal places of accuracy are retained. Values of pressure at the missing time steps are determined by linear interpolation of the tables. The values of β are reproduced faithfully but the values of α are in error by 10 - 15% throughout most of the calculation.

In conclusion, the results of the present study indicate that even with perfect knowledge of the plasma flux and the thermochemistry of the working fluid, and with the pressure specified to two decimal places, the values of α will still be subject to errors of the order of 2%. With regard to the accuracy with which the pressure is specified we should note that the effective limit is defined by the accuracy with which the code attempts to match the data. In all the present calculations this was 1 part in 10^4 so that specification of the pressure to greater accuracy would not be expected to have any benefit. If the pressure is given with an accuracy of roughly 1%, corresponding to the calculations with zero decimal places of accuracy, errors of the order of 20% are to be expected.

The present study has been based on water as the working fluid. It is suggested that the PMAP Code be used to screen possible alternative fluids to establish a stronger dependence of pressure on α. Even if the candidate fluid were not suitable for use in the ETG it could nevertheless be used in a test fixture to acquire valuable experimental characterizations of the rate of mixing. Such data would be very useful as a means of validating multi-dimensional numerical simulations of the mixing process and, possibly, as a means of defining empirical relations to be used in lower level codes.

On the other hand, working fluids which exhibit extreme insensitivity of pressure to α could be used to determine the plasma flux from measurements of pressure or, if the plasma flux were given, to verify BLAKE Code predictions of the dependence of effective energy on electrical energy output.

Table 2.17 Inverse Solution for $\alpha(t)$ and $\beta(t)$. Breech and base pressure given at every time step to zero decimal places of accuracy. Breech and base pressure histories smoothed.

Time (msec)	α(-) Exact	α(-) Calculated	α(-) % Error	β(-) Exact	β(-) Calculated	β(-) % Error
0.2	0.050	0.053	6.0	1.000	1.000	0.0
0.4	0.100	0.105	5.0	1.000	1.004	0.4
0.6	0.150	0.159	6.0	1.000	0.998	0.2
0.8	0.200	0.211	5.5	1.000	0.994	0.6
1.0	0.250	0.266	6.4	1.000	0.994	0.6
1.2	0.300	0.324	8.0	1.000	0.999	0.1
1.4	0.350	0.395	12.9	1.000	1.006	0.6
1.6	0.400	0.478	19.5	1.000	0.984	1.6
1.8	0.450	0.552	22.7	1.000	0.991	0.9
2.0	0.500	0.616	23.2	1.000	1.005	0.5
2.2	0.550	0.656	19.3	1.000	1.021	2.1
2.4	0.600	0.678	13.0	1.000	1.041	4.1
2.6	0.650	0.701	7.9	1.000	0.942	5.8
2.8	0.700	0.806	15.1	1.000	0.982	1.8
3.0	0.750	0.797	6.3	1.000	0.959	4.1

Table 2.18 Inverse Solution for $\alpha(t)$ and $\beta(t)$. Breech and base pressure given at every fifth time step to two decimal places of accuracy.

Time (msec)	α(-) Exact	α(-) Calculated	α(-) % Error	β(-) Exact	β(-) Calculated	β(-) % Error
0.2	0.050	0.056	12.0	1.000	1.000	0.0
0.4	0.100	0.112	12.0	1.000	1.000	0.0
0.6	0.150	0.169	11.3	1.000	1.000	0.0
0.8	0.200	0.224	12.0	1.000	1.000	0.0
1.0	0.250	0.282	12.8	1.000	1.000	0.0
1.2	0.300	0.342	14.0	1.000	1.000	0.0
1.4	0.350	0.402	14.8	1.000	1.000	0.0
1.6	0.400	0.462	15.5	1.000	1.000	0.0
1.8	0.450	0.522	16.0	1.000	1.000	0.0
2.0	0.500	0.582	16.4	1.000	1.000	0.0
2.2	0.550	0.592	7.6	1.000	1.000	0.0
2.4	0.600	0.659	9.8	1.000	1.000	0.0
2.6	0.650	0.668	2.8	1.000	1.000	0.0
2.8	0.700	0.782	11.7	1.000	1.001	0.1
3.0	0.750	0.768	2.4	1.000	1.001	0.1

3.0 ONE-DIMENSIONAL MODEL

In the previous chapter we described a lumped parameter model of the ETG and used it to demonstrate weak sensitivity of the interior ballistics of the ETG to the rate of decomposition of the working fluid. In the present chapter we continue to study the interaction between the manner of decomposition of the working fluid and the overall ballistics of the ETG. Our investigation is extended to include the influence of axial variations in the state variables. Obviously, a one-dimensional continuum analysis of the ETG leaves much to be desired since so much of the important phenomenology, such as the penetration of the working fluid by the plasma and the concomitant mixing process, is of an inherently two-dimensional nature. Nevertheless, it is of interest to determine to what extent the influence of axial wave propagation and axial non-uniformity in the distribution of the working fluid and its rate of decomposition might contribute to a greater dependency of the overall ballistics on the details of the interaction of the plasma and the working fluid.

The role of the one-dimensional model in the present study is to be viewed as permitting a degree of simulation beyond that possible with the lumped parameter model. No pretense is made of developing a truly predictive model which, given hard independent data, might be capable of predicting maximum pressure and muzzle velocity with any degree of accuracy. Accordingly, we do not develop a one-dimensional model from fundamental principles. Instead, we exploit an existing interior ballistics code, XKTC [8], and make suitable minor modifications in order to achieve our goal. We discuss the code in Section 3.1. In Section 3.2 we present some numerical results for an ETG configuration similar to that studied in Section 2.2.

3.1 Description of Model

The XKTC Code has been developed over several years and is a general purpose interior ballistics code. It is applicable to a wide variety of solid propellant charges including both conventional and traveling charge systems. The code supports a wide variety of form functions of which two are of greatest relevance here, namely the monolithic charge and the perforated stick charge. Our discussion focusses on these particular charge designs. The general details of the XKTC Code are not reviewed; the interested reader is directed to Reference 8 for a more complete discussion. Here we simply discuss those aspects of XKTC which pertain to the representation of the ETG.

Figure 3.1 illustrates the two types of ETG configuration which are admitted by the XKTC Code as revised in accordance with the present task objectives. The monolithic charge, shown in Figure 3.1(a), is configured rather like a solid propellant rocket motor. It is bonded to the sidewall of the tube and has a central port on whose surface the combustion occurs. Such a configuration can be used as an approximate representation of the working fluid of the ETG, provided that the working fluid is suitably packaged with a central duct. In the figure we show ullage inside the monolithic charge and also between the charge and the projectile base. We refer to the former as annular ullage and to the latter as axial ullage.

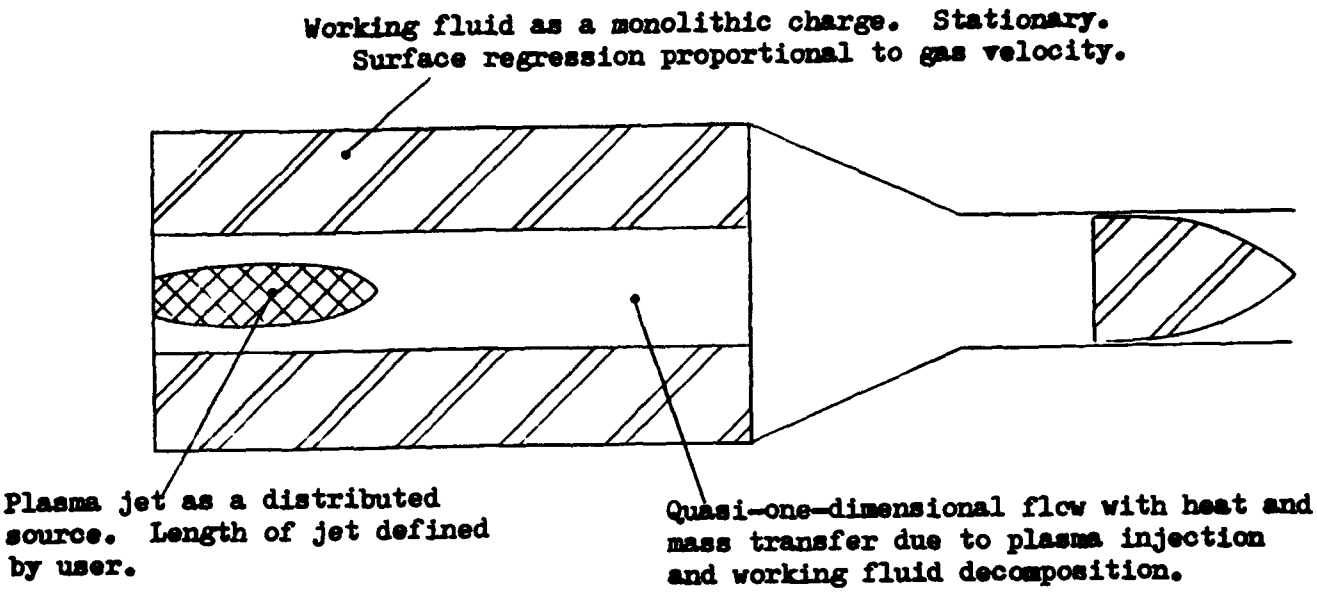

(a) Working Fluid as a Monolithic Charge.

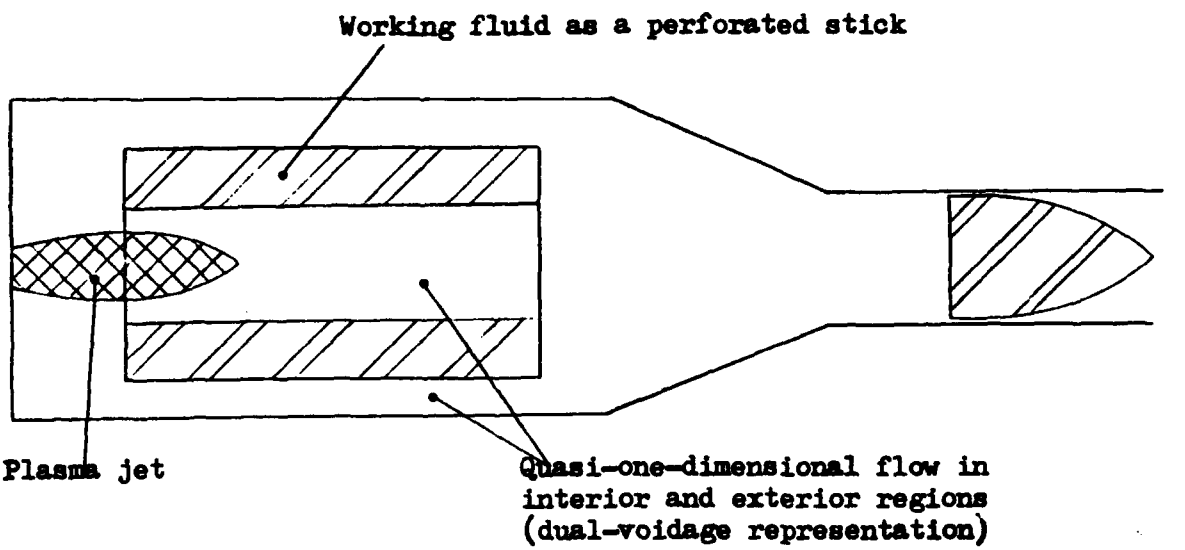

(b) Working fluid as a Perforated Stick

Figure 3.1 XKTC Representations of ETC with Annular Ullage.

Evidently the annular ullage will increase in time as the internal surface of the monolithic charge decomposes. The diameter of the duct, even if initially uniform, may vary with axial position in accordance with the local properties of the law governing the rate of decomposition. The axial ullage will grow in time due to the motion of the projectile; however, decomposition of the ends of the monolithic charge is not considered. We note that although Figure 3.1(a) shows the rear face of the monolithic charge in contact with the breech face, the code does admit the existence of axial ullage to the rear of the monolithic charge. Such a region would be of fixed length since the breechface is assumed to be stationary and the rear face of the monolithic charge, like the forward face, is assumed not to decompose.

The representation of Figure 3.1(b) admits certain additional features. The working fluid is represented as a perforated stick which is free to move in the axial direction in accordance with the gas-dynamic forces exerted on it by the mixture of plasma and products of decomposition. Annular ullage exists in the region exterior to the working fluid as well as in the central duct. Decomposition can occur on the outer and inner surfaces, but not at the ends. The properties of the gases in the external region of annular ullage are distinguished from those in the interior.

In XKTC the regions of annular ullage are always represented according to the equations of motion for a one-dimensional, unsteady, compressible fluid with variations in cross-sectional area and with mass and heat addition. The regions of axial ullage, at the ends of the charge regions, may be treated either as continua or as lumped parameter, depending on their lengths. The cross-sections of the tube at which the ends of the charge regions are located are treated mathematically as internal boundaries, permeable to the gas-phase, but across which all the gas-phase state variables may jump discontinuously as a result of the local discontinuity in flow area.

If the working fluid is represented as a monolithic charge, the solid-phase balance equations become trivial due to the assumption of immobility. However, if the working fluid is treated as a stick propellant, the motion of the working fluid is determined by the continuity and momentum equations for an elastic rod of varying cross-sectional area and with mass transfer to the ambient.

The gas-phase is assumed to obey the covolume equation of state, as in Chapter 2.0. However, the thermochemical properties are assumed to be constant; XKTC does not support the BLAKE Code formulation of variable properties.

The governing equations are a system of partial differential equations and are solved using an explicit finite difference scheme. The discontinuities at the internal boundaries defined by the ends of the charge regions are represented as such in the numerical algorithm.

The representation of the mixing of the plasma with the working fluid is visualized as a two-step process. The plasma mixes with the ambient gases. The motion of the gas, due at first to the non-uniform heating stimulus by the plasma, and subsequently to the rarefaction created by projectile motion, induces decomposition of the working fluid through a Helmholtz mechanism.

The working fluid is assumed to decompose at a rate

$$\dot{r}_p = \frac{k_w \left| \rho u - \rho_p u_p \right|}{\frac{1}{2} (\rho + \rho_p)} \tag{3.1}$$

where $\dot{r}_p$ is the local rate of surface regression; ρ is the density of the gas-phase (the mixture of plasma and products of decomposition); ρ_p is the density of the working fluid; u and u_p are respectively the velocity of the gas-phase and the velocity of the working fluid; and k_w is a dimensionless factor which we refer to as a wiping coefficient. Equation 3.1 has been previously proposed in connection with the regression of the cavity wall in bulk-loaded liquid propellant guns. Originally proposed to model decomposition due to the Helmholtz instability, Equation 3.1 can be shown to be closely related to the Prandtl theory of the mixing of a turbulent jet with the ambient fluid [18].

The influence of the plasma is reflected in the gas-phase balance equations as a source of mass, momentum and energy. As in the lumped parameter model of Chapter 2.0, we assume that the properties of the plasma are predetermined. The plasma is assumed to be added to the gas-phase over a distance referred to as the mixing length. At each time the specified plasma flux is converted to a distributed source term whose properties are essentially uniform over the mixing length. To permit resolution by the finite difference solver, the distribution is tapered linearly to zero over the last few mesh points. The magnitude of the source term follows from the value of the flux according to a simple quasi-steady mass balance.

Two representations of the plasma are admitted. In the simpler of the two we assume that the plasma mass flux is given and that the mixing length is a fixed value defined as an input datum. In the second representation we assume that the state of the plasma at the entrance to the mixing chamber is completely specified. The mixing length is then time dependent and follows from the Prandtl spreading rate for a turbulent jet. We take the Prandtl spreading rate for the plasma jet to be [18]

$$\dot{r}_j = \frac{k_j \left| \rho_j u_j - \rho u \right|}{\frac{1}{2} (\rho_j + \rho)} \quad , \tag{3.2}$$

---

18. *Edelman, R.B. "The Interior Ballistics of Liquid Propellant Guns" RDA-TR-4408-010* *1974*

where ρ_j and u_j are the density and velocity of the plasma jet as prescribed by a table of input data, and k_j is a dimensionless coefficient. The formal similarity to Equation 3.1 is obvious. We assume that the jet has an initial diameter d_j, specified as input, and that it is injected into the central ullage port whose diameter is d_i. We then take the mixing length to be the distance required for the jet boundary layer to expand to the point at which it touches either the wall of the cavity or the centerline of the jet. Thus we have the mixing length l_j defined by

$$l_j = \frac{u_j}{2r_j} \min [\, d_j,\ d_i - d_j] \quad . \tag{3.3}$$

Obviously, mixing will not be complete in a distance l_j which has rather the character of an e-folding length for the mixing process. However, Equation 3.3 expresses the essential physical relationship between the jet parameters and the rate of mixing with the ambient. The unknown coefficient k_j can be varied to compensate for the truncation inherent in Equation 3.3.

We note that Equation 3.2 is valid for subsonic jets. In fact, the plasma jet may be underexpanded and Equation 3.2 ought therefore to be applied to conditions downstream of the shock system which would be expected near the entrance to the mixing chamber. Consideration was given to a formulation similar to the Carfagno analysis of muzzle blast as modified by May and Einstein [19]. However, the analogy between the two sets of phenomena is not precise since the muzzle blast is essentially unconfined. In view of the other approximations inherent in the present application of XKTC, the extension to model a shock system in the chamber was not thought to be well motivated.

The goal of the present study is simply to assess the implications of one-dimensional axial structure of the flow in respect to the ballistic sensitivity to the rate of decomposition of the working fluid. Accordingly, the results presented in the next section are based on the simplest XKTC representation of the ETG. The working fluid is represented as a monolithic charge and the mixing length is taken to be a fixed input datum for each calculation.

---

19. May I.W. and Einstein , S.I. "Prediction of Gun Muzzle Flash" Proceedings of the 14th Jannaf Combustion Meeting 1977

3.2 Numerical Results

The calculations presented here are predicated on the same data as those in Section 2.2. The mixing chamber is assumed to have a cylindrical section 12.875 cm in length and a tapered section 3 cm in length over which the diameter decreases to that of the tube. To maintain the initial volume of 97.1 cm^3, the diameter of the cylindrical section is set equal to 2.944 cm. The working fluid is confined to the cylindrical section and the central port has a diameter of 2.059 cm. To maintain consistency with Section 2.2 the total plasma energy is set equal to 368.6 kJ which is the effective energy at 10 kJ/g of Table 2.2 corresponding to an input of 447.8 kJ as in Table 2.1. The values of γ and b are chosen consistently from Table 2.2. The plasma is represented as injecting at a uniform rate for 0.8 ms. At the initial instant the mixing chamber is assumed to be at atmospheric pressure and room temperature.

As will be seen, the solutions involve a great deal of structure and, accordingly, a total of 99 mesh points are used. XKTC treats the area discontinuity at the end of the monolithic charge as an explicit internal boundary. Within each of the two computational regions a uniform distribution of mesh points is used, the number being allocated to each region in proportion to length, except that the monolithic charge is always allocated a minimum of one half the total number.

We obtain results for three values of the plasma mixing length, namely 2.54 cm, 12.7 cm and a length which is variable but always equal to the distance from the breech to the base of the projectile. For each mixing length we obtain three solutions corresponding to values of k_w = 0.2, 0.4 and 0.8. The results are presented in Table 3.1 and in Figures 3.2 through 3.13.

Table 3.1 Ballistic Sensitivity of ETC to Plasma Mixing Length and Rate of Decomposition of Working Fluid According to One-Dimensional Continuum Analysis

Plasma Mixing Length (cm)	Wiping Coefficient (-)	α at 0.4 ms (-)	α at 0.8 ms (-)	Maximum Breech Pressure (MPa)	Muzzle Velocity (m/s)
2.54	0.2	0.32	0.56	563	2207
2.54	0.4	0.76	0.82	591	1938
2.54	0.8	0.89	0.92	580	1852
12.70	0.2	0.05	0.21	493	2676
12.70	0.4	0.27	0.57	545	2286
12.70	0.8	0.67	0.80	549	2146
*	0.2	0.01	0.06	473	2906
*	0.4	0.05	0.29	468	2856
*	0.8	0.19	0.66	462	2780

* Mixing length variable, taken to be distance from breech to base of projectile

In Table 3.1 we present the maximum breech pressure and the muzzle velocity for each of the nine solutions. We also tabulate the fraction of the working fluid which has been decomposed at 0.8 ms, when the plasma injection is complete, and at 0.4 ms, halfway through the injection process. Naturally, larger values of the wiping coefficient result in larger values of α at a given time. In general, the results of Table 3.1 are consistent with those of Section 2.2 based on the lumped parameter model. Higher pressures are obtained with more rapid rates of decomposition of the working fluid.

Precise comparisons between the continuum and the lumped parameter results cannot be made because the plasma injection rate in the latter were chosen to give a nearly constant breech pressure. In the continuum results the rate of energy deposition is more gradual so that maximum pressure occurs at about 0.4 - 0.8 ms, depending on the mixing parameters. The gradually rising pressure histories in the continuum solutions imply less projectile motion at the time of complete plasma addition and hence less volume and more pressure. Also, the plasma addition is complete in 0.8 ms in the continuum solutions whereas in the lumped parameter solutions the injection time was slightly longer, 1 ms.

Figures 3.2, 3.3 and 3.4 present distributions of density, pressure and velocity in the mixture of plasma and vaporized working fluid at various times for the shortest mixing length and the largest wiping coefficient. Figure 3.5 presents histories of breech pressure for the shortest mixing length and all three wiping coefficients. An extraordinary degree of structure is seen in the spacewise distributions. The short mixing length results in a blast wave type of response. A shock is formed and undergoes reflections from the projectile base and the face of the monolithic charge. A highly structured flow is developed. The rate of decomposition is very non-uniform and a slug of cool gas is formed as the high velocity results in rapid decomposition forward of the region where heat addition due to the plasma occurs. The wiggles in the pressure distribution at 0.2 ms indicate some strain on the numerical algorithm. We note that the maximum global pressure is much higher than the maximum breech pressure for this case. Yet in spite of the very non-uniform distributions the pressure histories are surprisingly indifferent to the wiping coefficient as shown in Figure 3.5. Greater wave structure is seen with the slower rates of decomposition since there is less damping of the initial explosive surge.

Comparable results are presented for the intermediate plasma mixing length in Figures 3.6 through 3.9. Although still highly structured, particularly as regards the density distribution, they show less blast wave structure than in the previous case. The histories of breech pressure show only a modest sensitivity to the wiping coefficient, even though the results in Table 3.1 indicate marked differences in the induced rates of decomposition. We see quite plainly the inflection due to termination of the energy supply at 0.8 ms. The lower pressure which occurs for the smallest value of the wiping coefficient is associated with a higher muzzle velocity, as shown in Table 3.1 and reflects the reduction in the pressure gradient due to the smaller mass of moving gas.

Finally, in Figures 3.10 through 3.13 we have the comparable results for the longest mixing length. The distributions are now quite smooth and the sensitivity of the pressure history to the rate of decomposition is almost nil, even though the values of α at 0.8 ms range from 0.06 to 0.66 as seen in Table 3.1 The density increases monotonically through the duct of the monolithic charge where the working fluid is decomposed and added to the mixture. In the developing region of ullage behind the projectile base, however, the density drops sharply as there is no further significant mass addition, only heating by the plasma.

Although a precise comparison with the results of Section 2.2 is precluded by the differences in plasma flux, it is fair to say that the results of Table 3.1 are consistent with those of Tables 2.8 and 2.9, for which the correspondence is expected to be greatest. Even though the continuum solutions reflect extremely non-uniform structure, they do not exhibit ballistic sensitivity to the rate of mixing in excess of that determined in the lumped parameter calculations.

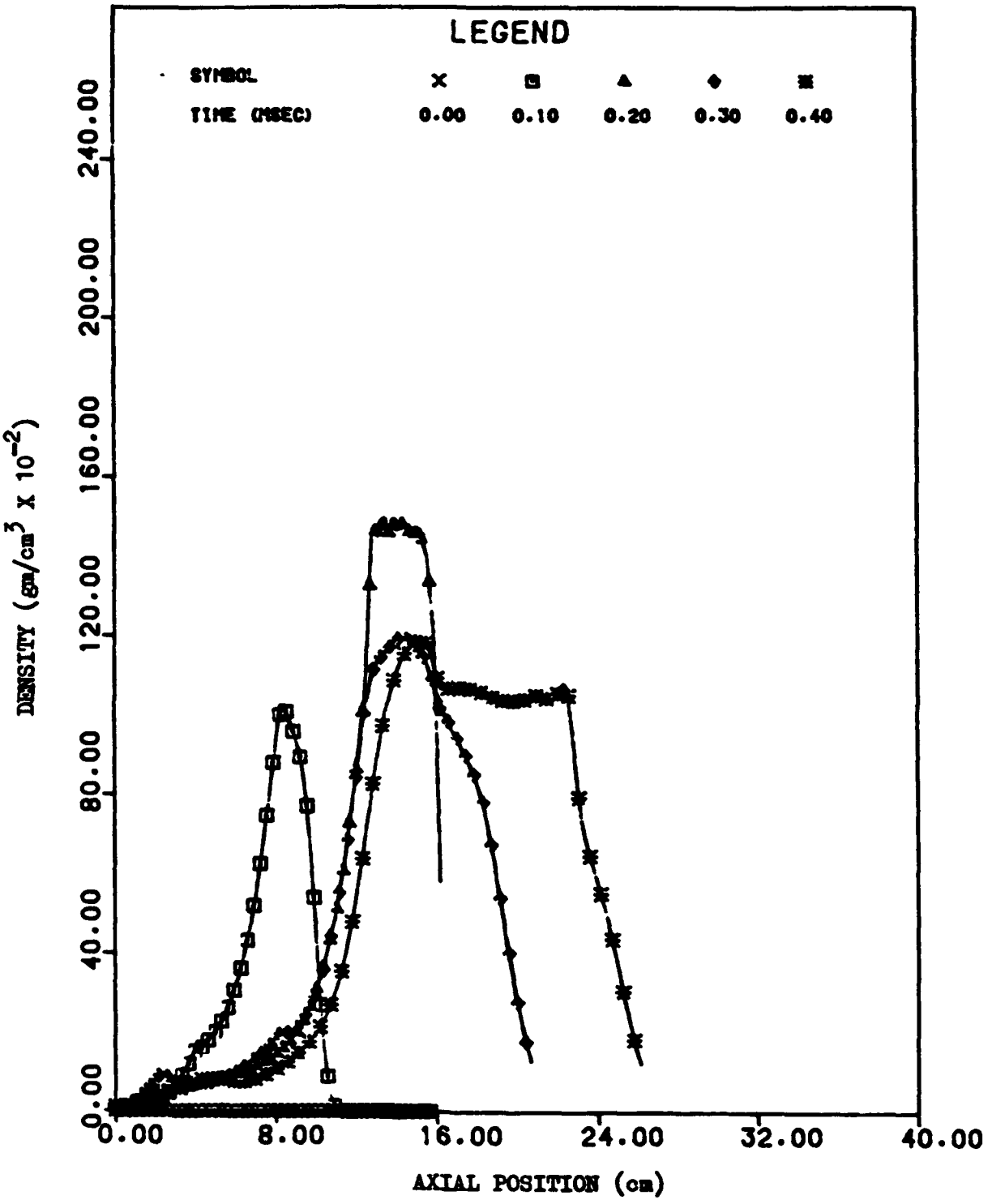

Figure 3.2 Distributions of density at various times for plasma mixing length 2.54 cm and wiping coefficient 0.8.

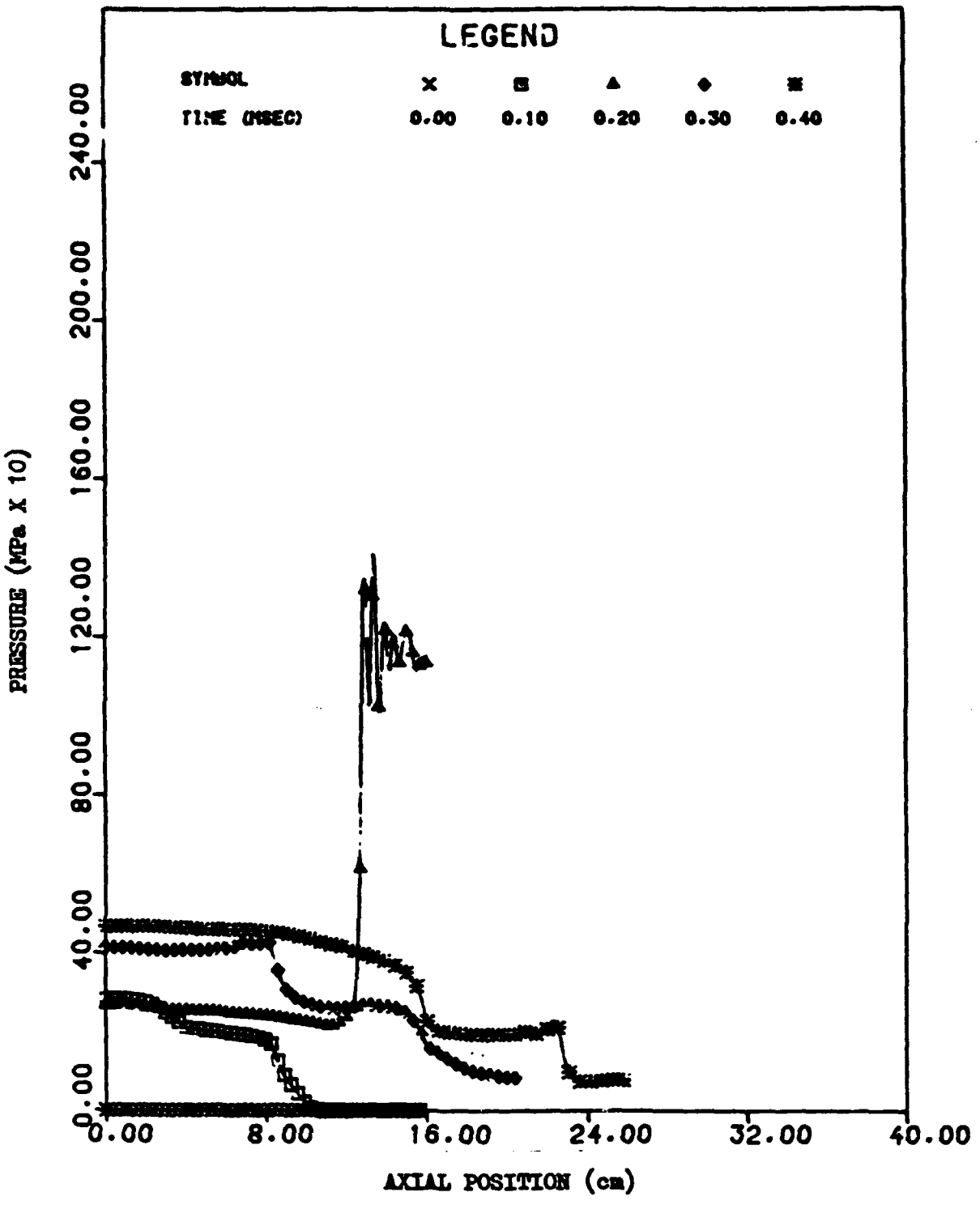

Figure 3.3 Distributions of pressure at various times for plasma mixing length 2.54 cm and wiping coefficient 0.8.

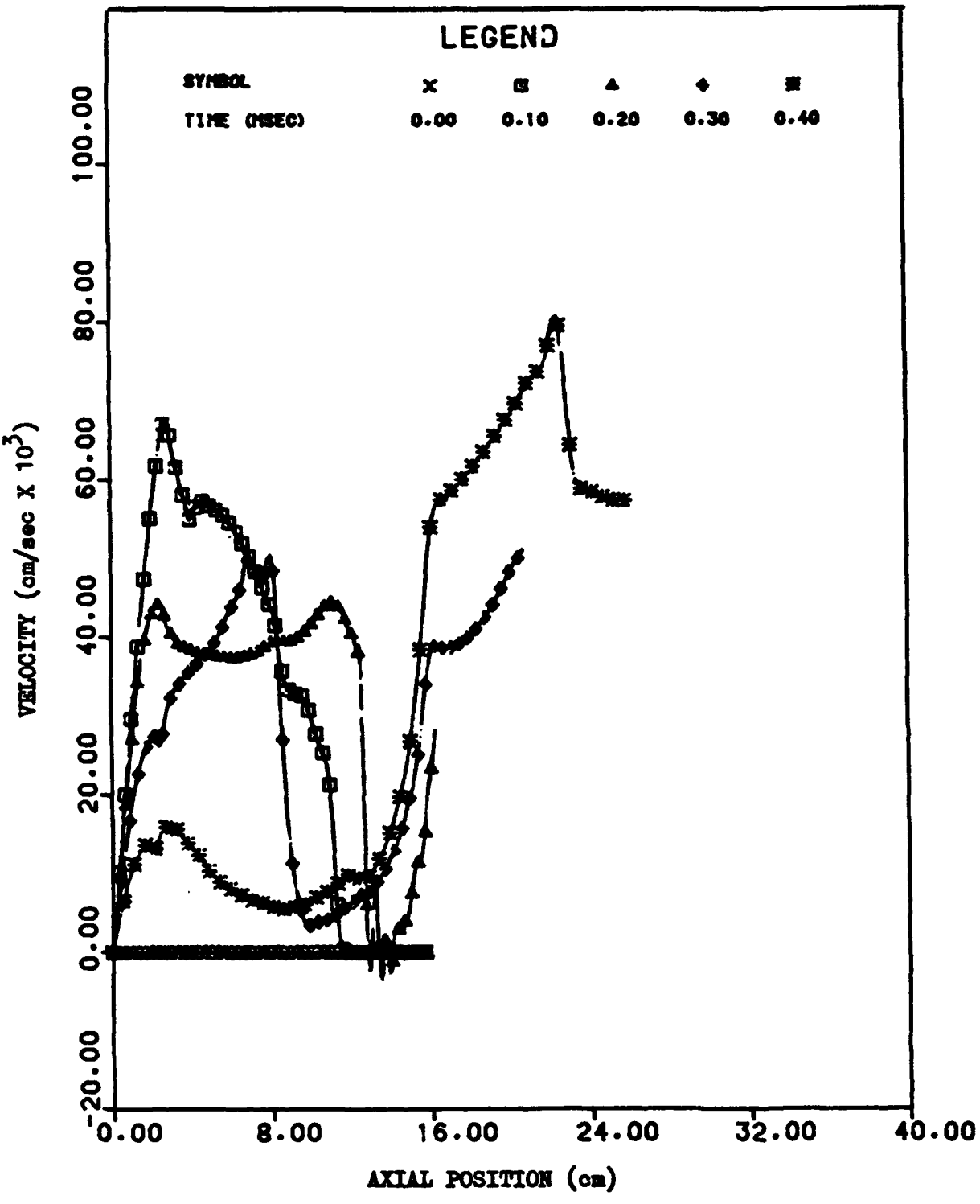

Figure 3.4 Distributions of velocity at various times for plasma mixing length 2.54 cm and wiping coefficient 0.8.

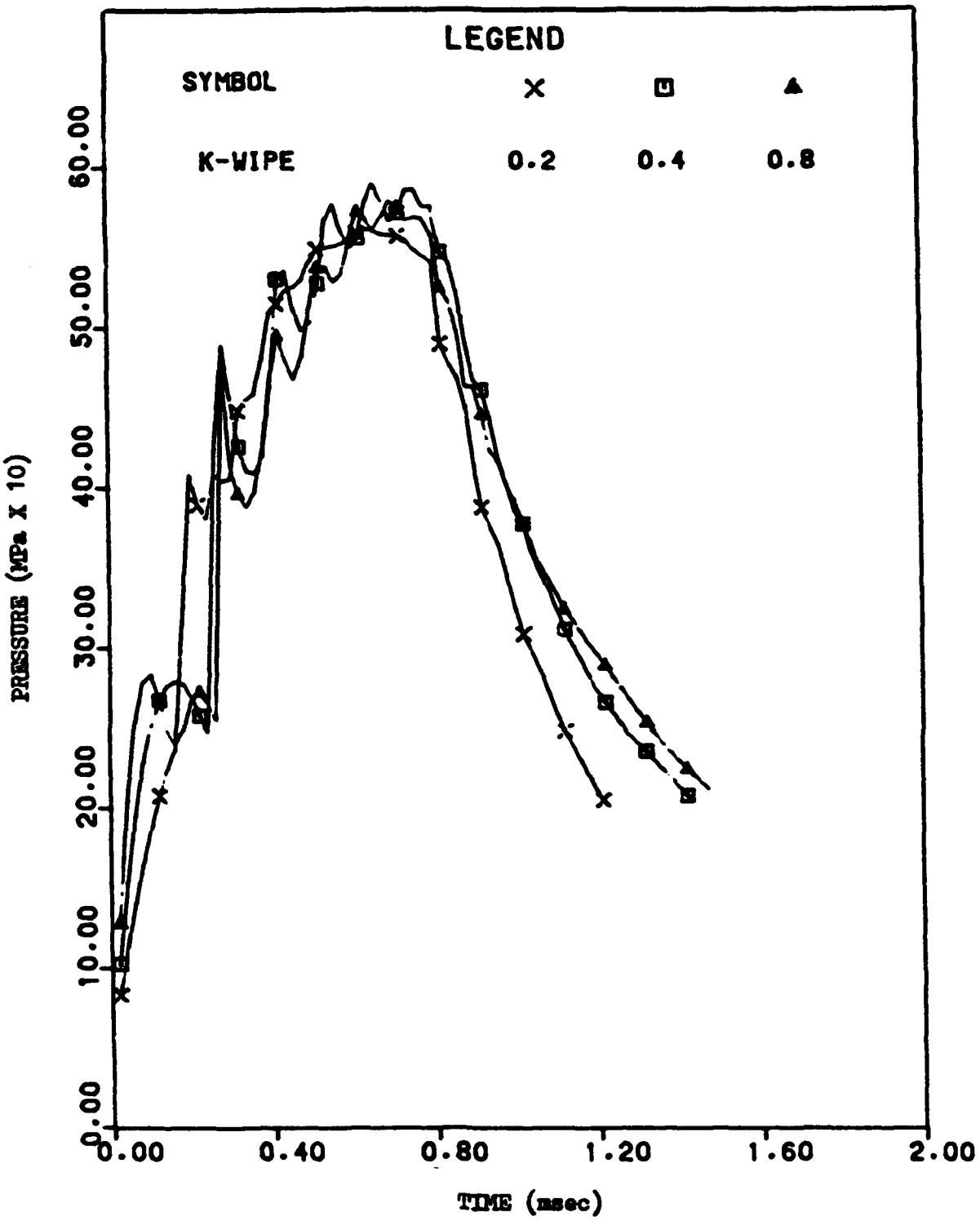

Figure 3.5 Histories of breech pressure for plasma mixing length 2.54 cm and three values of wiping coefficient.

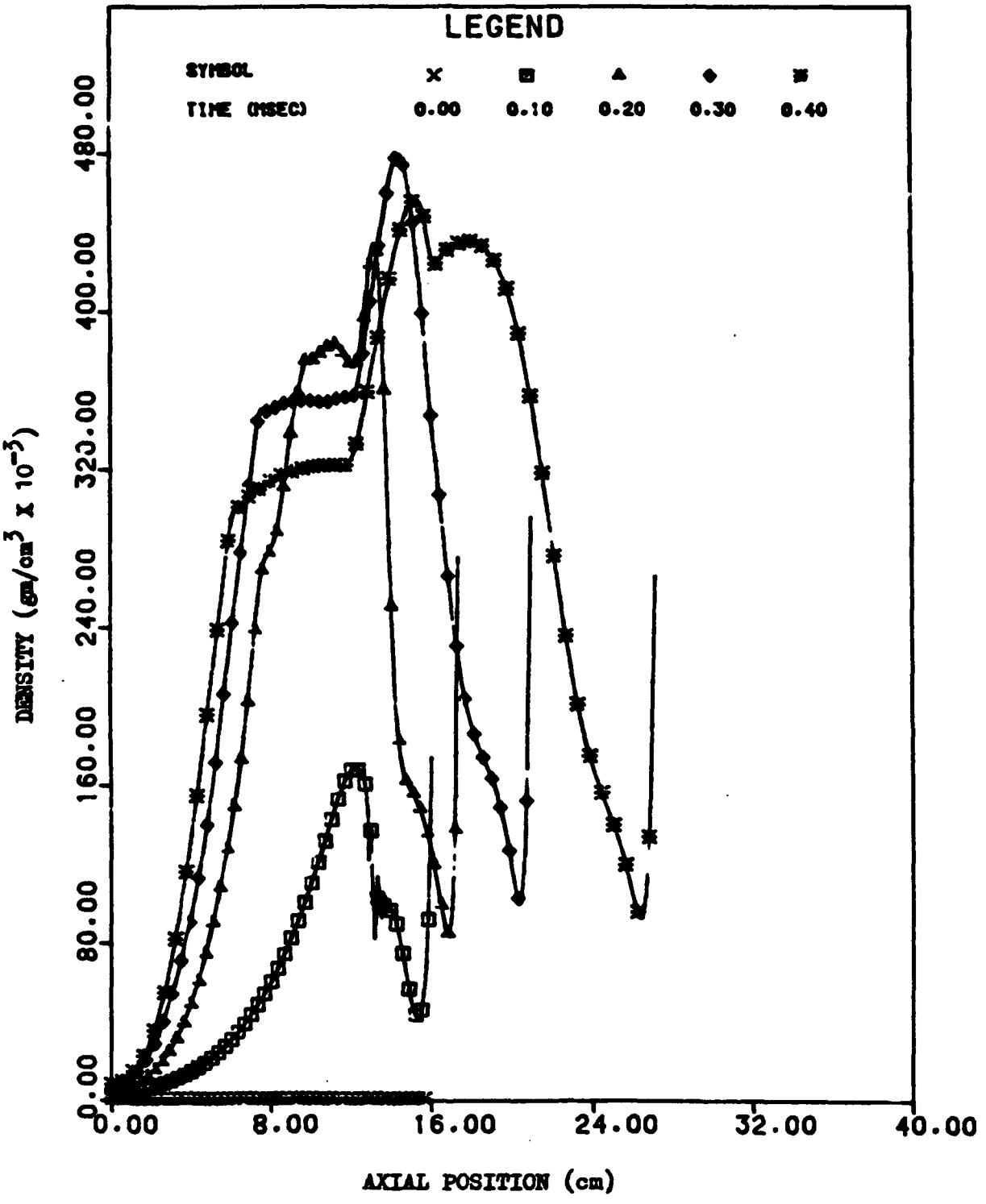

Figure 3.6 Distributions of density at various times for plasma mixing length 12.7 cm and wiping coefficient 0.8.

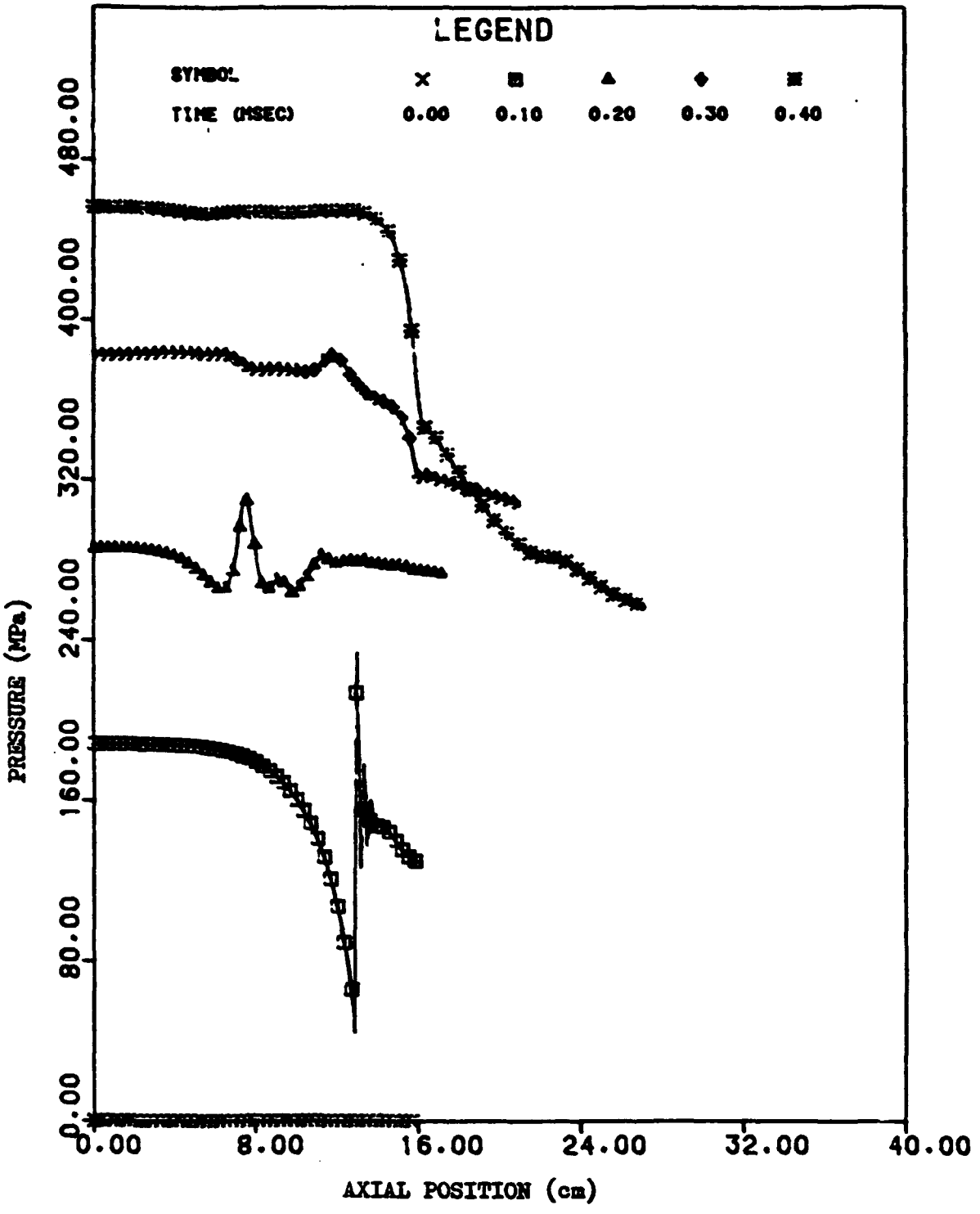

Figure 3.7 Distributions of pressure at various times for plasma mixing length 12.7 cm and wiping coefficient 0.8.

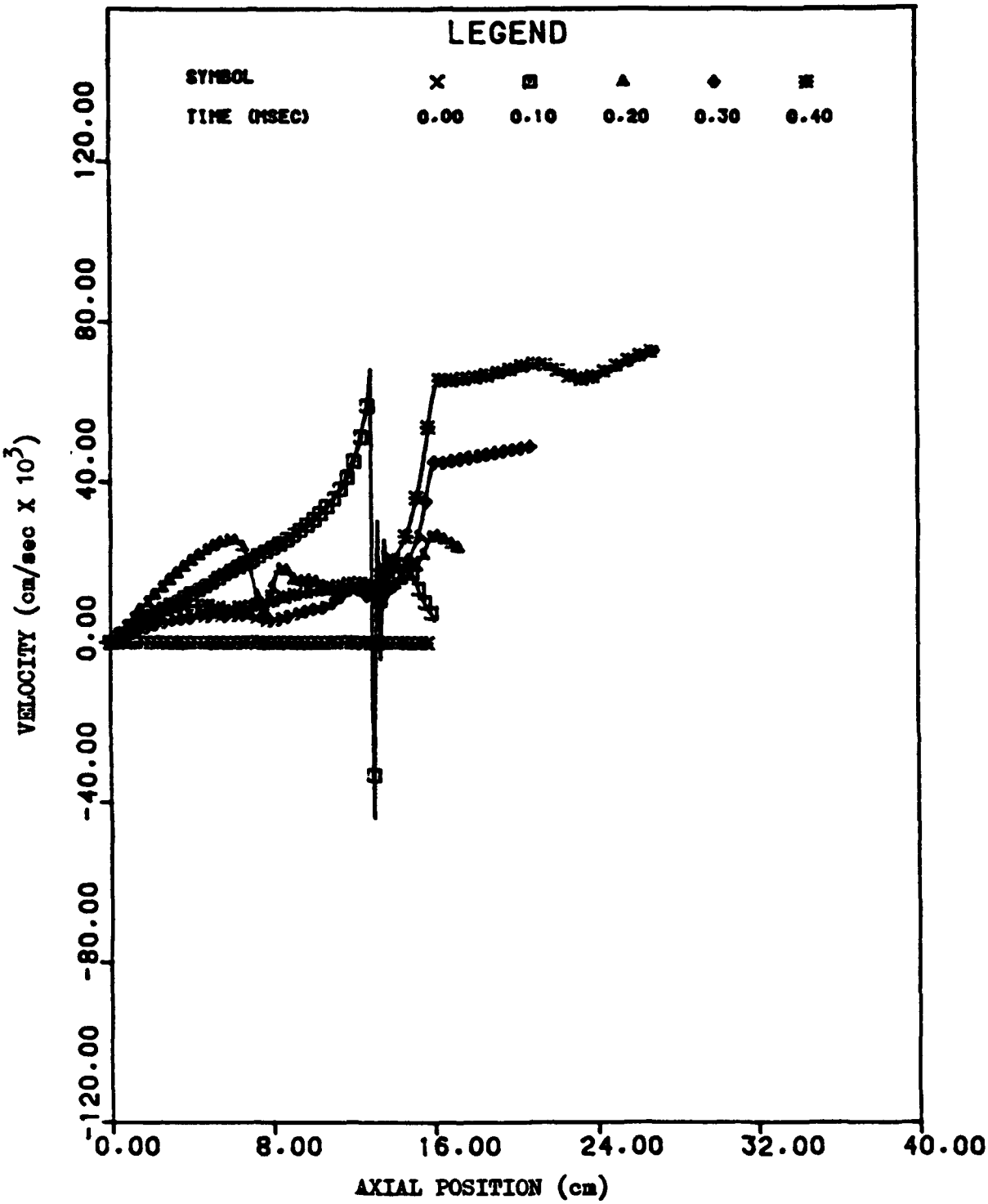

Figure 3.8 Distributions of velocity at various times for plasma mixing length 12.7 cm and wiping coefficient 0.8.

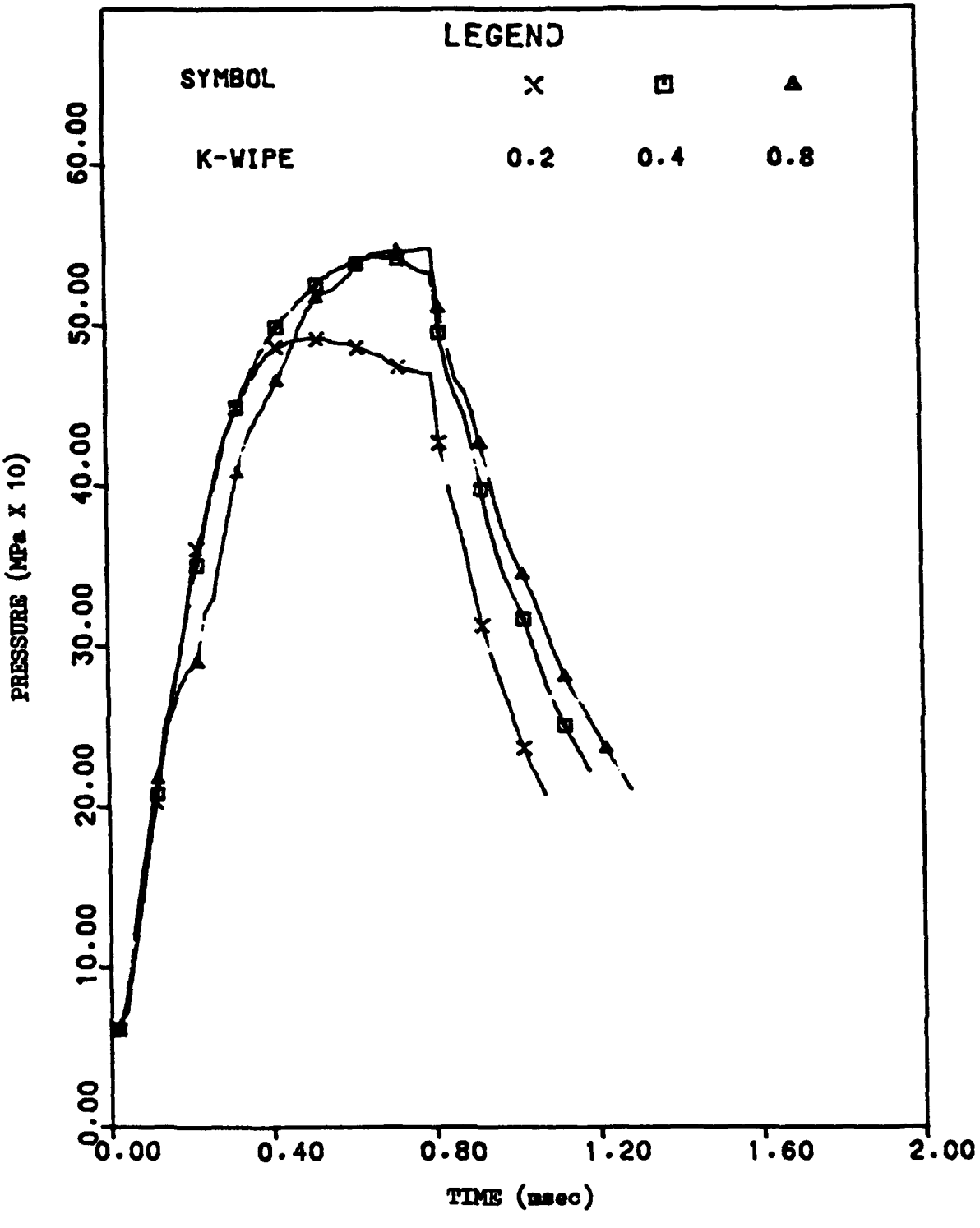

Figure 3.9 Histories of breech pressure for plasma mixing length 12.7 cm and various values of wiping coefficient.

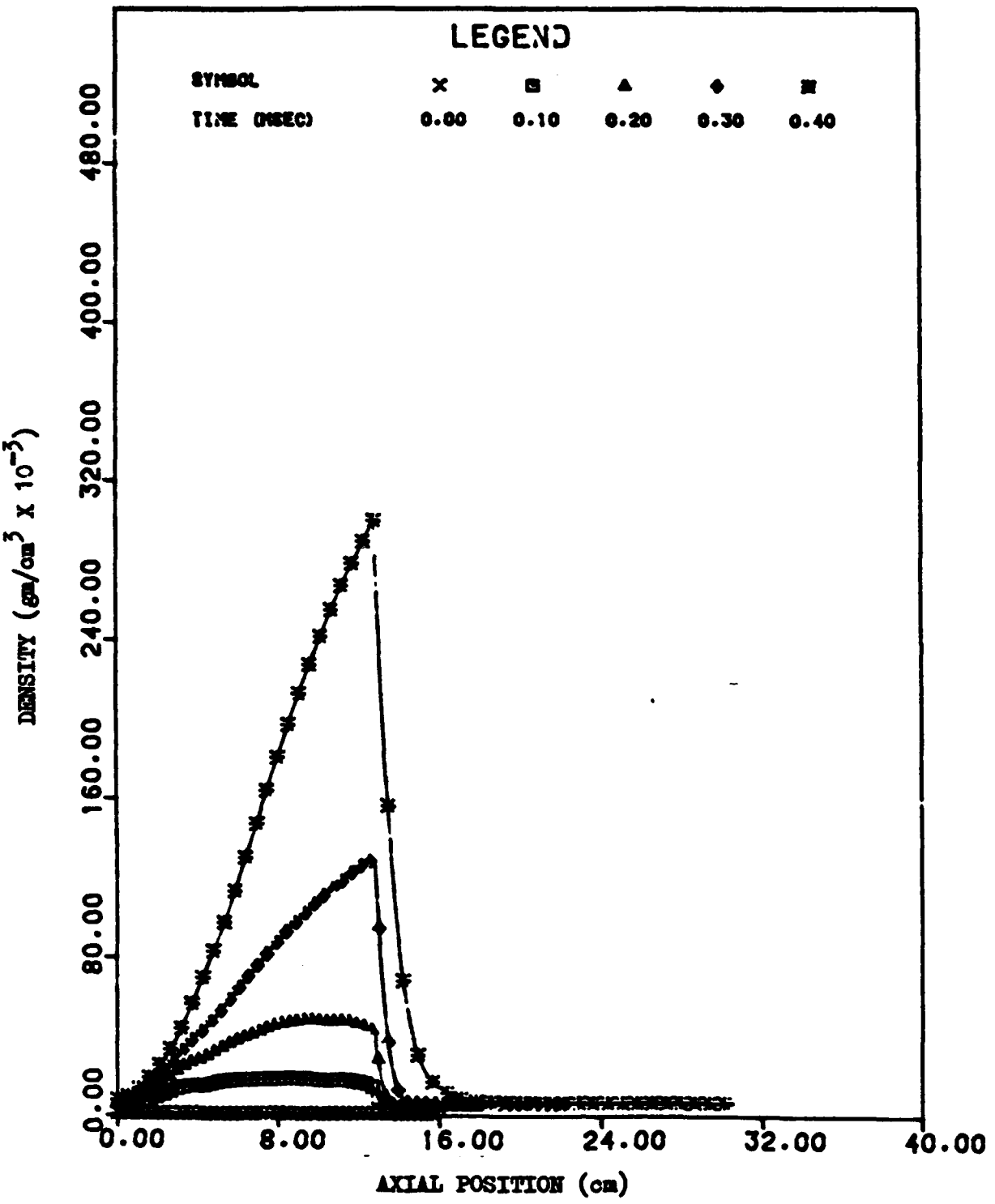

Figure 3.10 Distributions of density at various times for plasma mixing length extending to projectile base and wiping coefficient 0.8.

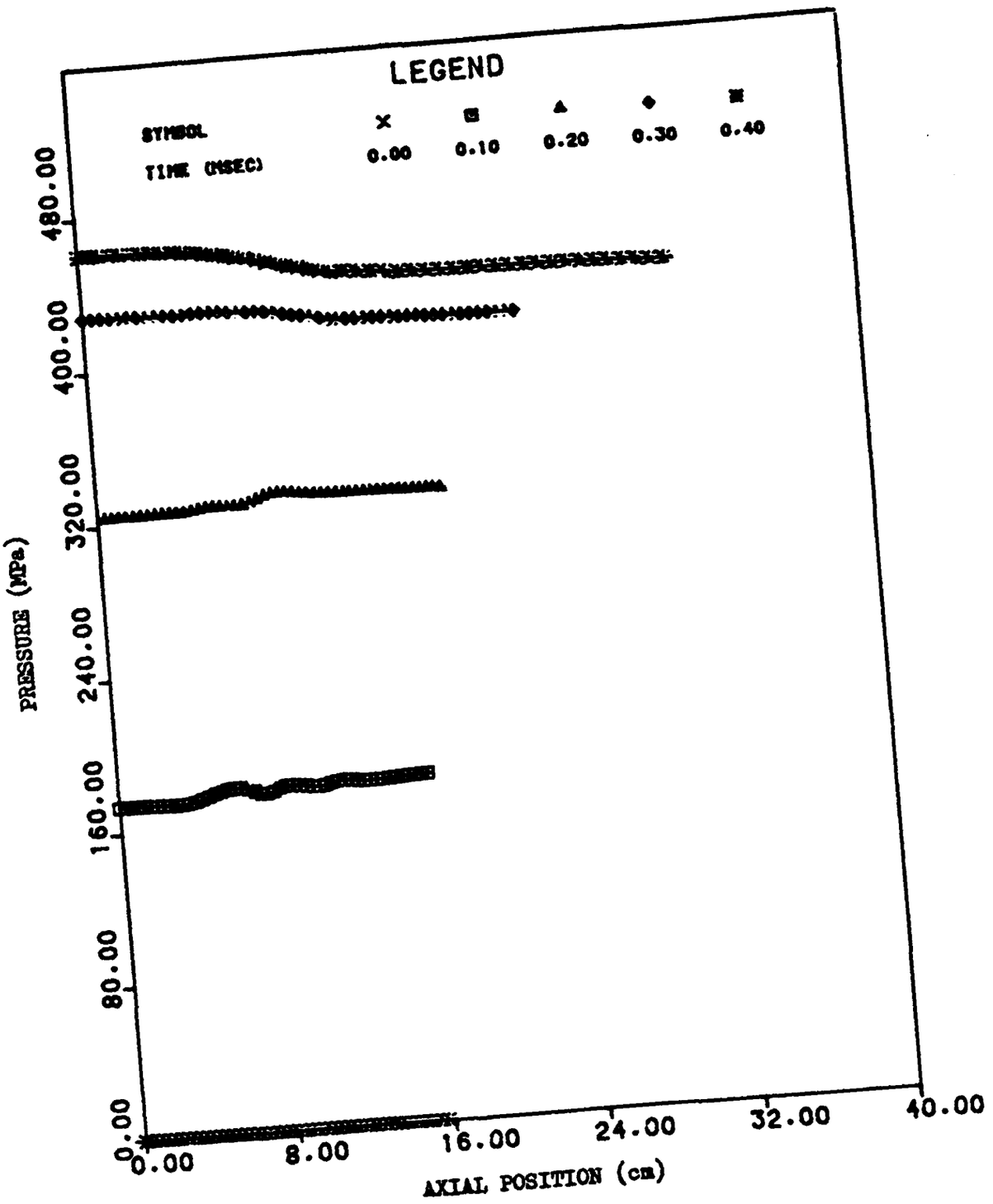

Figure 3.11 Distributions of pressure at various times for plasma mixing length extending to projectile base and wiping coefficient 0.8.

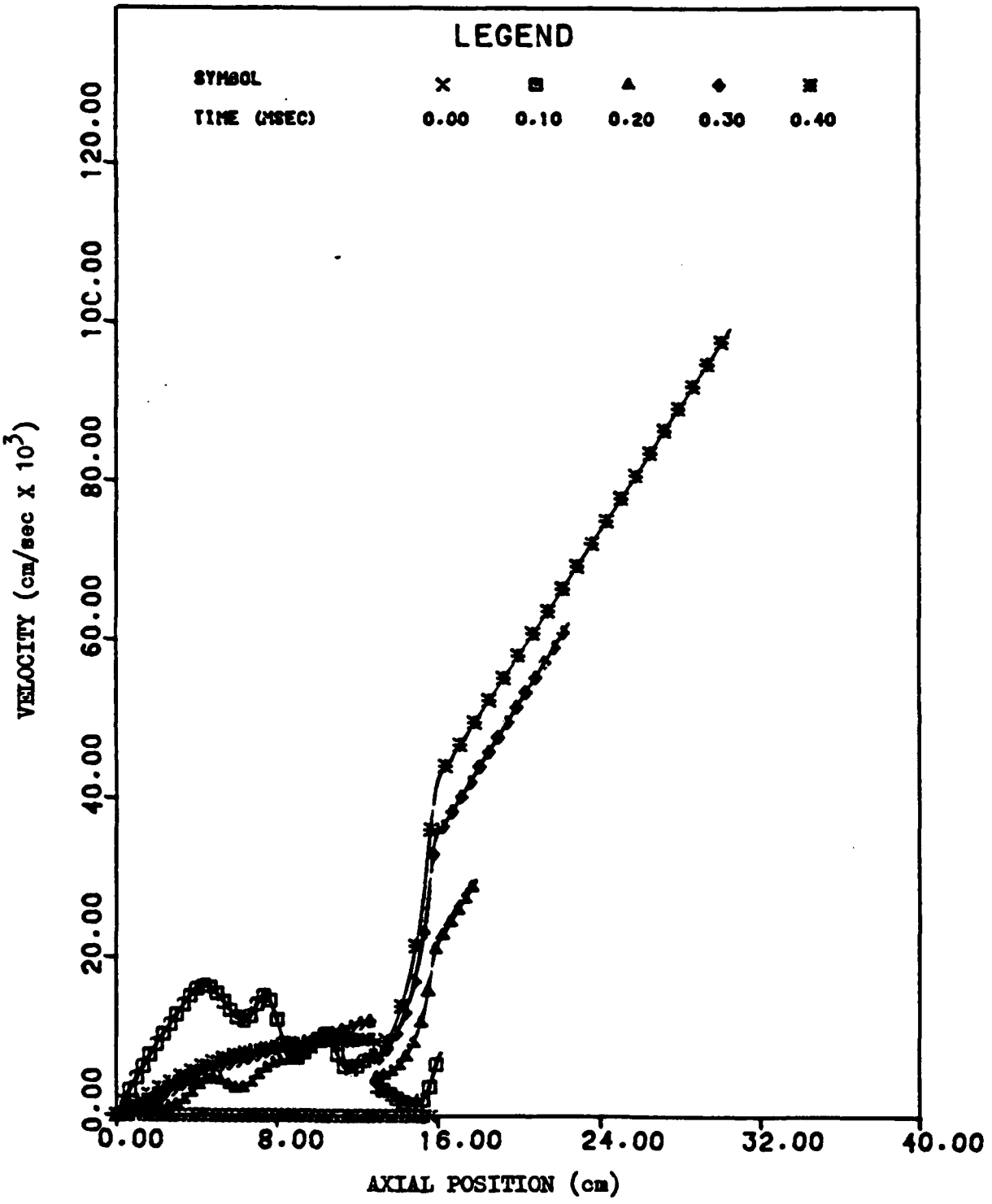

Figure 3.12 Distributions of velocity at various times for plasma mixing length extending to projectile base and wiping coefficient 0.8.

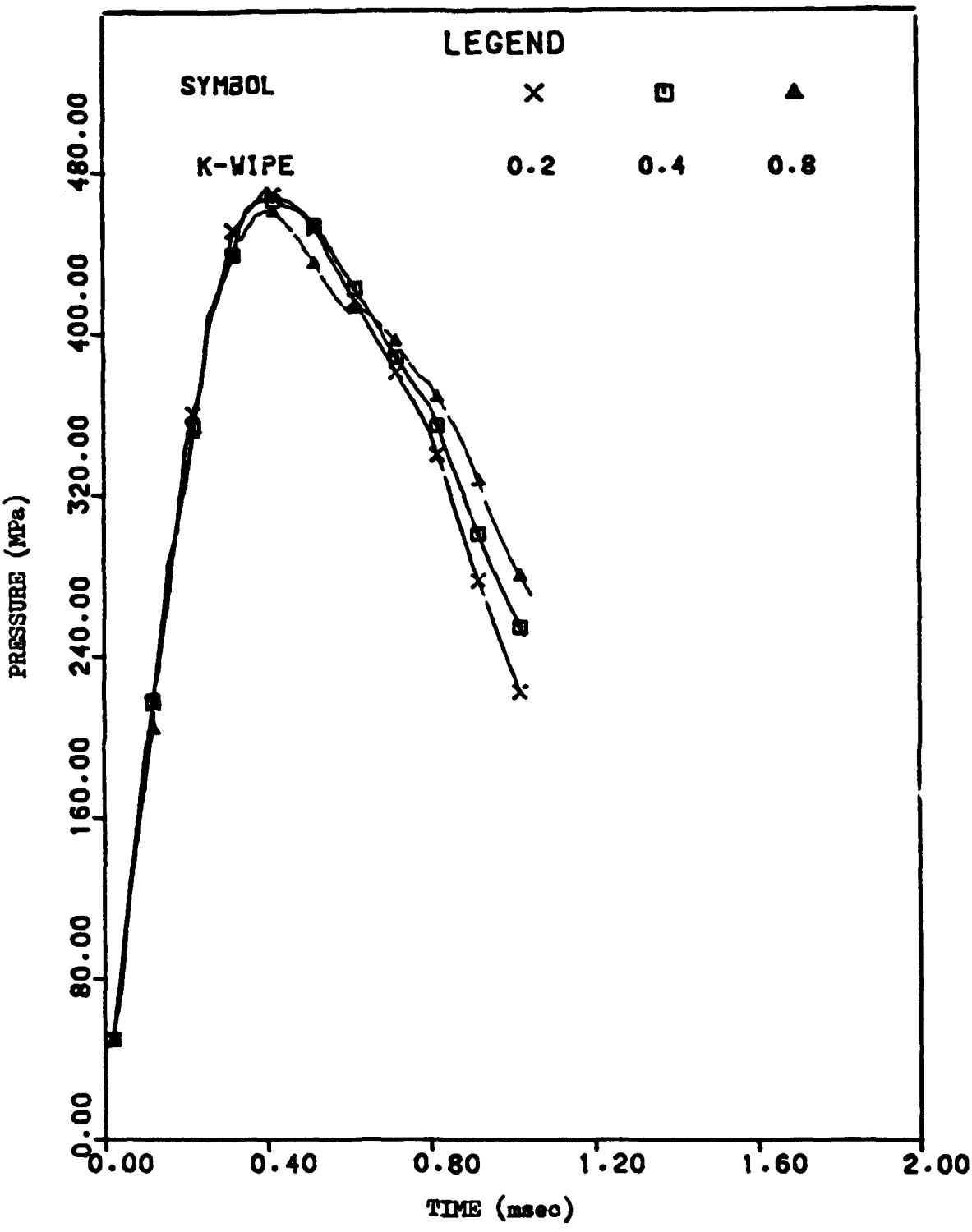

Figure 3.13 Histories of breech pressure for plasma mixing length extending to base of projectile and various values of wiping coefficient.

4.0 TWO-DIMENSIONAL MODEL

We now consider the formulation of a two-dimensional model of the ETG. Such a model would permit an assessment of the heat transfer to the tube as well as the overall ballistic response. Section 4.1 contains a brief summary of the approach that we consider to be most fruitful. Section 4.2 presents the principal governing equations, a discussion of the requirements for closure of the equations, and an appropriate solution technique. In the present formulation two-dimensional modeling is confined to the mixing chamber and the tube. The one-dimensional model of the capillary due to Powell [4] is used to describe the formation of the plasma. It is the mixing of the plasma with the working fluid which is an inherently two-dimensional process and is most naturally treated with a full resolution of radial as well as axial details of the flow. Moreover, an important feature of the model is the assessment of the heat transfer to the tube. This feature absolutely demands a fully two-dimensional treatment. Naturally, the solution of the equations requires an approach based on the method of finite differences.

4.1 Discussion of Formulation

The flow in the mixing chamber is very complex with as many as three distinct regions of highly structured flow each requiring detailed resolution. First, we must anticipate the formation of a shock near the plasma exit plane since the plasma is expected to be underexpanded at least part of the time. The attendant flow will be similar to that associated with muzzle blast and will therefore require a fairly large number of mesh points to permit adequate resolution by the finite difference solver. The second region of flow requiring careful resolution by the model is that defined by the penetration of the working fluid by the plasma and the entrainment of the working fluid by the hot central core flow. Eventually, the central cavity may penetrate completely the region occupied by the working fluid and a region of ullage may open behind the projectile. This is of importance since it allows the heated gases easier access to the tube wall, a problem of great practical concern. The third region requiring detailed resolution is the boundary layer near the tube wall.

These requirements for resolution of flow details in three regions — near the plasma exit plane, in the mixing layer between the core flow and the working fluid, and at the tube wall — motivate the principal modeling restriction, namely that the mixture be treated as locally homogeneous. The fluid in the mixing chamber and gun tube is viewed as a multicomponent, multiphase mixture in which all species and phases have the same velocity at each point and all gas-phase constituents have the same temperature. The response of the liquid-phase is assumed to be isothermal. Of course, the composition of the fluid is expected to vary from point to point and with respect to time. These variations result from convection of the flow, turbulent mixing and heat transfer and the dependence of composition on temperature and pressure. However, the assumption of local homogeneity implies that there is no explicit internal boundary between the unvaporized working fluid and the central region of hot gases. It also means that there is no requirement to formulate constitutive laws governing the formation of droplets and their time dependent diameters. Such data are hard to come by and the result of including analysis to treat the droplet phase moving

independently from the gases would be to increase substantially the complexity of the code (i.e. higher development costs and longer run times) without the likelihood of adding materially to the predictive capacity. It may be also pointed out that supercritical conditions may arise in which case models of the liquid phase as an aggregate of droplets are on very tenuous ground. A useful discussion has been provided by Edelman [18] in which he shows the relevance of a turbulent mixing law to the analysis of the cavity growth in the bulk loaded liquid propellant gun. The algebraic law of surface regression based on the slip velocity of the liquid and gas phases is shown to be related logically to a mixing law for a turbulent jet with strong density gradients. Finally, we note that the local equilibrium approach has been applied quite successfully to many types of turbulent jet flows including that of air penetrating water [20,21].

The model includes not only diffusion due to turbulence but also a contribution due to radiative transport subject to the simplifying assumption that the mixture is optically thick. The assumption of optical thickness implies that the radiative transport, which is expected to be significant, can be expressed as a diffusive mechanism [22,23]. A similar approach has been reported in studies of propulsion systems based on laser-heated plasmas [24] and by Powell in his analysis of the plasma capillary.

A two-equation model of turbulence which incorporates differential equations for the turbulent kinetic energy and dissipation is thought to be the most logical choice in connection with the two-dimensional model. The two-equation model has been used extensively in related studies of both turbulent jets and wall boundary layers and reasonably good agreement with a wide range of conditions has been reported using a fixed set of empirical coefficients [20]. A one-equation model, while not as general, may have some relevance here. Results have been reported by Garloff and Heiser in connection with the wall boundary layer in a gun tube [25]. Algebraic models may be useful for initial testing. However, they are not believed to reflect accurately the conditions in a gun, even for the simple case of one-phase flow from an initial all-burnt condition in which only the wall boundary layer is present. They would also necessitate the formulation of different laws for the mixing region and the wall boundary layer.

20. Kuo, K.K. "Principles of Combustion" Wiley/Interscience *1986*

21. Tross, S.R. "Characteristics of a Submerged Two-Phase Free Jet" M.S. Thesis, The Pennsylvania State University *1974*

22. Oran, E.S. and Boris, J.P. "Numerical Simulation of Reactive Flow" Elsevier *1987*

23. Zel'dovitch, Ya.B. and Raiser, Yu.P. "Physics of Shock Waves and High Temperature Hydrodynamic Phenomena" Academic Press *1966*

24. Glumb, R.J. and Krier, H. "Two-Dimensional Model of Laser-Sustained Plasmas in Axisymmetric Flowfields" AIAAJ. vol.24 n.8 pp.1331-1336 *1986*

25. Garloff, J. and Heiser, R. "A Contribution to the Turbulence of Interior Ballistic Flows" Proceedings of the AIAA/ASME/SAE/ASEE 25th Joint Propulsion Conference *1989*

4.2 Governing Equations

We adopt the system of equations presented by Garloff and Heiser to describe the motion of a compressible, viscous, heat conducting and turbulent gas [26]. We neglect the pressure-velocity correlations. However, we include a governing equation for the mass fraction of the fluid which is in the liquid-phase. It is understood that all variables are averaged quantities for the mixture of working fluid, its products of decomposition and the plasma unless otherwise noted.

Continuity Equation

$$\frac{D\rho}{Dt} = - \rho \nabla \cdot u \quad , \tag{4.1}$$

where D/Dt is the convective derivative.

Momentum Equation

$$\rho \frac{Du}{Dt} = - \nabla p + \nabla \cdot (\Pi + \Pi_t) \quad . \tag{4.2}$$

Energy Equation

$$\rho \frac{De}{Dt} = - p \nabla \cdot u + \phi - \nabla \cdot (Q + Q_t) + \rho \varepsilon \quad . \tag{4.3}$$

Turbulent Kinetic Energy Equation

$$\rho \frac{Dk}{Dt} = \nabla \cdot (\mu_k \nabla k) + \phi_t - \rho \varepsilon - 2\mu [\nabla (k^{1/2})]^2 \quad . \tag{4.4}$$

Dissipation Rate Equation

$$\rho \frac{D\varepsilon}{Dt} = c_1 f_1 \phi_t \frac{\varepsilon}{k} - c_2 f_2 \frac{\varepsilon}{k} (\varepsilon - 2\nu [\nabla (k^{1/2})]^2) \rho + \nabla \cdot (\mu_\varepsilon \nabla \varepsilon) \quad . \tag{4.5}$$

---

26. *Garloff, J. and Heiser, R. "Turbulence Modeling of One-Phase Interior Ballistics Flows by a Two-Equation Model" Ernst-Mach Institut Report 1/88* *1988*

Continuity of Liquid Phase

$$\rho \frac{DY}{Dt} = - \dot{r} - \nabla\cdot(\rho Y V) \quad . \tag{4.6}$$

In the foregoing we have used ρ, u, p, e, k and ε as density, velocity vector, pressure, internal energy, turbulent kinetic energy and dissipation rate respectively. We have $\mathbb{T}$ and $\mathbb{T}_t$ as the molecular and turbulent viscous stress tensors, Q and Q_t as the molecular and turbulent heat fluxes. We understand Q to embed the radiative heat transport approximated as a diffusive term. We refer to Garloff and Heiser [26] for further details of the turbulence terms. We have Y as the mass fraction in the liquid-phase and V is the diffusion velocity of the liquid. We neglect the molecular contribution to this term and resolve it as a purely turbulent phenomenon. The term $\dot{r}$ in Equation 4.6 represents the rate of decomposition of the working fluid. We take the gas-phase to be governed by a covolume equation of state as in Chapter 2.0 with the properties varying according to the energy density. The liquid-phase is assumed to be isothermal and governed by the equation of state presented in Chapter 2.0.

At present a law to describe $\dot{r}$, the rate of decomposition, has not been defined. Assuming that the rate of decomposition is a thermally dominated process, it seems logical to propose that $\dot{r}$ is proportional to the difference between the temperatures of the phases. Possibly, a dependence on the turbulent velocity fluctuation could be included on the assumption that the phases are only in velocity equilibrium in the mean. Further attention to this problem will be required in future work.

An appropriate solution technique for the governing equations is thought to be a linearized alternating direction implicit scheme of the type pioneered by Beam and Warming [27] and by Briley and McDonald [28]. Successful applications of this technique to the solution of single-phase flows in gun tubes have been reported by several authors [29,30,31].

---

27. Beam, R.M. and Warming, R.F. "An Implicit Factored Scheme for the Compressible Navier-Stokes Equations" AIAA J. vol.16 n.4 1978

28. Briley, W.R. and McDonald, H. "Solution of the Multi-Dimensional Compressible Navier-Stokes Equations by a Generalized Implicit Method" J. Comp. Phys. 24 pp.372-397 1977

29. Schmitt, J.A. "A Numerical Algorithm for the Multi-dimensional, Multiphase, Viscous Equations of Interior Ballistics" Proc. 2nd Army Conference on Applied Mathematics and Computing, RPI 1984

30. Gibeling, H.J. and McDonald, H. "An Implicit Numerical Analysis for Two-Dimensional Turbulent Interior Ballistic Flows" BRL Contract Report ARBRL-CR-00523 1984

31. Keller, G.E., Horst, A.W. and Gough, P.S. "The Effects of Viscosity on Interior Ballistics" Proc. 26th Jannaf Combustion Meeting 1989

5.0 CONCLUSIONS

[1] A lumped parameter model of the ETG has been developed. The code (LUMPET) requires a characterization of the plasma flux and the thermochemical properties of the mixture of plasma and working fluid. The code can be used to predict the pressure history and projectile motion; to determine the plasma flux required to achieve a constant pressure; to deduce the rate of decomposition of the working fluid given the pressure history in the mixing chamber.

[2] Calculations based on a nominal data base for the lumped parameter code indicate only a weak dependence of the interior ballistics on the rate of decomposition of the working fluid. Although the presence of ullage is expected to reduce the ballistic sensitivity to the rate of decomposition, the variation of thermochemical properties with energy density is found to exert a dominant influence.

[3] Calculations based on a nominal data base for the lumped parameter code run in the inverse mode show that very precise data will be required to achieve an accurate determination of the rate of decomposition if water is the working fluid. Even with the values of pressure given to an accuracy of 1%, errors of the order of 20% can arise in the calculated fraction of working fluid that has been decomposed.

[4] A code (PMAP) has been written to determine the pressure in a chamber as a function of the fraction of the working fluid that has decomposed, given values of the ratio of total energy to total mass of working fluid and the ratio of total mass of working fluid to total volume.

[5] The application of PMAP to the thermochemical properties of water determined from the BLAKE Code shows a complex dependence of pressure on the fraction of working fluid which has decomposed. The pressure is non-monotonic under some conditions; one or more maxima may be observed. Accordingly, the inverse analysis in which the rate of decomposition is to be determined from the pressure history may encounter multiple roots.

[6] An existing one-dimensional, two-phase flow model of solid propellant interior ballistics (XKTC) has been modified to permit simulations of a class of ETG configurations in which a central ullage port is present. As with the lumped parameter models, it is assumed that the plasma flux is provided as input data.

[7] The application of XKTC to a nominal data base revealed no ballistic sensitivity to the rate of decomposition of the working fluid in excess of that determined using the lumped parameter model. This was true in spite of the fact that the continuum solutions contained an extraordinary level of structure. However, the non-uniformity was such as to suggest that continuum modeling will be necessary to provide reliable estimates of the pressure gradient.

[8] A two-dimensional model of the ETG has been formulated.

INTENTIONALLY LEFT BLANK.

REFERENCES

1. Juhasz. A., Jamison, K., White, Y. and Wren, G. "Introduction to Electrothermal Gun Propulsion" Proceedings of the 25th Jannaf Combustion Meeting 1988

2. Oberle, W. "Electrothermal Guns -- A Theoretical Investigation of Factors for Optimal Performance" Ballistic Research Laboratory Report BRL-TR-2999 1989

3. Anderson, R.D. and Fickie, K.D. "IBHVG2 - A User's Guide" BRL Technical Report BRL-TR-2829 Ballistic Research Laboratory, Aberdeen Proving Ground, MD 1987

4. Powell, J.D. and Zielinski, A.E. "Analysis of the Plasma Discharge in an Electrothermal Gun" Proceedings of the 26th Jannaf Combustion Meeting 1989

5. Tidman, D.A., Thio, Y.C., Goldstein, S.A. and Spicer, D.S. "High Velocity Electrothermal Mass Launchers" GT Devices Technical Note Number GTD 86-7 1986

6. Loeb, A. and Kaplan, Z. "A Theoretical Model for the Physical Processes in the Confined High Pressure Discharges of Electrothermal Launchers" IEEE Trans. Magn. MAG-25, 342 1989

7. Chryssomallis, G.S., Marinos, C.D., Ricci, R.S. and Cook, D.C. "Combustion Augmented Plasma Gun" in Technology Efforts in ET Gun Propulsion, edited by A. A. *Juhasz* vol. 1 1988

8. Gough, P.S. "The XNOVAKTC Code" PGA-TR-86-1 Final Report, Task Order II, Contract DAAK11-85-D-0002 1986

9. Courant, R. and Friedrichs, K.O. "Supersonic Flow and Shock Waves" Interscience, New York 1948

10. Corner, J. "Theory of the Interior Ballistics of Guns" Wiley, New York 1950

11. Robbins, F.W., Anderson, R.D. and Gough, P.S. "Continued Studies of the Development of a Modified Pressure Gradient Equation for Lumped-Parameter Interior Ballistic Codes" Ballistic Research Laboratory Technical Report Undated

12. Vinti, J.P. "The Equations of Interior Ballistics" Ballistic Research Laboratory Report 307 1942

13. Morrison, W.F. and Wren, G.P. "A Lumped Parameter Description of Liquid Injection in a Regenerative Liquid Propellant Gun" Proceedings of the 23rd Jannaf Combustion Meeting 1988

14. Ralston, A. "A First Course in Numerical Analysis" McGraw-Hill 1965

15. Gough, P.S. "Influence on Interior Ballistics of Electrothermal Gun of Rate of Mixing of Plasma with Working Fluid" Proceedings of the 26th Jannaf Combustion Meeting 1989

16. Shuman, F.G. "Numerical Methods in Weather Predictions: II Smoothing and Filtering" Monthly Weather Review November 1957

17. Hoel, P.G. "Introduction to Mathematical Statistics" John Wiley and Sons 1966

18. Edelman, R.B. "The Interior Ballistics of Liquid Propellant Guns" RDA-TR-4408-010 1974

19. May I.W. and Einstein , S.I. "Prediction of Gun Muzzle Flash" Proceedings of the 14th Jannaf Combustion Meeting 1977

20. Kuo, K.K. "Principles of Combustion" Wiley/Interscience 1986

21. Tross, S.R. "Characteristics of a Submerged Two-Phase Free Jet" M.S. Thesis, The Pennsylvania State University 1974

22. Oran, E.S. and Boris, J.P. "Numerical Simulation of Reactive Flow" Elsevier 1987

23. Zel'dovitch, Ya.B. and Raiser, Yu.P. "Physics of Shock Waves and High Temperature Hydrodynamic Phenomena" Academic Press 1966

24. Glumb, R.J. and Krier, H. "Two-Dimensional Model of Laser-Sustained Plasmas in Axisymmetric Flowfields" AIAA J. vol.24 n.8 pp.1331-1336 1986

25. Garloff, J. and Heiser, R. "A Contribution to the Turbulence of Interior Ballistic Flows" Proceedings of the AIAA/ASME/SAE/ASEE 25th Joint Propulsion Conference 1989

26. Garloff, J. and Heiser, R. "Turbulence Modeling of One-Phase Interior Ballistics Flows by a Two-Equation Model" Ernst-Mach Institut Report 1/88 1988

27. Beam, R.M. and Warming, R.F. "An Implicit Factored Scheme for the Compressible Navier-Stokes Equations" AIAA J. vol.16 n.4 1978

28. Briley, W.R. and McDonald, H. "Solution of the Multi-Dimensional Compressible Navier-Stokes Equations by a Generalized Implicit Method" J. Comp. Phys. 24 pp.372-397 1977

29. Schmitt, J.A. "A Numerical Algorithm for the Multi-dimensional, Multiphase, Viscous Equations of Interior Ballistics" Proc. 2nd Army Conference on Applied Mathematics and Computing, RPI 1984

30. Gibeling, H.J. and McDonald, H. "An Implicit Numerical Analysis for Two-Dimensional Turbulent Interior Ballistic Flows" BRL Contract Report ARBRL-CR-00523 1984

31. Keller, G.E., Horst, A.W. and Gough, P.S. "The Effects of Viscosity on Interior Ballistics" Proc. 26th Jannaf Combustion Meeting 1989

INTENTIONALLY LEFT BLANK.

NOMENCLATURE

A	Pre-exponent in Arrhenius reaction rate law
$A(z)$	Cross-sectional area at distance z from rear of mixing chamber
A_b	Bore area
b	Covolume
C	Total mass of working fluid
c_p, c_v	Heat capacities at constant pressure and volume
c_1, c_2	Turbulence parameters
d_i	Diameter of cavity in working fluid
d_j	Diameter of plasma jet at capillary exit plane
E_A	Activation energy
$E_i(t)$	Total plasma energy delivered to mixing chamber at time t
E_{kin}	Kinetic energy of working fluid and mixture of products of decomposition and plasma
E_o	Internal energy of initial ambient in mixing chamber
e	Internal energy
e_{eff}	Effective internal energy
e_p	Energy of compression of working fluid
f_1, f_2	Turbulence parameters
g_o	Constant to reconcile units of measurement
H	Heat of formation
J_1, J_2 J_3, J_4	Integrals associated with chambrage analysis of pressure gradient
k	Turbulent kinetic energy
k_w	Dimensionaless coefficient to control decomposition of working fluid according to Helmholtz mechanism in XKTC Code
k_j	Dimensionless coefficient to contol rate of mixing of plasma jet with ambient in XKTC Code
K_p	Bulk modulus of working fluid

l_j	Mixing length of plasma jet
M	Mass of projectile
M_w	Molecular weight
$m_i(t)$	Total mass of plasma delivered to mixing chamber at time t
m_o	Mass of initial ambient in mixing chamber
p	Pressure
Q	Molecular heat flux vector
Q_t	Turbulent heat flux vector
Q_w	Heat loss to chamber and tube
R_u	Universal gas constant
$\dot{r}$	Rate of decomposition of working fluid
$\dot{r}_j$	Rate of mixing of plasma jet
T	Temperature
t	Time
u	Velocity of gas
u_p	Velocity of working fluid
u_j	Velocity of plasma jet at capillary exit plane
V	In Chapter 2.0, volume of gas In Chapter 4.0, diffusion velocity of working fluid
V_o	Volume of mixing chamber
V(z)	Volume contained between rear face of mixing chamber and position z
v_p	Projectile velocity
W_f	Work done against resistive forces acting on projectile
x_p	Displacement of projectile
Y	In Chapter 2.0, mass fraction of intermediate species of decomposition In Chapter 4.0, mass fraction of working fluid

Greek Symbols

$\alpha(t)$	Fraction of working fluid that has decomposed at time t
β	Lagrange coupling coefficient
γ	Ratio of specific heats
ε	Dissipation rate of turbulent kinetic energy
μ	Viscosity
μ_k	Effective viscosity in k-equation
μ_ε	Effective viscosity in ε-equation
ν	In Chapter 2.0, order of reaction In Chapter 4.0, kinematic viscosity
$\mathbb{\Pi}$	Molecular viscous stress tensor
$\mathbb{\Pi}_t$	Turbulent viscous stress tensor
ρ	Density of gas
ρ_j	Density of plasma jet at capillary exit plane
ρ_p	Density of working fluid
ϕ	In Chapter 2.0, parameter set equal to zero or one depending on representation of thermochemistry of products of decomposition of working fluid In Chapter 4.0, molecular mechanical dissipation function
ϕ_t	Turbulent mechanical dissipation function

INTENTIONALLY LEFT BLANK.

APPENDIX A

LUMPET: Code Listing and Description of Input

INTENTIONALLY LEFT BLANK.

```
C*MFST $STORAGE:2
C     PROGRAM TO PERFORM LUMPED PARAMETER SIMULATION OF ELECTROTHERMAL
C     GUN INTERIOR BALLISTICS.
C
C     VERSION 1.0 (DECEMBER 1989) WRITTEN FOR F77 COMPILER ON CRAY.
C
C     ************************************************************************
C     CODE MAY BE CONVERTED TO VERSION COMPATIBLE WITH MICROSOFT F77
C     COMPILER BY MEANS OF GLOBAL TEXT EDITING COMMAND OF THE FORM:
C
C     REPLACE 'C*MSFT ' WITH ' '.
C
C     ************************************************************************
C     MICROSOFT F77 VERSION PROMPTS AT TERMINAL FOR INPUT DATA FILE NAME
C     (FILNAM) AND OUTPUT FILE NAME (OUTFIL).  THE OUTPUT WILL BE
C     DIRECTED TO THE PRINTER IF OUTFIL IS ENTERED AS PRN.
C
C     ************************************************************************
C     DESCRIPTION OF INPUT DATA (ASSUMED TO BE LOCATED IN FILE LABELED
C     FILNAM):
C
C     FILE 1.0: "TITLE"    (A80)  ONE CARD.
C     TITLE     - PROBLEM TITLE. UP TO 80 CHARACTERS.
C
C     FILE 2.0: "INTEGRATION PARAMETERS" (6F10.0) ONE CARD.
C     DTNOM     - INTEGRATION TIME STEP (MSEC).
C     PTOL      - CONVERGENCE TOLERANCE IN SOLUTION FOR PRESSURE (-).
C                 DEFAULT IS 0.0001.  VALUES SMALLER THAN THIS MAY
C                 NOT BE ADVISABLE ON A PC UNLESS THE PROGRAM IS
C                 CONVERTED TO DOUBLE PRECISION.  FAILURE TO CONVERGE
C                 TO WITHIN THE VALUE OF PTOL RESULTS IN TERMINATION OF
C                 THE CALCULATION.
C     PTOLC     - CONVERGENCE TOLERANCE IN DETERMINATION OF CONSTANT
C                 PRESSURE SOLUTION (-).  DEFAULT IS 0.0001.  ONLY
C                 REQUIRED IF A CONSTANT PRESSURE SOLUTION IS BEING
C                 SOUGHT.  FAILURE TO CONVERGE TO WITHIN THE VALUE OF
C                 PTOLC RESULTS IN TERMINATION OF THE CALCULATION.
C     TTOL      - CONVERGENCE TOLERANCE IN SOLUTION FOR TEMPERATURE (-).
C                 DEFAULT IS 0.0001.  ONLY REQUIRED IF FINITE RATE
C                 CHEMISTRY IS CONSIDERED.  FAILURE TO CONVERGE
C                 TO WITHIN THE VALUE OF TTOL RESULTS IN TERMINATION
C                 OF THE CALCULATION.
C     ATOL1     - FIRST CONVERGENCE TOLERANCE IN SOLUTION FOR FRACTION
C                 OF WORKING FLUID WHICH HAS DECOMPOSED.  DEFAULT IS
C                 0.0001.  ONLY REQUIRED IF MATCHING TO OBSERVED
C                 BALLISTICS IS USED AS A MEANS OF DETERMINING THE
C                 RATE OF DECOMPOSITION.  FAILURE TO CONVERGE
C                 TO WITHIN THE VALUE OF ATOL1 RESULTS IN CONTINUATION
C                 OF THE CALCULATION AND PRINTING OF AN ERROR MESSAGE.
```

```
C     ATOL2      - SECOND CONVERGENCE TOLERANCE IN SOLUTION FOR FRACTION
C                  OF WORKING FLUID WHICH HAS DECOMPOSED.  DEFAULT IS
C                  0.01.  ONLY REQUIRED IF MATCHING TO OBSERVED
C                  BALLISTICS  IS USED AS A MEANS OF DETERMINING THE RATE
C                  OF DECOMPOSITION.  FAILURE TO CONVERGE TO WITHIN THE
C                  VALUE OF ATOL2 RESULTS IN TERMINATION OF THE
C                  CALCULATION.
C
C     FILE 3.0: "PRINT CYCLE COUNTER"      (I5) ONE CARD.
C     NPRT       - NUMBER OF STEPS BETWEEN SUCCESSIVE TABULATIONS OF
C                  SOLUTION.
C
C     FILE 4.0: "GENERAL DATA"      (8F10.0)     ONE CARD.
C     PRM        - PROJECTILE MASS (G).
C     PRTRV      - PROJECTILE TRAVEL (CM).
C     DB         - BORE DIAMETER (CM).
C     VO         - VOLUME OF MIXING CHAMBER (CC).
C     TEMPO      - INITIAL TEMPERATURE OF GAS IN MIXING CHAMBER (K).
C     PO         - INITIAL PRESSURE OF GAS IN MIXING CHAMBER (MPA).
C     PBSK       - DESIRED VALUE OF BREECH PRESSURE FOR CONSTANT
C                  PRESSURE BALLISTICS (MPA).  IF PBSK IS ENTERED
C                  AS ZERO, A CONSTANT PRESSURE SOLUTION IS NOT IMPOSED.
C                  THE PRESSURE FOLLOWS FROM THE RATE OF DEPOSITION OF
C                  PLASMA ENERGY SPECIFIED IN FILE 10.0.  IF PBSK IS
C                  ENTERED AS NON-ZERO, THE RATE OF PLASMA ADDITION TO
C                  ACHIEVE THE DESIRED CONSTANT PRESSURE IS DETERMINED
C                  AS PART OF THE SOLUTION, SUBJECT TO THE CONSTRAINT
C                  THAT THE TOTAL PLASMA ENERGY BE LIMITED TO THE VALUE
C                  TOTPE DEFINED IN FILE 9.0.  IT IS ALSO ASSUMED IN THIS
C                  CASE THAT THE RATE OF DECOMPOSITION OF THE WORKING
C                  FLUID IS PROPORTIONAL TO THE RATE OF ADDITION OF
C                  PLASMA ENERGY IN ACCORDANCE WITH THE VALUE OF RATE.
C     RATE       - FRACTIONAL RATE OF DECOMPOSITION OF WORKING FLUID
C                  DIVIDED BY FRACTIONAL RATE OF DEPOSITION OF PLASMA
C                  ENERGY (-).  IF RATE IS ENTERED AS ZERO, THE RATE OF
C                  DECOMPOSITION OF THE WORKING FLUID IS ASSUMED TO BE
C                  DEFINED BY THE DATA OF TABLE 12.0.  IF RATE IS NOT
C                  ENTERED AS ZERO, THE RATE OF DECOMPOSITION IS ASSUMED
C                  TO BE PROPORTIONAL TO THE FRACTIONAL RATE OF
C                  DEPOSITION OF PLASMA ENERGY AS DEFINED IN FILE 10.0
C                  SUBJECT TO THE CONSTRAINT THAT THE TOTAL FRACTION OF
C                  THE WORKING FLUID WHICH HAS DECOMPOSED AT ANY TIME
C                  BE LESS THAN OR EQUAL TO ONE.  A VALUE OF RATE = 1
C                  PRODUCES PROPORTIONAL DECOMPOSITION.  A VALUE > 1
C                  PRODUCES ACCELERATED DECOMPOSITION AND A VALUE < 1
C                  PRODUCES LAGGING DECOMPOSITION.
C                  HOWEVER, IF THE DATA OF FILE 16 ARE PROVIDED, AN
C                  INVERSE ANALYSIS IS PERFORMED IN WHICH THE RATE OF
C                  DECOMPOSITION IS DETERMINED TO MATCH THE OBSERVED
C                  PRESSURE HISTORY.  IN THIS CASE THE VALUE OF RATE
C                  IS IGNORED.
C
```

```
C     NOTES:       THE INITIAL CONDITION WILL ONLY YIELD TEMPO AND PO
C                  IF THE PLASMA IS SPECIFIED AS HAVING ZERO TRANSFER
C                  AT THE INITIAL TIME.  TEMPO AND PO MAY BE THOUGHT OF
C                  AS SPECIFYING THE AMBIENT CONDITION JUST BEFORE THE
C                  TRANSFER OF PLASMA BEGINS.
C
C     FILE 4.1: "NUMBER OF DATA TO DESCRIBE CHAMBER GEOMETRY"
C                        (2I5)          ONE CARD.
C     NSTA       - NUMBER OF PAIRS OF DATA IN FILE 4.2.  IF NSTA IS
C                  ZERO, FILE 4.2 IS NOT REQUIRED.
C                  NSTA ALSO CONTROLS THE MODEL OF THE PRESSURE GRADIENT.
C                  IF NSTA IS ZERO THE STANDARD LAGRANGE RELATIONS ARE
C                  USED TO RELATE THE BREECH, BASE AND SPACEMEAN
C                  PRESSURES AND TO DETERMINE THE KINETIC ENERGY OF
C                  THE MOVING FLUID.
C                  IF NSTA IS GREATER THAN OR EQUAL TO TWO, THE
C                  CHAMBRAGE RELATIONS AS DESCRIBED BY ROBBINS ET AL
C                  ARE USED.
C                  NSTA MUST NOT EXCEED TWENTY.
C     NSPLT      - NUMBER OF INCREMENTS FOR DETERMINATION OF CHAMBER
C                  INTEGRALS IN CHAMBRAGE ANALYSIS.  EACH INTERVAL
C                  (ZA(I-1),ZA(I)) IS SPLIT INTO NSPLT INCREMENTS.
C                  DEFAULT IS ONE.
C
C     FILE 4.21 "CHAMBER GEOMETRY"  (2F10.0)   NSTA CARDS.
C     N.B. THIS FILE IS REQUIRED IF AND ONLY IF NSTA > 1.
C     ZA(1)      - FIRST DISTANCE FROM REAR FACE OF CHAMBER (CM).
C     RA(1)      - CORRESPONDING RADIUS OF CHAMBER (CM).
C     ZA(2)      - SECOND DISTANCE.  STARTS A NEW CARD.
C                  .
C                  .
C     RA(NSTA)
C
C     NOTES:       THESE DATA ARE LINEARLY INTERPOLATED.
C
C     FILE 5.0: "RESISTANCE PARAMETERS"    (2I5)   ONE CARD.
C     NRES       - NUMBER OF PAIRS OF DATA TO CHARACTERIZE BORE
C                  RESISTANCE.  IF NRES IS ZERO, THE BORE RESISTANCE
C                  IS ASSUMED TO BE ZERO.  IF NRES IS GREATER THAN
C                  ZERO, FILE 6.0 IS REQUIRED.  NRES MAY NOT EXCEED
C                  20.
C     NSHK       - IF NSHK IS ZERO, THE RESISTANCE DUE TO THE AIR IN
C                  FRONT OF THE PROJECTILE IS NOT CONSIDERED.
C                  IF NSHK IS ONE, THE PRESSURE OF THE AIR IN FRONT
C                  OF THE PROJECTILE IS COMPUTED USING STEADY STATE
C                  SHOCKWAVE THEORY.  THE AIR PRESSURE IS ADDED TO
C                  THE BORE RESISTANCE PRESSURE.
C
```

```
C     FILE 6.0: " BORE RESISTANCE AS A FUNCTION OF PROJECTILE TRAVEL"
C                (2F10.0)  NRES CARDS.
C     N.B.  THIS FILE IS REQUIRED IF AND ONLY IF NRES > 0.
C     RESX(1)    - FIRST VALUE OF PROJECTILE DISPLACEMENT (CM).
C     RESP(1)    - CORRESPONDING VALUE OF RESISTIVE PRESSURE (MPA).
C     RESX(2)    - SECOND VALUE OF DISPLACEMENT. STARTS A NEW CARD.
C                  .
C                  .
C     RESP(NRES)
C
C     NOTES:       OUTSIDE THE TABLE RANGE THE FIRST OR LAST VALUE IS
C                  USED.  THUS A CONSTANT BORE RESISTANCE CAN BE
C                  CHARACTERIZED WITH ONE PAIR OF DATA.
C                  INSIDE THE TABLE RANGE THE DATA ARE LINEARLY
C                  INTERPOLATED.
C     FILE 7.0: "PROPERTIES OF UNDECOMPOSED WORKING FLUID"
C                                          (6F10.0) ONE CARD.
C     C          - TOTAL MASS OF WORKING FLUID (G).
C     RHOP0      - DENSITY OF WORKING FLUID AT ONE ATMOSPHERE (G/CC).
C     AK1        - BULK MODULUS AT ONE ATMOSPHERE (MPA).
C     AK2        - DERIVATIVE OF MODULUS WITH RESPECT TO PRESSURE (-).
C     QV         - HEAT OF VAPORIZATION OF WORKING FLUID (J/G).
C     BET        - LAGRANGE COUPLING COEFFICIENT (-).  MAY BE ENTERED AS
C                  ANY VALUE BETWEEN ZERO AND ONE.  IF BET IS ZERO, THE
C                  UNDECOMPOSED WORKING FLUID IS ASSUMED TO BE AT REST
C                  AT ALL TIMES.  IF BET IS ONE, THE UNDECOMPOSED FLUID
C                  IS ASSUMED TO HAVE THE SAME VELOCITY PROFILE
C                  (LAGRANGE) AS THE MIXTURE OF PLASMA AND DECOMPOSED
C                  FLUID.
C
C     NOTES:       QV SHOULD BE SET EQUAL TO ZERO IF THE PROPERTIES
C                  OF THE DECOMPOSED WORKING FLUID ARE CHARACTERIZED BY
C                  THE PARAMETRIC BLAKE CODE DATA OF FILE 14.0.  THE DATA
C                  OF FILE 14.0 AUTOMATICALLY INCLUDE THE ENERGY REQUIRED
C                  TO DECOMPOSE THE WORKING FLUID.
C
C     FILE 7.1: "PROPERTIES OF FINAL DECOMPOSITION PRODUCTS"
C                                (3F10.0)    ONE CARD.
C     B          - COVOLUME OF FINAL DECOMPOSITION PRODUCTS (CC/G).
C     GAM        - RATIO OF SPECIFIC HEATS OF FINAL DECOMPOSITION
C                  PRODUCTS (-).
C     GMOL       - MOLECULAR WEIGHT OF FINAL DECOMPOSITION
C                  PRODUCTS (G/GMOL).
C
C     NOTES:       IF THE DATA OF FILE 14.0 ARE PROVIDED THE VALUES OF
C                  B, GAM AND BET ARE ONLY USED TO DETERMINE THE INITIAL
C                  CONDITIONS.
C
```

```
C     FILE 7.2: "PROPERTIES OF INTERMEDIATE DECOMPOSITION PRODUCTS"
C                              (E10.2,7F10.0)     ONE CARD.
C     ARCB      - PRE-EXPONENTIAL FACTOR IN ARRHENIUS RATE LAW (UNITS
C                 YIELD G/CC-SEC).  IF ARCB=0, IT IS ASSUMED THAT
C                 INTERMEDIATE PRODUCTS ARE NOT FORMED AND THE
C                 REMAINING DATA IN THIS FILE ARE NOT REQUIRED.
C     ARXB      - TEMPERATURE EXPONENT IN ARRHENIUS LAW (-).
C     AREB      - ACTIVATION ENERGY IN ARRHENIUS RATE LAW (J/GMOL).
C     AROB      - ORDER OF REACTION WITH RESPECT TO CONCENTRATION OF
C                 INTERMEDIATE PRODUCTS (-).
C     ECHB      - CHEMICAL ENERGY RELEASED BY TRANSFORMATION OF
C                 INITIAL PRODUCTS OF DECOMPOSITION INTO FINAL
C                 EQUILIBRIUM PRODUCTS (J/G).  ECHB IS POSITIVE IF
C                 THE REACTION TO FINAL PRODUCTS IS EXOTHERMIC.
C     BI        - COVOLUME OF INTERMEDIATE DECOMPOSITION PRODUCTS (CC/G)
C     GAMI      - RATIO OF SPECIFIC HEATS OF INTERMEDIATE DECOMPOSITION
C                 PRODUCTS (-).
C     GMOLI     - MOLECULAR WEIGHT OF INTERMEDIATE DECOMPOSITION
C                 PRODUCTS (G/GMOL).
C
C     NOTES:      ECHB IS NOT USED IF THE PROPERTIES OF THE FINAL
C                 PRODUCTS ARE DEFINED BY THE DATA OF FILE 14.0.
C                 IT IS ASSUMED IN THAT CASE THAT THE HEAT OF
C                 REACTION IS INCORPORATED INTO THE EFFECTIVE
C                 INTERNAL ENERGY IN THE SAME WAY THAT THE HEAT
C                 OF VAPORIZATION IS CAPTURED BY THE EQUILIBRIUM
C                 ANALYSIS OF THE BLAKE CODE.  FILE 14.0 PROVIDES
C                 A TABULATION OF THE DIFFERENCE IN THE HEATS OF
C                 FORMATION OF THE INTERMEDIATE AND FINAL PRODUCTS
C                 WHICH SUPERSEDE THE VALUE OF ECHB.
C                 IT IS ASSUMED THAT THE RATE OF DECOMPOSITION OF
C                 THE WORKING FLUID IS GIVEN IN TABULAR FORM WHEN
C                 FINITE RATE CHEMISTRY IS CONSIDERED.
C
C     FILE 8.0: "NUMBER OF DATA TO CHARACTERIZE PLASMA DISCHARGE"
C                (I5)     ONE CARD.
C     NPLAS     - NUMBER OF SETS OF DATA IN FILE 10.0.  NPLAS MUST NOT
C                 BE LESS THAN TWO OR GREATER THAN ONE HUNDRED, EXCEPT
C                 IN THE SPECIAL CASE WHEN PBSK (FILE 4.0) > 0, AND THE
C                 VALUE NPLAS = 0 IS THEN ALLOWED.
C
C     FILE 9.0: "TOTAL PLASMA ENERGY AND MASS"    (2F10.0) ONE CARD.
C     TOTPE     - TOTAL PLASMA ENERGY (J).
C     TOTPM     - TOTAL PLASMA MASS (G).
C
```

```
C     FILE 10.0: "PLASMA DISCHARGE CHARACTERISTICS"
C                                          (3F10.0) NPLAS CARDS.
C     N.B. THIS FILE IS REQUIRED IF AND ONLY IF NPLAS > 1.
C     PLAST(1)  - FIRST VALUE OF TIME (MSEC).
C     PLASE(1)  - FRACTION OF TOTAL PLASMA ENERGY DELIVERED AT TIME
C                 PLAST(1)  (-).
C     PLASM(1)  - FRACTION OF TOTAL PLASMA MASS DELIVERED AT TIME
C                 PLAST(1)  (-).
C     PLAST(2)  - SECOND VALUE OF TIME (MSEC).
C               .
C               .
C     PLASM(NPLASM)
C
C     NOTES:      AT TIMES OUTSIDE THE TABLE RANGE THE FIRST OR LAST
C                 ENTRIES ARE USED.  LINEAR INTERPOLATION IS USED
C                 INSIDE THE TABLE RANGE.
C                 PLASE AND PLASM ARE EXPECTED TO BE MONOTONIC
C                 FUNCTIONS OF TIME AND TO BE GREATER THAN OR EQUAL
C                 TO ZERO AND LESS THAN OR EQUAL TO ONE.
C                 IF PBSK (FILE 4.0) IS NOT ZERO, THE VALUES OF
C                 PLASE AND PLASM ARE NOT USED.
C                 THE TABLES SHOULD BE SUFFICIENTLY COMPLETE TO SPECIFY
C                 THE CONDITION AT WHICH THE EFFECTIVE ENERGY OF THE
C                 MIXTURE IS ZERO, OTHERWISE CALCULATIONS IN WHICH THE
C                 PLASMA DISCHARGE YIELDS ENERGY INPUT BELOW THE TABLE
C                 RANGE WILL EXHIBIT ERRONEOUSLY HIGH PRESSURES DUE
C                 TO THE DEFAULT PROCEDURES.
C
C     FILE 11.0: "NUMBER OF DATA TO CHARACTERIZE RATE OF DECOMPOSITION
C                 OF WORKING FLUID"    (I5)    ONE CARD.
C     NALPH     - NUMBER OF SETS OF DATA IN FILE 12.0.  NALPH MUST BE
C                 AT LEAST TWO AND NOT GREATER THAN ONE HUNDRED  EXCEPT
C                 IN THE SPECIAL CASES WHEN RATE (FILE 4.0) > 0, OR
C                 PBSK > 0 (FILE 4.0), OR NBAL (FILE 15.0) > 0, AND THE
C                 VALUE NALPH = 0 IS THEN ALLOWED.
C
C     FILE 12.0: "RATE OF DECOMPOSITION OF WORKING FLUID"
C                           (2F10.0)     NALPH CARDS.
C     N.B. THIS FILE IS REQUIRED IF AND ONLY IF NALPH > 1.
C     ALPT(1)   - FIRST VALUE OF TIME (MSEC).
C     ALPH(1)   - FRACTION OF WORKING FLUID DECOMPOSED AT TIME ALPT(1)
C                 (-).
C     ALPT(2)   - SECOND VALUE OF TIME.  STARTS A NEW CARD.
C               .
C               .
C     ALPH(NALPH)
C
C     NOTES:      IF RATE (FILE 4.0) IS NOT ZERO, OR IF NBAL (FILE 15.0)
C                 IS NOT ZERO, THE DATA IN THIS FILE ARE NOT USED.
C                 THE VALUES OF ALPH ARE EXPECTED TO BE A MONOTONIC
C                 FUNCTION OF TIME AND TO BE GREATER THAN OR EQUAL TO
C                 ZERO AND LESS THAN OR EQUAL TO ONE.
C
```

```
C     FILE 13.0: "NUMBER OF DATA TO CHARACTERIZE COMPOSITION OF
C                 DECOMPOSED WORKING FLUID AS A FUNCTION OF PLASMA
C                 ENERGY"   (I5) ONE CARD.
C     NVDAT      - NUMBER OF SETS OF DATA IN FILE 14.0.  IF NVDAT
C                  IS ENTERED AS ZERO, THE COMPOSITION OF THE
C                  PROPULSION GASES IS ASSUMED TO BE CONSTANT AND
C                  TO BE CHARACTERIZED BY THE DATA OF FILE 4.0.
C                  NVDAT MAY NOT BE GREATER THAN 100.
C
C     FILE 14.0: "PROPERTIES OF FINAL DECOMPOSITION OF WORKING FLUID
C                 AS A FUNCTION OF TOTAL INJECTED PLASMA ENERGY"
C                 (6F10.0)      NVDAT CARDS.
C     N.B. THIS FILE IS REQUIRED IF AND ONLY IF NVDAT IS NOT ZERO.
C     VEIN(1)    - FIRST VALUE OF PLASMA ENERGY PER UNIT MASS
C                  OF WORKING FLUID (J/G).
C     VEFF(1)    - CORRESPONDING VALUE OF EFFECTIVE INTERNAL ENERGY
C                  (J/G).
C     VGAM(1)    - CORRESPONDING VALUE OF RATIO OF SPECIFIC HEATS (-).
C     VB(1)      - CORRESPONDING VALUE OF COVOLUME (CC/G).
C     VMOL(1)    - CORRESPONDING VALUE OF MOLECULAR WEIGHT (G/GMOL).
C     VECHB(1)   - CORRESPONDING VALUE OF DIFFERENCE IN HEATS OF
C                  FORMATION OF INTERMEDIATE AND FINAL PRODUCTS (J/G).
C                  THIS QUANTITY IS TAKEN TO BE POSITIVE WHEN THE
C                  REACTION FROM INTERMEDIATE TO FINAL PRODUCTS IS
C                  EXOTHERMIC.
C     VEIN(2)    - SECOND VALUE OF PLASMA ENERGY PER UNIT MASS
C                  OF WORKING FLUID (J/G).  STARTS A NEW CARD.
C                .
C                .
C     VECHB(NVDAT)
C
C     NOTES:       IF THE ENERGY DENSITY OF THE MIXTURE OF PLASMA
C                  AND DECOMPOSED WORKING FLUID LIES OUTSIDE THE
C                  RANGE OF THE TABLE THE FIRST OR LAST VALUES ARE
C                  USED TO DETERMINE THE EFFECTIVE PROPERTIES OF
C                  THE MIXTURE.
C                  THE ONLY EXCEPTION TO THIS RULE OCCURS FOR THE
C                  EFFECTIVE INTERNAL ENERGY AT VALUES OF ENERGY
C                  DENSITY LARGER THAN VEIN(NVDAT).  THE EFFECTIVE
C                  INTERNAL ENERGY IS DETERMINED IN THIS CASE BY
C                  LINEAR EXTRAPOLATION OF THE LAST TWO VALUES IN
C                  THE TABLE.
C                  INSIDE THE TABLE RANGE LINEAR INTERPOLATION IS
C                  USED TO DETERMINE VALUES OF ALL PROPERTIES.
C
```

```
C     FILE 15: "NUMBER OF SETS OF DATA TO DEFINE INTERIOR BALLISTIC
C              BEHAVIOR OF GUN"       (I5)     ONE CARD.
C     NBAL      - NUMBER OF SETS OF DATA IN FILE 16.  NBAL MAY BE
C                 EITHER ZERO OR ANY NUMBER GREATER THAN OR EQUAL
C                 TO TWO AND LESS THAN OR EQUAL TO ONE THOUSAND.
C                 IF NBAL IS NOT EQUAL TO ZERO, AN
C                 INVERSE ANALYSIS IS PERFORMED WITH THE RATE OF
C                 DECOMPOSITION OF THE WORKING FLUID BEING
C                 DETERMINED FROM THE OBSERVED HISTORY OF BREECH
C                 PRESSURE AND (IF APPLICABLE) THE HISTORY OF
C                 BASE PRESSURE, TOGETHER WITH A CHARACTERIZATION
C                 OF THE RATE OF PLASMA DISCHARGE AND THE THERMO-
C                 CHEMICAL PROPERTIES OF THE MIXTURE.
C     NSMTH     - IF NSMTH IS ZERO, THE BALLISTIC DATA ARE NOT SMOOTHED.
C                 IF NSMTH IS ONE, THE DATA ARE SMOOTHED USING A HIGH
C                 FREQUENCY NUMERICAL FILTER.
C     NDTR      - NUMBER OF DATA TO BE USED IN REGRESSION ANALYSIS OF
C                 RATE OF DECOMPOSITION OF WORKING FLUID.  SUGGESTED
C                 VALUE IS 10.  NDTR MAY TAKE ANY VALUE BETWEEN ZERO AND
C                 TWENTY.  IF NDTR IS LESS THAN TWO, A REGRESSION ANAL-
C                 YSIS IS NOT USED TO ESTIMATE THE TREND OF THE RATE OF
C                 DECOMPOSITION.
C
C     FILE 16: "OBSERVED BALLISTIC RESPONSE OF GUN" (3F10.0) NBAL CARDS.
C     N.B.  THIS FILE IS REQUIRED IF AND ONLY IF NBAL > 1.
C     BALT(1)   - FIRST VALUE OF TIME (MSEC).
C     BALP(1)   - CORRESPONDING VALUE OF BREECH PRESSURE (MPA).
C     BALPB(1)  - CORRESPONDING VALUE OF BASE PRESSURE (MPA).
C     BALT(2)   - SECOND VALUE OF TIME.  STARTS A NEW CARD.
C                 .
C                 .
C     BALPB(NBAL)
C
C     NOTES:      IF VALUES OF BALPB ARE NOT AVAILABLE THE ANALYSIS
C                 WILL USE THE VALUE OF BET GIVEN IN FILE 7.0 TO
C                 CHARACTERIZE THE MOTION OF THE UNDECOMPOSED
C                 WORKING FLUID.  IF VALUES OF BALPB ARE GIVEN, THE
C                 ANALYSIS WILL DETERMINE AN EFFECTIVE VALUE OF BET
C                 AT EACH TIME STEP IN ADDITION TO THE RATE OF
C                 DECOMPOSITION OF THE WORKING FLUID.
C
C     ****************************************************************
      PARAMETER (NYI=4,NYPD=4)
      CHARACTER*10 FILNAM,OUTFIL
      CHARACTER*80 TITLE
C
      COMMON/C1/ PRM,PRTRV,DB,AB,V0,C,RHOP0,AK1,AK2,QV,B,GAM,BET,
     *           DTNOM,XM0,P0,G,EG0,GMOL,TEMP,PBR,ALF,EFRAC,RATE,
     *           PBSK,PI,RU,ALFOLD,TOTPE,TOTPM,PLM,PLE
     *           ,GAM0,B0,GMOL0,ECHB0,EG00
      COMMON/C2/ RESX(20),RESP(20),NRES,NSHK
      COMMON/C3/ PLAST(100),PLASE(100),PLASM(100),NPLAS,MORE
      COMMON/C4/ ALPT(100),ALPH(100),NALPH
      COMMON/C5/ TITLE
```

```
      COMMON/C6/ TIME,YI(NYI),YDP(NYPD),YDT(NYI)
      COMMON/C7/ VEIN(100),VEFF(100),VGAM(100),VB(100),VMOL(100),
     *           VECHB(100),NVDAT
      COMMON/C8/ ARCB,ARXB,AREB,AROB,ECHB,BI,GAMI,GMOLI,CVI,CPI
      COMMON/C9/ BALT(1000),BALP(1000),BALPB(1000),NBAL
      COMMON/C10/ ZA(20),RA(20),NSTA,NSPLT
      COMMON/C11/ DXPLE,DXPLM,DXALF,RHO,VOL
      COMMON/C12/ DAT(20),DATA(20),DATEX,AEX,BEX,NDTR,NSTEP
      COMMON/C13/ PTOL,PTOLC,TTOL,ATOL1,ATOL2
C
      EQUIVALENCE (YI(1),XP),(YI(2),VP),(YI(3),WF),(YI(4),YFR),
     *            (YDP(1),PC),(YDP(2),PB),(YDP(3),RHOP),(YDP(4),RES),
     *            (YDT(2),VPRDOT)
C
C     NAME FILES FOR INPUT AND OUTPUT ON MICROCOMPUTER
C
C*MFST       WRITE(*,1)
C*MFST     1 FORMAT(' ENTER INPUT DATA FILE NAME: '\)
C*MFST       READ(*,2) FILNAM
C*MFST     2 FORMAT(A10)
C*MFST       OPEN(5,FILE=FILNAM)
C*MFST       WRITE(*,3)
C*MFST     3 FORMAT(' ENTER OUTPUT FILE NAME: '\)
C*MFST       READ(*,2) OUTFIL
C*MFST       OPEN(6,FILE=OUTFIL)
C
C     READ INPUT DATA
C
      READ(5,1004) TITLE
      READ(5,1000) DTNOM,PTOL,PTOLC,TTOL,ATOL1,ATOL2
      IF(PTOL.LT.1.E-10) PTOL=1.E-4
      IF(PTOLC.LT.1.E-10) PTOLC=1.E-4
      IF(TTOL.LT.1.E-10) TTOL=1.E-4
      IF(ATOL1.LT.1.E-10) ATOL1=1.E-4
      IF(ATOL2.LT.1.E-10) ATOL2=1.E-2
      READ(5,1001) NPRT
      READ(5,1000) PRM,PRTRV,DB,V0,TEMP0,P0,PBSK,RATE
      READ(5,1001) NSTA,NSPLT
      IF(NSTA.GE.2) READ(5,1002) (ZA(I),RA(I),I=1,NSTA)
      READ(5,1001) NRES,NSHK
      IF(NRES.GT.0) READ(5,1002) (RESX(I),RESP(I),I=1,NRES)
      READ(5,1000) C,RHOP0,AK1,AK2,QV,BET
      READ(5,1000) B,GAM,GMOL
      READ(5,1006) ARCB,ARXB,AREB,AROB,ECHB,BI,GAMI,GMOLI
      READ(5,1001) NPLAS
      READ(5,1000) TOTPE,TOTPM
      IF(NPLAS.GE.2)
     *      READ(5,1003) (PLAST(I),PLASE(I),PLASM(I),I=1,NPLAS)
      READ(5,1001) NALPH
      IF(NALPH.GE.2) READ(5,1002) (ALPT(I),ALPH(I),I=1,NALPH)
      READ(5,1001) NVDAT
      IF(NVDAT.GE.2) READ(5,1005)(VEIN(I),VEFF(I),VGAM(I),VB(I),
     *                            VMOL(I),VECHB(I),I=1,NVDAT)
      READ(5,1001) NBAL,NSMTH,NDTR
```

```
      IF(NBAL.GE.2) READ(5,1003) (BALT(I),BALP(I),BALPB(I),I=1,NBAL)
C
C     WRITE INPUT DATA
C
      WRITE(6,2000) TITLE
      WRITE(6,2010) DTNOM,PTOL,PTOLC,TTOL,ATOL1,ATOL2
      WRITE(6,2020) NPRT
      WRITE(6,2030) PRM,PRTRV,DB,V0,TEMP0,P0,PBSK,RATE
      WRITE(6,2032) NSTA,NSPLT
      IF(NSTA.GE.2) WRITE(6,2034) (ZA(I),RA(I),I=1,NSTA)
      WRITE(6,2040) NRES,NSHK
      IF(NRES.GT.0) WRITE(6,2050) (RESX(I),RESP(I),I=1,NRES)
      WRITE(6,2060) C,RHOP0,AK1,AK2,QV,BET
      WRITE(6,2062) B,GAM,GMOL
      WRITE(6,2064) ARCB,ARXB,AREB,AROB,ECHB,BI,GAMI,GMOLI
      WRITE(6,2070) NPLAS
      WRITE(6,2080) TOTPE,TOTPM
      IF(NPLAS.GE.2)
     *     WRITE(6,2090) (PLAST(I),PLASE(I),PLASM(I),I=1,NPLAS)
      WRITE(6,2100) NALPH
      IF(NALPH.GE.2) WRITE(6,2110) (ALPT(I),ALPH(I),I=1,NALPH)
      WRITE(6,2120) NVDAT
      IF(NVDAT.GE.2) WRITE(6,2130) (VEIN(I),VEFF(I),VGAM(I),VB(I),
     *                        VMOL(I),VECHB(I),I=1,NVDAT)
      WRITE(6,2140) NBAL,NSMTH,NDTR
      IF(NBAL.GE.2) WRITE(6,2150) (BALT(I),BALP(I),BALPB(I),I=1,NBAL)
C
C     INITIALIZE
C
      PI=3.1415927E0
      G=1.E+7
      RU=8.31434E0
      AB=PI*DB**2/4.E0
      DTNOM=DTNOM*1.E-3
      GAM0=GAM
      B0=B
      GMOL0=GMOL
      ECHB0=ECHB
C
C     RESCALE PLASMA DATA
C
      IF(NPLAS.EQ.0) GO TO 102
      DO 100 I=1,NPLAS
      PLAST(I)=PLAST(I)*1.E-3
      PLASE(I)=PLASE(I)*TOTPE
      PLASM(I)=PLASM(I)*TOTPM
  100 CONTINUE
  102 IF(NALPH.EQ.0) GO TO 112
      DO 110 I=1,NALPH
      ALPT(I)=ALPT(I)*1.E-3
  110 CONTINUE
  112 IF(NBAL.EQ.0) GO TO 160
      DO 120 I=1,NBAL
      BALT(I)=BALT(I)*1.E-3
```

```
  120 CONTINUE
      IF(NSMTH.EQ.1) CALL SMOOTH
  160 XP=0.E0
      VP=0.E0
      WF=0.E0
      YFR=0.E0
      ALFOLD=0.E0
      TIME=0.E0
      PMAX=0.E0
      IF(NVDAT.GT.0) ECHB=VECHB(1)
      TEMP=TEMP0
      PC=P0
      CALL EOSLIQ(PC,RHOP,DRHOP,EP,DEP)
      VF0=V0-C/RHOP
      RHO0=1.E0/(B+RU*TEMP0/GMOL/P0)
      XM0=RHO0*VF0
      CV=RU/GMOL/(GAM-1.E0)
      CP=CV*GAM
      EG00=CV*TEMP0
      EG0=EG00*XM0+EP
      IF(ARCB.GT.1.E-10) GO TO 170
      CVI=CV
      CPI=CP
      GMOLI=GMOL
      BI=B
      GAMI=GAM
      GO TO 180
  170 CVI=RU/GMOLI/(GAMI-1.E0)
      CPI=CVI*GAMI
  180 CALL GRAD(PC,PBR,PB,XP,VP,0.E0,TOTKE,1,1,0,0)
      NSTEP=0
      MORE=1
      IF(NPRT.LT.1) NPRT=1
      NSTOP=0
C
C     TEST FOR PRINT
C
  200 IF(MOD(NSTEP,NPRT).NE.0) GO TO 210
      CALL DEPEND
      IF(MOD(NSTEP/NPRT,50).EQ.0) WRITE(6,3000) TITLE
  205 TIMMS=TIME*1.E+3
      VPM=VP*1.E-2
      WRITE(6,3010) TIMMS,PBR,PB,TEMP,YFR,XP,VPM,ALF,BET,EFRAC
      IF(NSTOP.EQ.0) GO TO 210
      WRITE(6,3020) PMAX
      STOP
C
C     TEST FOR MAXIMUM PRESSURE
C
  210 IF(PBR.GT.PMAX) PMAX=PBR
C
C     SET TIME STEP AND PREPARE FOR STOP
C
      DT=DTNOM
```

```
      IF(XP+VP*DT+VPRDOT*DT*DT*0.5E0.LT.PRTRV) GO TO 240
      NSTOP=1
      IF( ABS(VPRDOT).LT.1.E-10) GO TO 230
      DT=( SQRT(VP*VP+2.E0*VPRDOT*(PRTRV-XP))-VP)/VPRDOT
      GO TO 240
  230 IF( ABS(VP).LT.1.E-10) GO TO 240
      DT=(PRTRV-XP)/VP
C
C     UPDATE TIME AND INDEPENDENT STATE VARIABLES
C
  240 CALL RKUT(DT)
      ALFOLD=ALF
      NSTEP=NSTEP+1
      IF(NDTR.LT.2) GO TO 260
      DO 250 I=2,NDTR
      DAT(I-1)=DAT(I)
      DATA(I-1)=DATA(I)
  250 CONTINUE
      DAT(NDTR)=TIME
      DATA(NDTR)=ALF
  260 IF(NSTOP.EQ.0) GO TO 200
      GO TO 205
C
C     FORMAT STATEMENTS
C
 1000 FORMAT(8F10.0)
 1001 FORMAT(16I5)
 1002 FORMAT(2F10.0)
 1003 FORMAT(3F10.0)
 1004 FORMAT(A80)
 1005 FORMAT(6F10.0)
 1006 FORMAT(E10.4,7F10.0)
 2000 FORMAT(' ',10X,'LUMPED PARAMETER SIMULATION OF ELECTROTHERMAL GUN
     *'//10X,A80//)
 2010 FORMAT(
     *' INTEGRATION TIME STEP(MS)                    ',F10.3/
     *' PRESSURE CONVERGENCE TOLERANCE(-)             ',G12.4/
     *' CONVERGENCE TOLERANCE FOR CONSTANT PRESSURE'/
     *' SOLUTION(-)                                  ',G12.4/
     *' TEMPERATURE CONVERGENCE TOLERANCE(-)          ',G12.4/
     *' FIRST CONVERGENCE TOLERANCE FOR FRACTION'/
     *' OF WORKING FLUID DECOMPOSED(-)                ',G12.4/
     *' SECOND CONVERGENCE TOLERANCE FOR FRACTION'/
     *' OF WORKING FLUID DECOMPOSED(-)                ',G12.4//)
 2020 FORMAT(
     *' NUMBER OF STEPS FOR SOLUTION PRINTOUT         ',I5)
 2030 FORMAT(
     *' PROJECTILE MASS(G)                            ',F10.2/
     *' PROJECTILE TRAVEL(CM)                         ',F10.2/
     *' BORE DIAMETER(CM)                             ',F10.2/
     *' VOLUME OF MIXING CHAMBER(CC)                  ',F10.1/
     *' INITIAL TEMPERATURE OF GAS(K)                 ',F10.1/
     *' INITIAL PRESSURE(MPA)                         ',F10.1/
     *' CONSTANT BREECH PRESSURE(MPA)                 ',F10.1/
```

```
     *' RATE OF DECOMPOSITION OVER RATE OF ENERGY'/
     *' ADDITION(-)                                    ',F10.3//)
2032 FORMAT(
     *' NUMBER OF DATA TO DESCRIBE CHAMBER GEOMETRY    ',I5/
     *' (0 IMPLIES LAGRANGE GRADIENT; >1 IMPLIES CHAMBRAGE GRADIENT)'/
     *' NUMBER OF SUBDIVISIONS FOR CHAMBER INTEGRALS   ',I5//)
2034 FORMAT(' ',5X,'CHAMBER GEOMETRY'//
     *' ',5X,'DISTANCE(CM)',5X,'RADIUS(CM)'//(' ',2F15.3))
2040 FORMAT(
     *' NUMBER OF BORE RESISTANCE DATA                 ',I5/
     *' AIR SHOCK RESISTANCE (0=NO;1=YES)              ',I5//)
2050 FORMAT(' ',5X,'TRAVEL(CM)',5X,'RESISTANCE(MPA)'//
     *(' ',F15.2,5X,F15.1))
2060 FORMAT(' '//
     *' ',5X,'PROPERTIES OF UNDECOMPOSED WORKING FLUID'//
     *' MASS OF WORKING FLUID(G)                       ',F10.1/
     *' DENSITY OF FLUID AT 1 ATM.(G/CC)               ',F10.4/
     *' BULK MODULUS AT 1 ATM.(MPA)                    ',F10.1/
     *' DERIVATIVE OF MODULUS W.R.T. PRESSURE(-)       ',F10.3/
     *' HEAT OF VAPORIZATION(J/G)                      ',F10.1/

     *' LAGRANGE COUPLING COEFFICIENT(-)               ',F10.2/
     *' (0=LIQUID AT REST;1=LIQUID HAS LAGRANGE VELOCITY)'//)
2062 FORMAT(' ',5X,'PROPERTIES OF FINAL PRODUCTS OF DECOMPOSITION'//
     *' COVOLUME (CC/G)                               ',F10.4/
     *' RATIO OF SPECIFIC HEATS (-)                   ',F10.4/
     *' MOLECULAR WEIGHT (G/GMOL)                     ',F10.4//)
2064 FORMAT(' ',5X,'PROPERTIES OF INTERMEDIATE PRODUCTS OF DECOMPOSITIO
     *N'//
     *' PRE-EXPONENT IN ARRHENIUS REACTION RATE LAW'/
     *'  (UNITS YIELD G/CC-SEC)                       ',G15.5/
     *' TEMPERATURE EXPONENT IN REACTION RATE LAW (-) ',G15.5/
     *' ACTIVATION ENERGY (J/GMOL)                    ',G15.5/
     *' REACTION ORDER (-)                            ',G15.5/
     *' CHEMICAL ENERGY OF REACTION (J/G)              ',G15.5/
     *' COVOLUME (CC/G)                               ',F10.4/
     *' RATIO OF SPECIFIC HEATS (-)                   ',F10.4/
     *' MOLECULAR WEIGHT (G/GMOL)                     ',F10.4//)
2070 FORMAT(
     *' NUMBER OF DATA TO DESCRIBE PLASMA DISCHARGE    ',I5)
2080 FORMAT(
     *' TOTAL PLASMA ENERGY(J)                        ',G15.6/
     *' TOTAL PLASMA MASS(G)                          ',F10.3//)
2090 FORMAT(' ',5X,'TIME(MS)',5X,'FRACTION OF ENERGY(-)',5X,'FRACTION O
     *F MASS(-)'//(' ',F15.3,5X,2F15.6))
2100 FORMAT(' '//
     *' NUMBER OF DATA TO DESCRIBE DECOMPOSITION'/
     *'                           OF WORKING FLUID    ',I5//)
2110 FORMAT(' ',5X,'TIME(MS)',5X,'FRACTION OF FLUID DECOMPOSED(-)'//
     *(' ',5X,F15.3,5X,F15.6))
2120 FORMAT(' '//
     *' NUMBER OF DATA TO DETERMINE THERMOCHEMISTRY   ',I5//)
```

```
2130 FORMAT(' ',5X,'ENERGY(J/G)',5X,'EFF.ENGY.(J/G)',8X,'GAMMA(-)',
    *5X,'COVOLUME(CC/G)',12X,'MOL. WGT.'8X,'DELTA HOF(J/G)'//
    *(' ',2F15.1,5X,2F15.4,10X,F15.4,F15.1))
2140 FORMAT(' '//
    *' NUMBER OF DATA TO SPECIFY OBSERVED BALLISTICS  ',I5/
    *' DATA SMOOTHING REQUIRED (0=NO;1=YES)           ',I5/
    *' NUMBER OF DATA FOR REGRESSION ANALYSIS OF RATE'/
    *'          OF DECOMPOSITION                      ',I5//)
2150 FORMAT(' ',5X,'TIME(MSEC)',5X,'BREECH PRESS. (MPA)',5X,
    *'BASE PRESS. (MPA)'//(' ',3G20.6))
3000 FORMAT('1',10X,A80/
    *' ',5X,'TIME(MS)',5X,'P-BR(MPA)',5X,'P-BASE(MPA)',5X,'TEMP(K)',
    *4X,'YFR(-)',3X,'PR. DISP(CM)',2X,'PR. VEL(M/S)',2X,'ALPHA(-)',4X,
    *'BETA(-)',4X,'E-FRAC(-)'//)
3010 FORMAT(' ',F10.3,3F15.2,F10.3,F12.2,F12.1,F12.3,F11.3,F13.3)
3020 FORMAT(' '//' MAXIMUM PRESSURE(MPA): ',F10.1)
     END
```

```
      SUBROUTINE RKUT(DT)
C
C     FOURTH ORDER RUNGE-KUTTA ALGORITHM
C
      PARAMETER (NYI=4,NYPD=4)
C
      COMMON/C6/ TIME,YI(NYI),YDP(NYPD),YDT(NYI)
C
      EQUIVALENCE (YI(1),XP),(YI(2),VP),(YI(3),WF),(YI(4),YFR),
     *            (YDP(1),PC),(YDP(2),PB),(YDP(3),RHOP),(YDP(4),RES),
     *            (YDT(2),VPRDOT)
C
      DIMENSION YB(NYI),CW(4),Q(NYI,4)
C
      DATA CW/0.E0,0.5E0,0.5E0,1.0E0/
C
      TB=TIME
      DO 10 J=1,NYI
      YB(J)=YI(J)
   10 CONTINUE
      DO 100 I=1,4
      TIME=TB+CW(I)*DT
      DO 20 J=1,NYI
      YI(J)=YB(J)
      IF(I.EQ.1) GO TO 20
      YI(J)=YB(J)+CW(I)*DT*Q(J,I-1)
      IF(J.NE.4) GO TO 20
      IF(YI(J).GT.1.E0) YI(J)=1.E0
      IF(YI(J).GE.0.E0) GO TO 20
      Q(J,I-1)=-YB(J)/CW(I)/DT
      YI(J)=0.E0
   20 CONTINUE
      CALL DEPEND
      CALL DERIV
      DO 40 J=1,NYI
      Q(J,I)=YDT(J)
   40 CONTINUE
  100 CONTINUE
      TIME=TB+DT
      DO 200 J=1,NYI
      YI(J)=YB(J)+DT/6.E0*(Q(J,1)+2.E0*Q(J,2)+2.E0*Q(J,3)+Q(J,4))
  200 CONTINUE
      IF(YFR.LT.0.E0) YFR=0.E0
      IF(YFR.GT.1.E0) YFR=1.E0
      RETURN
      END
```

```
      SUBROUTINE DERIV
C
C     TIME DERIVATIVES OF INDEPENDENT STATE VARIABLES
C
      PARAMETER (NYI=4,NYPD=4)
C
      COMMON/C1/ PRM,PRTRV,DB,AB,V0,C,RHOP0,AK1,AK2,QV,B,GAM,BET,
     *           DTNOM,XM0,P0,G,EG0,GMOL,TEMP,PBR,ALF,EFRAC,RATE,
     *           PBSK,PI,RU,ALFOLD,TOTPE,TOTPM,PLM,PLE
     *           ,GAM0,B0,GMOL0,ECHB0,EG00
      COMMON/C6/ TIME,YI(NYI),YDP(NYPD),YDT(NYI)
      COMMON/C8/ ARCB,ARXB,AREB,AROB,ECHB,BI,GAMI,GMOLI,CVI,CPI
      COMMON/C9/ BALT(1000),BALP(1000),BALPB(1000),NBAL
      COMMON/C11/ DXPLE,DXPLM,DXALF,RHO,VOL
C
      EQUIVALENCE (YI(1),XP),(YI(2),VP),(YI(3),WF),(YI(4),YFR),
     *            (YDP(1),PC),(YDP(2),PB),(YDP(3),RHOP),(YDP(4),RES),
     *            (YDT(2),VPRDOT)
C
      YDT(1)=VP
      YDT(2)=G*AB/PRM*(PB-RES)
      IF(YDT(2).LT.0.E0) YDT(2)=0.E0
      YDT(3)=AB*RES*VP
      YDT(4)=0.E0
      IF(ARCB.LT.1.E-10) RETURN
      BIT=AREB/RU/TEMP
      EXPON=0.E0
      IF(BIT.LT.50.E0) EXPON= EXP(-BIT)
      YDT(4)=((1.E0-YFR)*C*DXALF-YFR*DXPLM)/RHO/VOL
     *      -ARCB/RHO*TEMP**ARXB*(YFR*RHO)**AROB*EXPON
      RETURN
      END
```

```
      SUBROUTINE DEPEND
C
C     CALCULATION OF DEPENDENT STATE VARIABLES
C
      PARAMETER (NYI=4,NYPD=4)
C
      COMMON/C1/ PRM,PRTRV,DB,AB,V0,C,RHOP0,AK1,AK2,QV,B,GAM,BET,
     *           DTNOM,XM0,P0,G,EG0,GMOL,TEMP,PBR,ALF,EFRAC,RATE,
     *           PBSK,PI,RU,ALFOLD,TOTPE,TOTPM,PLM,PLE
     *           ,GAM0,B0,GMOL0,ECHB0,EG00
      COMMON/C2/ RESX(20),RESP(20),NRES,NSHK
      COMMON/C3/ PLAST(100),PLASE(100),PLASM(100),NPLAS,MORE
      COMMON/C4/ ALPT(100),ALPH(100),NALPH
      COMMON/C6/ TIME,YI(NYI),YDP(NYPD),YDT(NYI)
      COMMON/C7/ VEIN(100),VEFF(100),VGAM(100),VB(100),VMOL(100),
     *           VECHB(100),NVDAT
      COMMON/C8/  ARCB,ARXB,AREB,AROB,ECHB,BI,GAMI,GMOLI,CVI,CPI
      COMMON/C9/ BALT(1000),BALP(1000),BALPB(1000),NBAL
      COMMON/C11/ DXPLE,DXPLM,DXALF,RHO,VOL
      COMMON/C12/ DAT(20),DATA(20),DATEX,AEX,BEX,NDTR,NSTEP
      COMMON/C13/ PTOL,PTOLC,TTOL,ATOL1,ATOL2
C
      EQUIVALENCE (YI(1),XP),(YI(2),VP),(YI(3),WF),(YI(4),YFR),
     *            (YDP(1),PC),(YDP(2),PB),(YDP(3),RHOP),(YDP(4),RES),
     *            (YDT(2),VPRDOT)
C
      DATA AIRGAM/1.4E0/,AIRP0/0.101E0/,AIRT0/293.E0/,
     *           AIRMW/28.96E0/
C
      QW=0.E0
      RES=0.E0
      IF(NRES.EQ.0) GO TO 5
      CALL INTERP(XP,RES,DXRES,RESX,RESP,0,NRES)
    5 IF(NSHK.EQ.0) GO TO 10
C
C     RESISTANCE DUE TO SHOCK AHEAD OF PROJECTILE
C
      BIT=(AIRGAM-1.E0)/(AIRGAM+1.E0)
      BITC= SQRT(G*AIRGAM*RU*AIRT0/AIRMW)
      BITL=1.E0-BIT
      BITU=(VP+ SQRT(VP*VP+4.E0*BITL*BITL*BITC*BITC))
     *     /(2.E0*BITL*BITC)
      RES=RES+AIRP0*((1.E0+BIT)*BITU*BITU-BIT)
   10 IF(PBSK.GT.1.E-10) GO TO 20
C
C     PLASMA ENERGY FROM TABLE
C
      CALL INTERP(TIME,PLE,DXPLE,PLAST,PLASE,0,NPLAS)
      CALL INTERP(TIME,PLM,DXPLM,PLAST,PLASM,0,NPLAS)
      EFRAC=PLE/PLASE(NPLAS)
      IF(NBAL.EQ.0) GO TO 14
C
C     RATE OF DECOMPOSITION TO MATCH OBSERVED BALLISTICS
C
```

```
      NPASS=2
      ITER=0
      NSRCH=0
      ALF=ALFOLD
C
C     COMPUTE EXPECTED VALUE FROM LINEAR REGRESSION LINE
C
      DATEX=0.E0
      IF(NDTR.GT.1.AND.NSTEP.GE.NDTR) CALL REGR
      IF(DATEX.GT.1.E-10) ALF=DATEX
      ALF1=ALF
      CALL INTERP(TIME,PBRSK,DXPBR,BALT,BALP,0,NBAL)
      IF(BALPB(NBAL).LT.1.E-10) GO TO 13
      CALL INTERP(TIME,PBASK,BITAXL,BALT,BALPB,0,NBAL)
C
C     CALL TO GRAD TO SET SLIP COEFFICIENT
C
   12 IF(BALPB(NBAL).LT.1.E-10) GO TO 13
      CALL GRAD(PSEEK,PBRSK,PBASK,XP,VP,RES,TOTKE,2,0,0,1)
C
C     CALL TO GRAD TO GET SPACEMEAN PRESSURE AND KINETIC ENERGY
C
   13 CALL GRAD(PSEEK,PBRSK,PB,XP,VP,RES,TOTKE,2,0,0,0)
      IF(TIME.LT.1.E-6.AND.PSEEK.LT.P0) PSEEK=P0
      GO TO 28
   14 IF(RATE.GT.1.E-10) GO TO 16
C
C     RATE OF DECOMPOSITION FROM TABLE
C
      CALL INTERP(TIME,ALF,DXALF,ALPT,ALPH,0,NALPH)
      GO TO 18
C
C     RATE OF DECOMPOSITION PROPORTIONAL TO PLASMA ENERGY FLUX
C     ACCORDING TO VALUE OF RATE.
C
   16 ALF=EFRAC
      IF(TIME.GT.PLAST(NPLAS)) ALF=TIME/PLAST(NPLAS)
      ALF=ALF*RATE
      IF(ALF.GT.1.E0) ALF=1.E0
   18 NPASS=2
C
C     CALL GRAD TO GET KINETIC ENERGY
C
      CALL GRAD(PC,PBR,PB,XP,VP,RES,TOTKE,1,0,0,0)
      GO TO 28
C
C     PLASMA ENERGY TO PROVIDE CONSTANT BREECH PRESSURE PBSK.  RATE
C     OF DECOMPOSITION PROPORTIONAL TO ENERGY FLUX.
C
   20 ITER=0
      NPASS=1
      PLEL=0.
      PLEH=TOTPE
      IF(MORE.EQ.0) PLEL=PLEH
```

```
   26 PLE=0.5E0*(PLEL+PLEH)
      EFRAC=PLE/TOTPE
      PLM=TOTPM*EFRAC
      ALF=EFRAC
      IF(MORE.EQ.0) ALF=TIME*ERATE*RATE
      IF(ALF.GT.1.E0) ALF=1.E0
C
C     CALL GRAD TO GET KINETIC ENERGY
C
      CALL GRAD(PSEEK,PBSK,PB,XP,VP,RES,TOTKE,2,0,0,0)
   28 NIT=0
   30 CALL EOSLIQ(PC,RHOP,DRHOP,EP,DEP)
      VOL=V0+AB*XP
      YFRM=1.E0-YFR
      BIT0=PLM+XM0+ALF*C
      BIT2=VOL-B*BIT0
      BIT3=-(1.E0-ALF)*C
      BIT4=BIT2+BIT3/RHOP
      BIT5=VOL+BIT3/RHOP
      RHO=BIT0/BIT5
      DRHO=BIT0/BIT5/BIT5*BIT3/RHOP/RHOP*DRHOP
      NITE=0
   32 PLEIN=PLE+EG0-QW-WF-PRM/G/2.E0*VP**2-TOTKE
     *      -ALF*C*YFR*ECHB-EP
      IF(YFR.LT..999E0) PLEIN=PLEIN-BIT0*YFR*CVI*TEMP
      IF(NVDAT.EQ.0.OR.YFR.GE..999E0) PLEIN=PLEIN+ALF*C*(ECHB-QV)
      PLEIN=PLEIN/BIT0
      IF(YFR.LT..999E0) PLEIN=PLEIN/YFRM
      IF(NVDAT.GT.1.AND.YFR.LT..999E0) GO TO 36
C
C     FIXED THERMOCHEMISTRY
C
      EMIX=PLEIN
      DXEMIX=1.E0
      DXECHB=0.E0
      DXTEMP=0.E0
      DPLEIN=0.E0
      DXGAM=0.E0
      DXGMOL=0.E0
      GO TO 40
C
C     VARIABLE THERMOCHEMISTRY
C
   36 CALL INTERP(PLEIN,EMIX,DXEMIX,VEIN,VEFF,1,NVDAT)
      IF(EMIX.GE.EG00) GO TO 38
      EMIX=EG00
      GAM=GAM0
      B=B0
      GMOL=GMOL0
      ECHB=ECHB0
      GO TO 40
   38 CALL INTERP(PLEIN,GAM,DXGAM,VEIN,VGAM,0,NVDAT)
      CALL INTERP(PLEIN,B,DXB,VEIN,VB,0,NVDAT)
      CALL INTERP(PLEIN,GMOL,DXGMOL,VEIN,VMOL,0,NVDAT)
```

```
      CALL INTERP(PLEIN,ECHB,DXECHB,VEIN,VECHB,0,NVDAT)
   40 CV=RU/GMOL/(GAM-1.E0)
      CP=GAM*CV
      CV=YFRM*CV+YFR*CVI
      CP=YFRM*CP+YFR*CPI
      B=YFRM*B+YFR*BI
      GMOLF=GMOL
      GMOL=1.E0/(YFRM/GMOL+YFR/GMOLI)
      GAM=CP/CV
      IF(YFR.GT.1.E-3.AND.YFR.LT.0.999E0) GO TO 42
      TEMP=EMIX/CV
      GO TO 48
C
C     NEED TO ITERATE FOR VALUE OF TEMPERATURE
C
   42 FPE=TEMP-EMIX/CV
      IF( ABS(FPE).LT.TTOL*TEMP) GO TO 48
      IF(NITE.LT.50) GO TO 46
      WRITE(6,44) FPE,TEMP
   44 FORMAT(' MORE THAN 50 ITERATIONS TO DETERMINE TEMPERATURE IN DEPEN
     *D.  TERMINATING.'/' FPE =',G15.6,' TEMP =',G15.6)
      STOP
   46 DXCV=YFRM*RU*(DXGAM/GMOL-(GAM-1.E0)/GMOLF/GMOLF*DXGMOL)
      DFPE=1.E0+(DXEMIX/CV-EMIX/CV/CV*DXCV)*YFR*CVI/YFRM
      TEMP=TEMP-FPE/DFPE
      NITE=NITE+1
      GO TO 32
   48 IF(YFR.LT..999E0) DXTEMP=RU/GMOL*((1.E0/RHO-B)-PC/RHO/RHO*DRHO)
      BIT=-YFR
      IF(NVDAT.EQ.0) BIT=1.E0-YFR
      DPLEIN=(-DEP-BIT0*YFR*CVI*DXTEMP)/BIT0
      IF(YFR.LT..999E0) DPLEIN=DPLEIN/YFRM/(1.E0-BIT*ALF*C*DXECHB/BIT0
     *                                      /YFRM)
      BIT1=(GAM-1.E0)*BIT0*EMIX
      BIT2=VOL-B*BIT0
      BIT4=BIT2+BIT3/RHOP
      IF(ALF.LT..99999E0) GO TO 50
      IF(YFR.GT.1.E-10.AND.YFR.LT..999E0) GO TO 50
      PC=BIT1/BIT2
      GO TO 100
C
C     PRESSURE AND LIQUID DENSITY ARE COUPLED NONLINEARLY
C
   50 FP=PC-BIT1/BIT4
      IF( ABS(FP).LT.PTOL*PC) GO TO 100
      IF(NIT.LT.50) GO TO 80
      WRITE(6,60) FP,PC
   60 FORMAT(' MORE THAN 50 ITERATIONS TO DETERMINE PRESSURE IN DEPEND.
     *TERMINATING.'/
     *' FP =',G15.6,' PC =',G15.6)
      STOP
   80 DFP=1.E0-DRHOP*BIT1*BIT3/(BIT2*RHOP+BIT3)**2
     *       -DPLEIN*DXEMIX*(GAM-1.E0)*BIT0*RHOP/(BIT2*RHOP+BIT3)
      PC=PC-FP/DFP
```

```
      NIT=NIT+1
      GO TO 30
  100 IF(NPASS.EQ.2) GO TO 160
C
C     CHECK WHETHER CONSTANT PRESSURE SOLUTION HAS BEEN OBTAINED
C
      IF(MORE.EQ.0) GO TO 220
      IF( ABS(PC-PSEEK).LT.PTOLC*PSEEK) GO TO 220
      IF(ITER.LT.100) GO TO 120
      WRITE(6,110) PC,PLE,PLEL,PLEH
  110 FORMAT(' MORE THAN 100 ITERATIONS IN SEARCH FOR CONSTANT PRESSURE
     *SOLUTION. TERMINATING.'/
     *' PC,PLE,PLEL,PLEH ',4G15.6)
      STOP
  120 IF(PC.GT.PSEEK) PLEH=PLE
      IF(PLEH.GT.TOTPE) PLEH=TOTPE
      IF(PC.LT.PSEEK) PLEL=PLE
      IF(PLE.LT.0.E0) PLEL=0.E0
      IF(PLEL.GT.TOTPE) PLEL=TOTPE
      ITER=ITER+1
      IF(PLEL.LT.0.999*TOTPE) GO TO 26
      MORE=0
      ERATE=1.E0/TIME
      GO TO 26
  160 IF(NBAL.EQ.0) GO TO 220
C
C     CHECK WHETHER OBSERVED BALLISTICS ARE MATCHED
C
      IF(ALFOLD.GT.0.999E0) GO TO 220
      FP=PC/PSEEK-1.E0
      IF( ABS(FP).LT.ATOL1) GO TO 200
      IF(ITER.LT.100) GO TO 170
      IF(NSRCH.EQ.1) GO TO 210
      IF( ABS(FP).GT.ATOL2) GO TO 164
      WRITE(6,162) TIME,FP
  162 FORMAT(' AT TIME =',G12.5,' ALPHA SEARCH HAS FP = ',G12.5,
     *       ' CONTINUING.')
      GO TO 200
  164 WRITE(6,165) TIME,PC,PSEEK,ALF,BET
  165 FORMAT(' MORE THAN 100 ITERATIONS TO MATCH BALLISTICS. TERMINATING
     *.'/' TIME =',G12.5,' PC =',G12.5,' PSEEK =',G12.5,' ALPHA =',
     *  G12.5,' BETA =',G12.5)
      STOP
  170 IF(ITER.GT.0) GO TO 175
  172 ALFW=ALF
      FPW=FP
      ALF=ALF+0.01
      GO TO 180
  175 DFP=(FP-FPW)/(ALF-ALFW)
      ALFW=ALF
      FPW=FP
      IF( ABS(DFP).LT.1.E-5) GO TO 172
      ALF=ALF-FP/DFP
      IF(NSRCH.EQ.1.AND.ALF.LT.ALF1) GO TO 205
```

```
      IF(ALF.LT.0.E0) ALF=ALFW/2.E0
      IF(ALF.GT.1.E0) ALF=(1.E0+ALFW)/2.E0
      IF(NSRCH.EQ.0) GO TO 180
      IF( ABS(ALF-ALFW).LT.1.E-6) GO TO 205
  180 ITER=ITER+1
      GO TO 12
C
C     CHECK FOR MONOTONICITY OF ALPHA
C
  200 IF(NVDAT.EQ.0) GO TO 220
      IF(ALF.LT.ALFOLD-1.E-3) GO TO 204
      IF(NSRCH.EQ.0) GO TO 220
C
C     ACCEPT LOWER ROOT IF CLOSER TO EXPECTED VALUE AND DOWNTREND HAS
C     NOT BEEN ESTABLISHED
C
      IF(DATEX.LT.1.E-10) GO TO 220
      IF(BEX.LT.-1.E-10) GO TO 220
      IF( ABS(ALF-DATEX).LT. ABS(ALF2-DATEX)) GO TO 220
      GO TO 210
  204 IF(NSRCH.EQ.0) ALF2=ALF
      NSRCH=1
  205 IF(ALF1.GE..989E0) GO TO 210
      ALF1=ALF1+0.01E0
      ALF=ALF1
      ITER=0
      GO TO 12
  210 ALF=ALF2
C
C     CAIL TO GRAD TO GET BREECH AND BASE PRESSURES
C
  220 CALL GRAD(PC,PBR,PB,XP,VP,RES,TOTKE,1,0,0,0)
      VOL=BIT5
      RETURN
      END
```

```
      SUBROUTINE EOSLIQ(PIN,RHOP,DRHOP,EP,DEP)
C
C     DETERMINES DENSITY (RHOP) AND INTERNAL ENERGY (EP) OF WORKING
C     FLUID AS A FUNCTION OF PRESSURE (PIN) TOGETHER WITH DERIVATIVES
C     DRHOP AND DEP.
C
      COMMON/C1/ PRM,PRTRV,DB,AB,V0,C,RHOP0,AK1,AK2,QV,B,GAM,BET,
     *           DTNOM,XM0,P0,G,EG0,GMOL,TEMP,PRR,ALF,EFRAC,RATE,
     *           PBSK,PI,RU,ALFOLD,TOTPE,TOTPM,PLM,PLE
     *           ,GAM0,B0,GMOL0,ECHB0,EG00
C
      P=PIN-0.101E0
      IF(P.GT.0.E0) GO TO 10
      RHOP=RHOP0
      DRHOP=0.E0
      EP=0.E0
      DEP=0.E0
      GO TO 80
   10 IF( ABS(AK2).GT.1.E-6) GO TO 20
      RHOP=RHOP0*(1.E0+P/AK1)
      DRHOP=RHOP0/AK1
      GO TO 40
   20 RHOP=RHOP0*(1.E0+AK2/AK1*P)**(1.E0/AK2)
      DRHOP=RHOP0/AK1*(1.E0+AK2/AK1*P)**((1.E0-AK2)/AK2)
   40 EP=-P/RHOP
      DEP=-1.E0/RHOP+P/RHOP/RHOP*DRHOP
      IF( ABS(AK2).GT.1.E-6.AND. ABS(AK2-1.E0).GT.1.E-6) GO TO 60
      EP=EP+AK1/RHOP0*ALOG(1.E0+P/AK1)
      DEP=DEP+1.E0/RHOP/(1.E0+P/AK1)
      GO TO 80
   60 EP=EP+(AK1+AK2*P)/(AK2-1.E0)/RHOP-AK1/(AK2-1.E0)/RHOP0
      DEP=DEP+(AK2-(AK1+AK2*P)/RHOP*DRHOP)/(AK2-1.E0)/RHOP
   80 EP=(1.E0-ALF)*C*EP
      DEP=(1.E0-ALF)*C*DEP
      RETURN
      END
```

```
      SUBROUTINE INTERP(X,Y,DYDX,XA,YA,NXTRAP,N)
C
C     INTERPOLATE (XA,YA) ARRAYS TO GET Y(X) AND DERIVATIVE DYDX.
C     IF X IS OUTSIDE RANGE OF XA, Y IS SET EQUAL TO FIRST OR LAST
C     VALUE OF YA UNLESS NXTRAP = 1 IN WHICH CASE LINEAR EXTRAPOLATION
C     IS USED FOR X > XA(N).
C     IF N IS LESS THAN TWO, Y IS SET EQUAL TO ZERO.
C
      DIMENSION XA(N),YA(N)
C
      Y=0.E0
      DYDX=0.E0
      IF(N.LT.2) GO TO 50
      IF(X.LT.XA(1)) GO TO 30
      IF(X.GT.XA(N)) GO TO 40
      DO 10 I=2,N
      IF(XA(I).GT.X) GO TO 20
   10 CONTINUE
      GO TO 40
C
C     X IS IN TABLE RANGE. INTERPOLATE.
C
   20 BIT=XA(I)-XA(I-1)
      IF(BIT.GT.1.E-10) DYDX=(YA(I)-YA(I-1))/BIT
      Y=YA(I-1)+(X-XA(I-1))*DYDX
      GO TO 50
C
C     X IS OUTSIDE TABLE RANGE. USE FIRST OR LAST VALUE OF YA.
C
   30 Y=YA(1)
      GO TO 50
   40 IF(NXTRAP.EQ.1) GO TO 45
      Y=YA(N)
      GO TO 50
   45 I=N
      GO TO 20
   50 RETURN
      END
```

```
      SUBROUTINE GRAD(PC,PBRCH,PB,XP,VP,RES,TOTKE,IND,INIT,KALC,MODE)
C
C     ACTION DEPENDS ON VALUE OF INPUT DATUM MODE.  WHEN MODE = 0, GRAD
C     COMPUTES EFFECT OF PRESSURE GRADIENT.  PC, PBRCH AND PB ARE
C     SPACEMEAN, BREECH AND BASE PRESSURES RESPECTIVELY.
C     XP AND VP ARE PROJECTILE DISPLACEMENT AND VELOCITY RESPECTIVELY.
C     RES IS BORE RESISTANCE PRESSURE.  TOTKE IS KINETIC ENERGY OF
C     MOVING FLUID.
C     IND = 1, 2 OR 3 ACCORDING AS PC, PBRCH OR PB IS SUPPLIED AS INPUT
C     TO ROUTINE.
C     INIT = 1 FOR INITIALIZATION CALL (NECESSARY IF CHAMBER GEOMETRY
C     IS NEWLY ENTERED TO PROGRAM) AND 0 SUBSEQUENTLY.
C     KALC = 0 IF THE CHAMBER INTEGRALS NEED TO BE UPDATED AT A STEP
C     DURING THE SOLUTION AND 1 IF THE VALUES ARE ALREADY KNOWN.
C
C     INPUT ARE XP, VP, RES, IND, INIT, KALC AND MODE AND ONE OF PC, PBR
C     OR PB.
C
C     WHEN MODE=1, GRAD COMPUTES THE VALUE OF THE SLIP COEFFICIENT BET
C     (COMMON BLOCK /C1/) TO MATCH THE VALUES OF PBRCH AND PB.
C
C     INPUT ARE XP, VP, RES, IND, INIT, KALC AND MODE AND BOTH PBRCH
C     AND PB.
C
      PARAMETER (NYI=4,NYPD=4)
C
      COMMON/C1/ PRM,PRTRV,DB,AB,V0,C,RHOP0,AK1,AK2,QV,B,GAM,BET,
     *           DTNOM,XM0,P0,G,EG0,GMOL,TEMP,PBR,ALF,EFRAC,RATE,
     *           PBSK,PI,RU,ALFOLD,TOTPE,TOTPM,PLM,PLE
     *           ,GAM0,B0,GMOL0,ECHB0,EG00
      COMMON/C6/ TIME,YI(NYI),YDP(NYPD),YDT(NYI)
      COMMON/C10/ ZA(20),RA(20),NSTA,NSPLT
C
      IF(INIT.EQ.0) GO TO 100
C
C     INITIALIZATION
C
      IF(NSTA.EQ.0) RETURN
      IF(NSTA.LT.2.OR.NSTA.GT.20) GO TO 320
      IF(NSPLT.LT.1) NSPLT=1
      VOL0=0.E0
      AJ10=0.E0
      AJ30=0.E0
      AJ40=0.E0
      Z=0.E0
      CALL INTERP(0.E0,R,DUM,ZA,RA,0,NSTA)
      AL=PI*R*R
      VOL0L=0.E0
      AJ10L=0.E0
      AJ2L=0.E0
      DO 80 I=2,NSTA
      DZ=(ZA(I)-ZA(I-1))/ FLOAT(NSPLT)
      DO 60 J=1,NSPLT
      Z=Z+DZ
```

```
      CALL INTERP(Z,R,DUM,ZA,RA,0,NSTA)
      A=PI*R*R
      VOLO=VOLO+DZ*(A+AL)/2.E0
      AJ10=AJ10+DZ*(VOLO+VOLOL)/(A+AL)
      AJ2=(VOLO/A)**2
      AJ30=AJ30+DZ*(A+AL)*(AJ10+AJ10L)/4.E0
      AJ40=AJ40+DZ*(A+AL)*(AJ2+AJ2L)/4.E0
      AL=A
      VOLOL=VOLO
      AJ10L=AJ10
      AJ2L=AJ2
   60 CONTINUE
   80 CONTINUE
      WRITE(6,90) VOLO,AJ10,AJ30,AJ40
   90 FORMAT(//' GRAD INTEGRALS ... VOLO:',G12.4,' AJ10:',G12.4,' AJ30:'
     *,G12.4,' AJ40:',G12.4//)
      RETURN
C
C     COMPUTE PRESSURE GRADIENT
C
  100 IF(MODE.EQ.0) GO TO 102
      IF(NSTA.EQ.0) GO TO 140
      GO TO 200
  102 IF(IND.LT.1.OR.IND.GT.3) GO TO 300
      XK=(C*(ALF+BET*(1.E0-ALF))+PLM+XM0)/PRM
      IF(NSTA.GT.0) GO TO 200
C
C     LAGRANGE GRADIENT ANALYSIS
C
      XK2=1.E0+XK/2.E0
      XK3=1.E0+XK/3.E0
      TOTKE=XK*PRM/6.E0/G*VP*VP
      GO TO (110,120,130),IND
C
C     MEAN PRESSURE IS GIVEN
C
  110 PBRCH=PC*XK2/XK3
      PB=PC/XK3
      RETURN
C
C     BREECH PRESSURE IS GIVEN
C
  120 PC=PBRCH*XK3/XK2
      PB=PBRCH/XK2
      RETURN
C
C     BASE PRESSURE IS GIVEN
C
  130 PC=PB*XK3
      PBRCH=PB*XK2
      RETURN
C
C     COMPUTE SLIP COEFFICIENT
C
```

```
  140 BET=1.E0
      IF(ALF.GT..999E0) RETURN
      BET=(2.E0*PRM/C*(PBRCH/PB-1.E0)-ALF-(PLM+XM0)/C)/(1.E0-ALF)
C      IF(BET.LT.0.E0) BET=0.E0
C      IF(BET.GT.1.E0) BET=1.E0
      RETURN
C
C     CHAMBRAGE PRESSURE GRADIENT ANALYSIS
C
  200 IF(KALC.EQ.1) GO TO 205
      XP2=XP*XP
      VOL=VOL0+AB*XP
      AJ1=AJ10+VOL0/AB*XP+0.5E0*XP2
      AJ2=VOL*VOL/AB/AB
      AJ3=AJ30+AB*AJ10*XP+VOL0/2.E0*XP2+AB/6.E0*XP*XP2
      AJ4=AJ40+(VOL**3-VOL0**3)/3.E0/AB/AB
      A1T=XK*PRM*AB/G/VOL/VOL*(AB*VP*VP/VOL+G*AB/PRM*RES)
      A2T=-XK/AJ2
      BT=-XK*PRM/2.E0/G*VP*VP/AJ2/VOL
      IF(MODE.EQ.1) GO TO 240
      XK1=A1T*AJ1+BT*AJ2-A1T*AJ3/VOL-BT*AJ4/VOL
      XK2=1.E0-A2T*AJ1+A2T*AJ3/VOL
      XK3=1.E0-A2T*AJ1
      XK4=-A1T*AJ1-BT*AJ2
      TOTKE=XK*PRM/2.E0/G*AJ4/AJ2/VOL*VP*VP
  205 GO TO (210,220,230),IND
C
C     MEAN PRESSURE IS GIVEN
C
  210 PBRCH=XK3/XK2*PC+XK3*XK1/XK2+XK4
      PB=(PC+XK1)/XK2
      RETURN
C
C     BREECH PRESSURE IS GIVEN
C
  220 PC=XK2/XK3*(PBRCH-XK3*XK1/XK2-XK4)
      PB=(PBRCH-XK4)/XK3
      RETURN
C
C     BASE PRESSURE IS GIVEN
C
  230 PC=XK2*PB-XK1
      PBRCH=XK3*PB+XK4
      RETURN
C
C     COMPUTE SLIP COEFFICIENT
C
  240 A1T=A1T/XK
      A2T=A2T/XK
      BT=BT/XK
      XK=-(PBRCH-PB)/(A2T*AJ1*PB+A1T*AJ1+BT*AJ2)
      BET=(PRM/C*XK-ALF-(PLM+XM0)/C)/(1.E0-ALF)
      IF(BET.LT.0.E0) BET=0.E0
      IF(BET.GT.1.E0) BET=1.E0
```

```
      RETURN
  300 WRITE(6,310) IND
  310 FORMAT(' GRAD CALLED WITH INVALID ARGUMENT IND =',I5,' TERMINATING
     *.')
      STOP
  320 WRITE(6,330) NSTA
  330 FORMAT(' GRAD CALLED WITH INVALID ARGUMENT NSTA =',I5,
     *' TERMINATING.')
      STOP
      END
```

```
      SUBROUTINE SMOOTH
C
C     ROUTINE TO FILTER HIGH FREQUENCY COMPONENTS OF DATA ARRAYS
C
      COMPLEX ARRAY,XND
      COMMON/C9/ BALT(1000),BALP(1000),BALPB(1000),NBAL
      DIMENSION ARG(2000),ARRAY(1000,2),XND(3)
C
      EQUIVALENCE (ARG(1),BALP(1))
C
      DATA XND/(0.49965,0.),(-0.22227,0.64240),(-0.22227,-0.64240)/
C
      DO 100 IC=1,2
      IBIAS=1000*(IC-1)
      DO 10 I=1,NBAL
      I1=I+IBIAS
      ARRAY(I,1)=ARG(I1)
   10 CONTINUE
      J1=2
      J2=NBAL-1
      DO 30 I=1,3
      K=MOD(I,2)+1
      L=MOD(I+1,2)+1
      DO 20 J=J1,J2
      ARRAY(J,K)=ARRAY(J,L)+0.5*XND(I)*(ARRAY(J-1,L)+ARRAY(J+1,L)-
     +           2.*ARRAY(J,L))
   20 CONTINUE
      ARRAY(1,K)=ARRAY(1,L)
      ARRAY(NBAL,K)=ARRAY(NBAL,L)
   30 CONTINUE
      DO 40 J=1,NBAL
      J1=J+IBIAS
      BIT=REAL(ARRAY(J,K))
      ARG(J1)=BIT
   40 CONTINUE
  100 CONTINUE
      RETURN
      END
```

```
      SUBROUTINE REGR
C
C     COMPUTES LEAST SQUARES FIT TO (DAT,DATA).
C
      PARAMETER (NYI=4,NYPD=4)
C
      COMMON/C6/ TIME,YI(NYI),YDP(NYPD),YDT(NYI)
      COMMON/C12/ DAT(20),DATA(20),DATEX,AEX,BEX,NDTR,NSTEP
C
      XNDTR=NDTR
      TAV=0.E0
      AEX=0.E0
      STA=0.E0
      ST=0.E0
      DO 10 I=1,NDTR
      TAV=TAV+DAT(I)
      AEX=AEX+DATA(I)
      STA=STA+DAT(I)*DATA(I)
      ST=ST+DAT(I)*DAT(I)
   10 CONTINUE
      TAV=TAV/XNDTR
      AEX=AEX/XNDTR
      BEX=(STA-XNDTR*TAV*AEX)/(ST-XNDTR*TAV*TAV)
      DATEX=AEX+BEX*(TIME-TAV)
      RETURN
      END
```

APPENDIX B

PMAP: Code Listing and Description of Input

INTENTIONALLY LEFT BLANK.

```
C*MFST $STORAGE:2
C     PROGRAM TO STUDY DEPENDENCE OF PRESSURE ON FRACTION OF WORKING
C     FLUID CONVERTED TO GAS.  ASSUMES BLAKE CODE CHARACTERIZATION OF
C     EQUATION OF STATE.
C
C     VERSION 1.0 (DECEMBER 1989) WRITTEN FOR F77 COMPILER ON CRAY.
C
C     ************************************************************************
C     CODE MAY BE CONVERTED TO VERSION COMPATIBLE WITH MICROSOFT F77
C     COMPILER BY MEANS OF GLOBAL TEXT EDITING COMMAND OF THE FORM:
C
C     REPLACE 'C*MSFT ' WITH ' '.
C
C     ************************************************************************
C     MICROSOFT F77 VERSION PROMPTS AT TERMINAL FOR INPUT DATA FILE NAME
C     (FILNAM) AND OUTPUT FILE NAME (OUTFIL).  THE OUTPUT WILL BE
C     DIRECTED TO THE PRINTER IF OUTFIL IS ENTERED AS PRN.
C
C     ************************************************************************
C     DESCRIPTION OF INPUT DATA (ASSUMED TO BE LOCATED IN FILE LABELED
C     FILNAM):
C
C     FILE 1.0:  "FILE COUNTERS" (3I5) ONE CARD.
C     NVDAT      - NUMBER OF SETS OF DATA IN FILE 2.0.
C                  NVDAT MAY NOT BE GREATER THAN 100.
C     NCOV       - NUMBER OF DATA IN FILE 3.0.
C                  NCOV MAY NOT BE GREATER THAN 10.
C     NEOV       - NUMBER OF DATA IN FILE 4.0.
C                  NEOV MAY NOT BE GREATER THAN 5.
C
C     FILE 2.0:  "PROPERTIES OF FINAL DECOMPOSITION OF WORKING FLUID
C                 AS A FUNCTION OF TOTAL INJECTED PLASMA ENERGY"
C                 (4F10.0)       NVDAT CARDS.
C     VEIN(1)    - FIRST VALUE OF PLASMA ENERGY PER UNIT MASS
C                  OF WORKING FLUID (J/G).
C     VEFF(1)    - CORRESPONDING VALUE OF EFFECTIVE INTERNAL ENERGY
C                  (J/G).
C     VGAM(1)    - CORRESPONDING VALUE OF RATIO OF SPECIFIC HEATS (-).
C     VB(1)      - CORRESPONDING VALUE OF COVOLUME (CC/G).
C     VEIN(2)    - SECOND VALUE OF PLASMA ENERGY PER UNIT MASS
C                  OF WORKING FLUID (J/G).  STARTS A NEW CARD.
C                .
C                .
C     VB(NVDAT)
C
C     NOTES:       IF THE ENERGY DENSITY OF THE MIXTURE OF PLASMA
C                  AND DECOMPOSED WORKING FLUID LIES OUTSIDE THE
C                  RANGE OF THE TABLE THE FIRST OR LAST VALUES ARE
C                  USED TO DETERMINE THE EFFECTIVE PROPERTIES OF
C                  THE MIXTURE.
```

```
C                  THE ONLY EXCEPTION TO THIS RULE OCCURS FOR THE
C                  EFFECTIVE INTERNAL ENERGY AT VALUES OF ENERGY
C                  DENSITY LARGER THAN VEIN(NVDAT).  THE EFFECTIVE
C                  INTERNAL ENERGY IS DETERMINED IN THIS CASE BY
C                  LINEAR EXTRAPOLATION OF THE LAST TWO VALUES IN
C                  THE TABLE.
C                  INSIDE THE TABLE RANGE LINEAR INTERPOLATION IS
C                  USED TO DETERMINE VALUES OF ALL PROPERTIES.
C
C     FILE 3.0:  "VALUES OF C/V"   (8F10.0) ONE OR TWO CARDS.
C     DEN(1)     - FIRST VALUE OF C/V (G/CC), THE RATIO OF THE TOTAL
C                  MASS OF WORKING FLUID TO THE TOTAL CHAMBER VOLUME.
C     DEN(2)     - SECOND VALUE OF C/V.
C                  .
C                  .
C     DEN(NCOV)
C
C     FILE 4.0:  "VALUES OF E/C"   (8F10.0) ONE CARD.
C     EDEN(1)    - FIRST VALUE OF E/C (J/G), THE RATIO OF THE TOTAL
C                  ENERGY TO THE TOTAL MASS OF THE WORKING FLUID.
C     EDEN(2)    - SECOND VALUE OF E/C (J/G).
C                  .
C                  .
C     EDEN(NEOV)
C
C     FILE 5.0: "PROPERTIES OF UNDECOMPOSED WORKING FLUID"
C                                          (3F10.0) ONE CARD.
C     RHOP0      - DENSITY OF WORKING FLUID AT ONE ATMOSPHERE (G/CC).
C     AK1        - BULK MODULUS AT ONE ATMOSPHERE (MPA).
C     AK2        - DERIVATIVE OF MODULUS WITH RESPECT TO PRESSURE (-).
C
C     ***************************************************************
      CHARACTER*10 FILNAM,OUTFIL
C
      COMMON/C1/ RHOP0,AK1,AK2
C
      DIMENSION PRES(50,10),DEN(10),EDEN(5),VEIN(100),VEFF(100),
     *          VGAM(100),VB(100)
C
C     NAME FILES FOR INPUT AND OUTPUT ON MICROCOMPUTER
C
C*MFST       WRITE(*,1)
C*MFST    1 FORMAT(' ENTER INPUT DATA FILE NAME: '\)
C*MFST      READ(*,2) FILNAM
C*MFST    2 FORMAT(A10)
C*MFST      OPEN(5,FILE=FILNAM)
C*MFST      WRITE(*,3)
C*MFST    3 FORMAT(' ENTER OUTPUT FILE NAME: '\)
C*MFST      READ(*,2) OUTFIL
C*MFST      OPEN(6,FILE=OUTFIL)
C
```

```
C     READ AND WRITE INPUT DATA
C
      READ(5,1001) NVDAT,NCOV,NEOV
      READ(5,1005)(VEIN(I),VEFF(I),VGAM(I),VB(I),I=1,NVDAT)
      READ(5,1002) (DEN(I),I=1,NCOV)
      READ(5,1002) (EDEN(I),I=1,NEOV)
      READ(5,1002) RHOP0,AK1,AK2
      WRITE(6,2120) NVDAT,NCOV,NEOV
      WRITE(6,2130) (VEIN(I),VEFF(I),VGAM(I),VB(I),I=1,NVDAT)
      WRITE(6,2132) (DEN(I),I=1,NCOV)
      WRITE(6,2134) (EDEN(I),I=1,NEOV)
      WRITE(6,2060) RHOP0,AK1,AK2
C
C     CALCULATE VALUES OF PRESSURE
C
      DO 300 K=1,NEOV
      EOC=EDEN(K)
      DO 200 J=1,NCOV
      COV=DEN(J)
      DO 100 I=1,50
      ALF=0.02E0* FLOAT(I)
      PLEIN=EOC/ALF
      CALL INTERP(PLEIN,EMIX,DXEMIX,VEIN,VEFF,1,NVDAT)
      CALL INTERP(PLEIN,GAM,DXGAM,VEIN,VGAM,0,NVDAT)
      CALL INTERP(PLEIN,B,DXB,VEIN,VB,0,NVDAT)
      BIT1=(GAM-1.E0)*ALF*EMIX
      BIT2=1.E0/COV-B*ALF
      BIT3=-(1.E0-ALF)
      PC=0.E0
      BIT4=BIT2+BIT3/RHOP0
      IF(BIT4.LT.1.E-3) GO TO 90
      PC=BIT1/BIT4
      NIT=0
   30 CALL EOSLIQ(PC,RHOP,DRHOP,EP,DEP)
      BIT4=BIT2+BIT3/RHOP
C
C     PRESSURE AND LIQUID DENSITY ARE COUPLED NONLINEARLY
C
   50 FP=PC-BIT1/BIT4
      IF( ABS(FP).LT.1.E-4*PC) GO TO 90
      IF(NIT.LT.50) GO TO 80
      WRITE(6,60) FP,PC
   60 FORMAT(' MORE THAN 50 ITERATIONS TO DETERMINE PRESSURE IN DEPEND.
     *TERMINATING.'/
     *' FP =',G15.6,' PC =',G15.6)
      STOP
   80 DFP=1.E0-DRHOP*BIT1*BIT3/(BIT2*RHOP+BIT3)**2
      PC=PC-FP/DFP
      NIT=NIT+1
      GO TO 30
   90 PRES(I,J)=PC
  100 CONTINUE
  200 CONTINUE
C
```

```
C     PRINT TABLE OF RESULTS
C
      WRITE(6,2090)
      WRITE(6,3000) EDEN(K),(DEN(J),J=1,NCOV)
      DO 260 I=1,50
      ALF=0.02E0* FLOAT(I)
      WRITE(6,3010) ALF,(PRES(I,J),J=1,NCOV)
  260 CONTINUE
  300 CONTINUE
      STOP
C
C     FORMAT STATEMENTS
C
 1001 FORMAT(16I5)
 1002 FORMAT(8F10.0)
 1005 FORMAT(4F10.0)
 2060 FORMAT(' '//
     *' ',5X,'PROPERTIES OF UNDECOMPOSED WORKING FLUID'//
     *' DENSITY OF FLUID AT 1 ATM.(G/CC)              ',F10.4/
     *' BULK MODULUS AT 1 ATM.(MPA)                   ',F10.1/
     *' DERIVATIVE OF MODULUS W.R.T. PRESSURE(-)      ',F10.3//)
 2120 FORMAT(' PRESSURE AS A FUNCTION OF FRACTION OF WORKING FLUID CONVE
     *RTED TO GAS'//
     *' NUMBER OF DATA TO DETERMINE THERMOCHEMISTRY  ',I5/
     *' NUMBER OF VALUES OF C/V                      ',I5/
     *' NUMBER OF VALUES OF E/C                      ',I5//)
 2130 FORMAT(' ',5X,'ENERGY(J/G)',5X,'EFF.ENGY.(J/G)',8X,'GAMMA(-)',
     *5X,'COVOLUME(CC/G)'//(' ',2F15.1,5X,2F15.4))
 2132 FORMAT(' '//' VALUES OF C/V (G/CC):'//(' ',10G12.5))
 2134 FORMAT(' '//' VALUES OF E/C (J/G):'//(' ',5G12.5))
 2090 FORMAT('1')
 3000 FORMAT(' ',10X,'PRESSURE AS A FUNCTION OF ALPHA AND C/V FOR E/C ='
     *,G12.5//' ',6X,'ALPHA',40X,'C/V'/' ',10X,10F10.3//)
 3010 FORMAT(' ',F10.4,10F10.1)
      END
```

```
      SUBROUTINE INTERP(X,Y,DYDX,XA,YA,NXTRAP,N)
C
C     INTERPOLATE (XA,YA) ARRAYS TO GET Y(X) AND DERIVATIVE DYDX.
C     IF X IS OUTSIDE RANGE OF XA, Y IS SET EQUAL TO FIRST OR LAST
C     VALUE OF YA UNLESS NXTRAP = 1 IN WHICH CASE LINEAR EXTRAPOLATION
C     IS USED FOR X > XA(N).
C     IF N IS LESS THAN TWO, Y IS SET EQUAL TO ZERO.
C
      DIMENSION XA(N),YA(N)
C
      Y=0.E0
      DYDX=0.E0
      IF(N.LT.2) GO TO 50
      IF(X.LT.XA(1)) GO TO 30
      IF(X.GT.XA(N)) GO TO 40
      DO 10 I=2,N
      IF(XA(I).GT.X) GO TO 20
   10 CONTINUE
      GO TO 40
C
C     X IS IN TABLE RANGE. INTERPOLATE.
C
   20 BIT=XA(I)-XA(I-1)
      IF(BIT.GT.1.E-10) DYDX=(YA(I)-YA(I-1))/BIT
      Y=YA(I-1)+(X-XA(I-1))*DYDX
      GO TO 50
C
C     X IS OUTSIDE TABLE RANGE. USE FIRST OR LAST VALUE OF YA.
C
   30 Y=YA(1)
      GO TO 50
   40 IF(NXTRAP.EQ.1) GO TO 45
      Y=YA(N)
      GO TO 50
   45 I=N
      GO TO 20
   50 RETURN
      END
```

```
      SUBROUTINE EOSLIQ(PIN,RHOP,DRHOP,EP,DEP)
C
C     DETERMINES DENSITY (RHOP) AND INTERNAL ENERGY (EP) OF WORKING
C     FLUID AS A FUNCTION OF PRESSURE (PIN) TOGETHER WITH DERIVATIVES
C     DRHOP AND DEP.  PMAP VERSION SETS EP=DEP=0.E0
C
      COMMON/C1/ RHOP0,AK1,AK2
C
      P=PIN-0.101E0
      IF(P.GT.0.E0) GO TO 10
      RHOP=RHOP0
      DRHOP=0.E0
      EP=0.E0
      DEP=0.E0
      RETURN
   10 IF( ABS(AK2).GT.1.E-6) GO TO 20
      RHOP=RHOP0*(1.E0+P/AK1)
      DRHOP=RHOP0/AK1
      GO TO 40
   20 RHOP=RHOP0*(1.E0+AK2/AK1*P)**(1.E0/AK2)
      DRHOP=RHOP0/AK1*(1.E0+AK2/AK1*P)**((1.E0-AK2)/AK2)
   40 EP=0.E0
      DEP=0.E0
      RETURN
      END
```

APPENDIX C

Nominal Data Base for Lumped Parameter Study of Ballistic Implications of Rate of Mixing

INTENTIONALLY LEFT BLANK.

LUMPED PARAMETER SIMULATION OF ELECTROTHERMAL GUN

r971 - CONSTANT PRESSURE SOLUTION FOR V=97.1

INTEGRATION TIME STEP(MS)	0.010
PRESSURE CONVERGENCE TOLERANCE(-)	0.1000E-03
CONVERGENCE TOLERANCE FOR CONSTANT PRESSURE SOLUTION(-)	0.1000E-03
TEMPERATURE CONVERGENCE TOLERANCE(-)	0.1000E-03
FIRST CONVERGENCE TOLERANCE FOR FRACTION OF WORKING FLUID DECOMPOSED(-)	0.1000E-03
SECOND CONVERGENCE TOLERANCE FOR FRACTION OF WORKING FLUID DECOMPOSED(-)	0.1000E-01

NUMBER OF STEPS FOR SOLUTION PRINTOUT	5
PROJECTILE MASS(G)	18.00
PROJECTILE TRAVEL(CM)	145.00
BORE DIAMETER(CM)	1.40
VOLUME OF MIXING CHAMBER(CC)	97.1
INITIAL TEMPERATURE OF GAS(K)	300.0
INITIAL PRESSURE(MPA)	0.1
CONSTANT BREECH PRESSURE(MPA)	435.0
RATE OF DECOMPOSITION OVER RATE OF ENERGY ADDITION(-)	1.000

NUMBER OF DATA TO DESCRIBE CHAMBER GEOMETRY (0 IMPLIES LAGRANGE GRADIENT; >1 IMPLIES CHAMBRAGE GRADIENT)	0
NUMBER OF SUBDIVISIONS FOR CHAMBER INTEGRALS	0

NUMBER OF BORE RESISTANCE DATA	2
AIR SHOCK RESISTANCE (0=NO;1=YES)	0

TRAVEL(CM)	RESISTANCE(MPA)
0.00	0.0
1.27	0.0

PROPERTIES OF UNDECOMPOSED WORKING FLUID

MASS OF WORKING FLUID(G)	44.8
DENSITY OF FLUID AT 1 ATM.(G/CC)	1.0000
BULK MODULUS AT 1 ATM.(MPA)	5000.0
DERIVATIVE OF MODULUS W.R.T. PRESSURE(-)	8.000
HEAT OF VAPORIZATION(J/G)	0.0
SLIP COEFFICIENT(-) (0=LIQUID AT REST;1=LIQUID HAS LAGRANGE VELOCITY)	1.00

PROPERTIES OF FINAL PRODUCTS OF DECOMPOSITION

COVOLUME (CC/G)	0.6090
RATIO OF SPECIFIC HEATS (-)	1.2035
MOLECULAR WEIGHT (G/GMOL)	17.6330

PROPERTIES OF INTERMEDIATE PRODUCTS OF DECOMPOSITION

PRE-EXPONENT IN ARRHENIUS REACTION RATE LAW (UNITS YIELD G/CC-SEC)	0.00000
TEMPERATURE EXPONENT IN REACTION RATE LAW (-)	0.00000
ACTIVATION ENERGY (J/GMOL)	0.00000
REACTION ORDER (-)	0.00000
CHEMICAL ENERGY OF REACTION (J/G)	0.00000
COVOLUME (CC/G)	0.0000
RATIO OF SPECIFIC HEATS (-)	0.0000
MOLECULAR WEIGHT (G/GMOL)	0.0000

NUMBER OF DATA TO DESCRIBE PLASMA DISCHARGE	2
TOTAL PLASMA ENERGY(J)	447800.
TOTAL PLASMA MASS(G)	1.000

TIME(MS)	FRACTION OF ENERGY(-)	FRACTION OF MASS(-)
0.000	0.000000	0.000000
0.800	1.000000	1.000000

NUMBER OF DATA TO DESCRIBE DECOMPOSITION OF WORKING FLUID 2

TIME(MS)	FRACTION OF FLUID DECOMPOSED(-)
0.000	0.000000
0.800	1.000000

NUMBER OF DATA TO DETERMINE THERMOCHEMISTRY 22

ENERGY(J/G)	EFF.ENGY.(J/G)	GAMMA(-)	COVOLUME(CC/G)	MOL. WGT.	DELTA HOF(J/G)
0.0	0.0	1.9414	-1.8340	18.0150	0.0
3000.0	440.0	1.9414	-1.8340	18.0150	0.0
4000.0	1630.0	1.4000	-0.3420	18.0140	0.0
5000.0	2860.0	1.2987	0.0820	18.0140	0.0
6000.0	4080.0	1.2557	0.2830	18.0010	0.0
7000.0	5240.0	1.2323	0.4040	17.9670	0.0
8000.0	6320.0	1.2182	0.4880	17.8960	0.0
9000.0	7310.0	1.2093	0.5540	17.7830	0.0
10000.0	8230.0	1.2035	0.6090	17.6330	0.0
11000.0	9070.0	1.1998	0.6590	17.4500	0.0
12000.0	9850.0	1.1975	0.7050	17.2420	0.0
13000.0	10590.0	1.1962	0.7480	17.0150	0.0
14000.0	11290.0	1.1958	0.7880	16.7750	0.0
15000.0	11950.0	1.1959	0.8260	16.5260	0.0
16000.0	12590.0	1.1964	0.8630	16.2720	0.0
17000.0	13210.0	1.1973	0.8980	16.0150	0.0
18000.0	13810.0	1.1985	0.9310	15.7570	0.0
19000.0	14400.0	1.1998	0.9640	15.5010	0.0
20000.0	14970.0	1.2014	0.9950	15.2480	0.0
21000.0	15550.0	1.2030	1.0250	14.9980	0.0
22000.0	16110.0	1.2048	1.0540	14.7530	0.0
23000.0	16680.0	1.2066	1.0820	14.5120	0.0

NUMBER OF DATA TO SPECIFY OBSERVED BALLISTICS 0
DATA SMOOTHING REQUIRED (0=NO;1=YES) 0
NUMBER OF DATA FOR REGRESSION ANALYSIS OF RATE OF DECOMPOSITION 0

r971 - CONSTANT PRESSURE SOLUTIONS FOR V=97.1

TIME(MS)	P-BR(MPA)	P-BASE(MPA)	TEMP(K)	YFR(-)	PR. DISP(CM)	PR. VEL(M/S)	ALPHA(-)	BETA(-)	E-FRAC(-)
0.000	434.99	193.10	3479.95	0.000	0.00	0.0	0.278	1.000	0.278
0.050	435.02	193.11	3477.66	0.000	0.21	82.6	0.280	1.000	0.280
0.100	435.04	193.11	3470.96	0.000	0.83	165.1	0.285	1.000	0.285
0.150	435.04	193.08	3460.32	0.000	1.86	247.7	0.295	1.000	0.295
0.200	435.01	193.04	3446.45	0.000	3.30	330.3	0.308	1.000	0.308
0.250	434.96	192.98	3430.15	0.000	5.16	412.8	0.325	1.000	0.325
0.300	435.04	192.96	3412.29	0.000	7.43	495.3	0.345	1.000	0.345
0.350	435.01	192.89	3393.60	0.000	10.11	577.8	0.370	1.000	0.370
0.400	435.02	192.83	3374.76	0.000	13.21	660.3	0.398	1.000	0.398
0.450	435.01	192.75	3356.25	0.000	16.72	742.7	0.429	1.000	0.429
0.500	435.03	192.68	3338.45	0.000	20.64	825.1	0.465	1.000	0.465
0.550	435.03	192.58	3321.59	0.000	24.97	907.5	0.504	1.000	0.504
0.600	434.97	192.45	3305.77	0.000	29.71	989.8	0.547	1.000	0.547
0.650	435.04	192.37	3291.15	0.000	34.86	1072.1	0.594	1.000	0.594
0.700	434.96	192.22	3277.61	0.000	40.43	1154.3	0.645	1.000	0.645
0.750	434.96	192.09	3265.44	0.000	46.41	1236.5	0.699	1.000	0.699
0.800	435.01	191.98	3254.47	0.000	52.80	1318.6	0.757	1.000	0.757
0.850	435.02	191.84	3244.42	0.000	59.59	1400.6	0.818	1.000	0.818
0.900	435.01	191.68	3235.22	0.000	66.80	1482.6	0.884	1.000	0.884
0.950	434.97	191.50	3226.79	0.000	74.42	1564.6	0.953	1.000	0.953
1.000	423.99	186.56	3212.10	0.000	82.45	1646.1	1.000	1.000	1.000
1.050	393.89	173.31	3184.45	0.000	90.87	1723.0	1.000	1.000	1.000
1.100	366.47	161.25	3157.26	0.000	99.67	1794.5	1.000	1.000	1.000
1.150	341.54	150.28	3130.62	0.000	108.81	1861.0	1.000	1.000	1.000
1.200	318.88	140.31	3104.58	0.000	118.27	1923.1	1.000	1.000	1.000
1.250	298.27	131.24	3079.18	0.000	128.03	1981.1	1.000	1.000	1.000
1.300	279.52	122.99	3054.45	0.000	138.08	2035.5	1.000	1.000	1.000
1.334	267.83	117.85	3038.15	0.000	145.00	2070.2	1.000	1.000	1.000

MAXIMUM PRESSURE(MPA): 435.0

APPENDIX D

Nominal Data Base for Inverse Analysis

INTENTIONALLY LEFT BLANK.

LUMPED PARAMETER SIMULATION OF ELECTROTHERMAL GUN

TEST CASE BASED ON 40MTC3

INTEGRATION TIME STEP(MS)	.010
PRESSURE CONVERGENCE TOLERANCE(-)	.1000E-03
CONVERGENCE TOLERANCE FOR CONSTANT PRESSURE SOLUTION(-)	.1000E-03
TEMPERATURE CONVERGENCE TOLERANCE(-)	.1000E-03
FIRST CONVERGENCE TOLERANCE FOR FRACTION OF WORKING FLUID DECOMPOSED(-)	.1000E-03
SECOND CONVERGENCE TOLERANCE FOR FRACTION OF WORKING FLUID DECOMPOSED(-)	.1000E-01

NUMBER OF STEPS FOR SOLUTION PRINTOUT	1
PROJECTILE MASS(G)	160.00
PROJECTILE TRAVEL(CM)	400.00
BORE DIAMETER(CM)	4.00
VOLUME OF MIXING CHAMBER(CC)	444.6
INITIAL TEMPERATURE OF GAS(K)	300.0
INITIAL PRESSURE(MPA)	.1
CONSTANT BREECH PRESSURE(MPA)	.0
RATE OF DECOMPOSITION OVER RATE OF ENERGY ADDITION(-)	.000

NUMBER OF DATA TO DESCRIBE CHAMBER GEOMETRY (0 IMPLIES LAGRANGE GRADIENT; >1 IMPLIES CHAMBRAGE GRADIENT)	0
NUMBER OF SUBDIVISIONS FOR CHAMBER INTEGRALS	0

NUMBER OF BORE RESISTANCE DATA	2
AIR SHOCK RESISTANCE (0=NO;1=YES)	0

TRAVEL(CM)	RESISTANCE(MPA)
.00	.0
1.27	.0

PROPERTIES OF UNDECOMPOSED WORKING FLUID

MASS OF WORKING FLUID(G)	420.0
DENSITY OF FLUID AT 1 ATM.(G/CC)	1.0000
BULK MODULUS AT 1 ATM.(MPA)	5000.0
DERIVATIVE OF MODULUS W.R.T. PRESSURE(-)	8.000
HEAT OF VAPORIZATION(J/G)	.0
LAGRANGE COUPLING COEFFICIENT(-) (0=LIQUID AT REST;1=LIQUID HAS LAGRANGE VELOCITY)	1.00

PROPERTIES OF FINAL PRODUCTS OF DECOMPOSITION

COVOLUME (CC/G)	-1.8340
RATIO OF SPECIFIC HEATS (-)	1.9414
MOLECULAR WEIGHT (G/GMOL)	18.0150

PROPERTIES OF INTERMEDIATE PRODUCTS OF DECOMPOSITION

PRE-EXPONENT IN ARRHENIUS REACTION RATE LAW (UNITS YIELD G/CC-SEC)	.00000
TEMPERATURE EXPONENT IN REACTION RATE LAW (-)	.00000
ACTIVATION ENERGY (J/GMOL)	.00000
REACTION ORDER (-)	.00000
CHEMICAL ENERGY OF REACTION (J/G)	.00000
COVOLUME (CC/G)	.0000
RATIO OF SPECIFIC HEATS (-)	.0000
MOLECULAR WEIGHT (G/GMOL)	.0000

NUMBER OF DATA TO DESCRIBE PLASMA DISCHARGE	2
TOTAL PLASMA ENERGY(J)	.200000E+07
TOTAL PLASMA MASS(G)	.000

TIME(MS)	FRACTION OF ENERGY(-)	FRACTION OF MASS(-)
.000	.000000	.000000
2.000	1.000000	1.000000

NUMBER OF DATA TO DESCRIBE DECOMPOSITION OF WORKING FLUID 2

TIME(MS)	FRACTION OF FLUID DECOMPOSED(-)
.000	.000000
4.000	1.000000

NUMBER OF DATA TO DETERMINE THERMOCHEMISTRY 22

ENERGY(J/G)	EFF.ENGY.(J/G)	GAMMA(-)	COVOLUME(CC/G)	MOL. WGT.	DELTA HOF(J/G)
.0	.0	1.9414	-1.8340	18.0150	.0
3000.0	440.0	1.9414	-1.8340	18.0150	.0
4000.0	1630.0	1.4000	-.3420	18.0140	.0
5000.0	2860.0	1.2987	.0820	18.0140	.0
6000.0	4080.0	1.2557	.2830	18.0010	.0
7000.0	5240.0	1.2323	.4040	17.9670	.0
8000.0	6320.0	1.2182	.4880	17.8960	.0
9000.0	7310.0	1.2093	.5540	17.7830	.0
10000.0	8230.0	1.2035	.6090	17.6330	.0
11000.0	9070.0	1.1998	.6590	17.4500	.0
12000.0	9850.0	1.1975	.7050	17.2420	.0
13000.0	10590.0	1.1962	.7480	17.0150	.0
14000.0	11290.0	1.1958	.7880	16.7750	.0
15000.0	11950.0	1.1959	.8260	16.5260	.0
16000.0	12590.0	1.1964	.8630	16.2720	.0
17000.0	13210.0	1.1973	.8980	16.0150	.0
18000.0	13810.0	1.1985	.9310	15.7570	.0
19000.0	14400.0	1.1998	.9640	15.5010	.0
20000.0	14970.0	1.2014	.9950	15.2480	.0
21000.0	15550.0	1.2030	1.0250	14.9980	.0
22000.0	16110.0	1.2048	1.0540	14.7530	.0
23000.0	16680.0	1.2066	1.0820	14.5120	.0

NUMBER OF DATA TO SPECIFY OBSERVED BALLISTICS 0
DATA SMOOTHING REQUIRED (0=NO;1=YES) 0
NUMBER OF DATA FOR REGRESSION ANALYSIS OF RATE OF DECOMPOSITION 0

TEST CASE BASED ON 40MTC3

TIME(MS)	P-BR(MPA)	P-BASE(MPA)	TEMP(K)	YFR(-)	PR. DISP(CM)	PR. VEL(M/S)	ALPHA(-)	BETA(-)	E-FRAC(-)
.000	.12	.05	300.00	.000	.00	.0	.000	1.000	.000
.010	69.83	30.19	3344.89	.000	.00	1.3	.002	1.000	.005
.020	123.43	53.37	3349.85	.000	.00	4.6	.005	1.000	.010
.030	168.89	73.03	3346.30	.000	.01	9.5	.008	1.000	.015
.040	208.98	90.37	3341.96	.000	.02	16.0	.010	1.000	.020
.050	245.00	105.94	3337.69	.000	.04	23.7	.013	1.000	.025
.060	277.66	120.07	3333.51	.000	.07	32.6	.015	1.000	.030
.070	307.38	132.92	3329.33	.000	.11	42.5	.018	1.000	.035
.080	334.42	144.61	3325.05	.000	.16	53.4	.020	1.000	.040
.090	358.95	155.22	3320.60	.000	.22	65.2	.023	1.000	.045
.100	381.09	164.79	3315.91	.000	.29	77.8	.025	1.000	.050
.110	400.93	173.37	3310.94	.000	.37	91.1	.028	1.000	.055
.120	418.56	180.99	3305.66	.000	.47	105.0	.030	1.000	.060
.130	434.04	187.69	3300.06	.000	.58	119.5	.033	1.000	.065
.140	447.45	193.49	3294.12	.000	.71	134.5	.035	1.000	.070
.150	458.85	198.42	3287.86	.000	.85	149.9	.038	1.000	.075
.160	468.40	202.55	3281.28	.000	1.01	165.6	.040	1.000	.080
.170	476.15	205.90	3274.39	.000	1.18	181.6	.043	1.000	.085
.180	482.21	208.52	3267.39	.000	1.37	197.9	.045	1.000	.090
.190	486.71	210.46	3260.20	.000	1.58	214.4	.048	1.000	.095
.200	489.74	211.77	3252.77	.000	1.80	231.0	.050	1.000	.100
.210	491.43	212.50	3245.14	.000	2.04	247.6	.053	1.000	.105
.220	491.89	212.70	3237.33	.000	2.30	264.3	.055	1.000	.110
.230	491.24	212.42	3229.36	.000	2.57	281.0	.058	1.000	.115
.240	489.61	211.72	3221.27	.000	2.86	297.7	.060	1.000	.120
.250	487.11	210.64	3213.09	.000	3.16	314.3	.063	1.000	.125
.260	483.83	209.22	3204.84	.000	3.49	330.8	.065	1.000	.130
.270	479.90	207.52	3196.56	.000	3.82	347.1	.068	1.000	.135
.280	475.40	205.57	3188.26	.000	4.18	363.4	.070	1.000	.140
.290	470.43	203.42	3179.97	.000	4.55	379.4	.072	1.000	.145
.300	465.06	201.10	3171.72	.000	4.94	395.3	.075	1.000	.150
.310	459.37	198.64	3163.51	.000	5.34	411.0	.077	1.000	.155
.320	453.42	196.07	3155.39	.000	5.76	426.5	.080	1.000	.160
.330	447.28	193.41	3147.34	.000	6.20	441.8	.082	1.000	.165
.340	441.00	190.70	3139.41	.000	6.64	456.9	.085	1.000	.170
.350	434.62	187.94	3131.59	.000	7.11	471.8	.087	1.000	.175
.360	428.19	185.16	3123.89	.000	7.59	486.4	.090	1.000	.180
.370	421.74	182.37	3116.33	.000	8.08	500.8	.092	1.000	.185
.380	415.29	179.58	3108.92	.000	8.59	515.1	.095	1.000	.190
.390	408.89	176.81	3101.65	.000	9.11	529.0	.097	1.000	.195
.400	402.54	174.07	3094.54	.000	9.65	542.8	.100	1.000	.200
.410	396.26	171.35	3087.59	.000	10.20	556.4	.102	1.000	.205
.420	390.08	168.68	3080.80	.000	10.76	569.7	.105	1.000	.210
.430	383.99	166.05	3074.17	.000	11.34	582.9	.107	1.000	.215
.440	378.02	163.46	3067.71	.000	11.93	595.8	.110	1.000	.220
.450	372.16	160.93	3061.41	.000	12.53	608.6	.112	1.000	.225
.460	366.43	158.45	3055.27	.000	13.14	621.1	.115	1.000	.230
.470	360.83	156.03	3049.30	.000	13.77	633.5	.117	1.000	.235
.480	355.36	153.66	3043.49	.000	14.41	645.6	.120	1.000	.240
.490	350.02	151.36	3037.83	.000	15.06	657.6	.122	1.000	.245

TEST CASE BASED ON 40HTC3

TIME(MS)	P-BR(MPA)	P-BASE(MPA)	TEMP(K)	YFR(-)	PR. DISP(CM)	PR. VEL(M/S)	ALPHA(-)	BETA(-)	E-FRAC(-)
.500	344.81	149.10	3032.33	.000	15.72	669.4	.125	1.000	.250
.510	339.74	146.91	3026.99	.000	16.40	681.0	.127	1.000	.255
.520	334.80	144.77	3021.80	.000	17.09	692.5	.130	1.000	.260
.530	329.98	142.69	3016.75	.000	17.79	703.8	.132	1.000	.265
.540	325.30	140.67	3011.85	.000	18.49	714.9	.135	1.000	.270
.550	320.74	138.70	3007.09	.000	19.21	725.9	.137	1.000	.275
.560	316.31	136.78	3002.47	.000	19.95	736.7	.140	1.000	.280
.570	312.00	134.92	2997.98	.000	20.69	747.3	.142	1.000	.285
.580	307.81	133.10	2993.62	.000	21.44	757.9	.145	1.000	.290
.590	303.73	131.34	2989.38	.000	22.20	768.3	.147	1.000	.295
.600	299.76	129.62	2985.28	.000	22.98	778.5	.150	1.000	.300
.610	295.91	127.96	2981.28	.000	23.76	788.6	.152	1.000	.305
.620	292.15	126.33	2977.41	.000	24.55	798.6	.155	1.000	.310
.630	288.51	124.76	2973.65	.000	25.36	808.5	.157	1.000	.315
.640	284.96	123.22	2970.00	.000	26.17	818.2	.160	1.000	.320
.650	281.52	121.73	2966.57	.000	26.99	827.8	.163	1.000	.325
.660	278.18	120.29	2963.35	.000	27.83	837.3	.165	1.000	.330
.670	274.93	118.88	2960.22	.000	28.67	846.7	.168	1.000	.335
.680	271.76	117.52	2957.17	.000	29.52	856.0	.170	1.000	.340
.690	268.68	116.18	2954.21	.000	30.38	865.2	.173	1.000	.345
.700	265.68	114.89	2951.33	.000	31.25	874.3	.175	1.000	.350
.710	262.76	113.62	2948.53	.000	32.13	883.2	.178	1.000	.355
.720	259.91	112.39	2945.81	.000	33.02	892.1	.180	1.000	.360
.730	257.14	111.19	2943.16	.000	33.91	900.9	.183	1.000	.365
.740	254.44	110.02	2940.58	.000	34.82	909.6	.185	1.000	.370
.750	251.80	108.88	2938.08	.000	35.73	918.2	.188	1.000	.375
.760	249.23	107.77	2935.64	.000	36.66	926.7	.190	1.000	.380
.770	246.73	106.69	2933.27	.000	37.59	935.1	.193	1.000	.385
.780	244.28	105.63	2930.96	.000	38.53	943.4	.195	1.000	.390
.790	241.90	104.60	2928.71	.000	39.47	951.7	.198	1.000	.395
.800	239.57	103.60	2926.52	.000	40.43	959.9	.200	1.000	.400
.810	237.30	102.62	2924.39	.000	41.39	968.0	.203	1.000	.405
.820	235.09	101.66	2922.32	.000	42.36	976.0	.205	1.000	.410
.830	232.92	100.72	2920.30	.000	43.34	983.9	.208	1.000	.415
.840	230.81	99.81	2918.33	.000	44.33	991.8	.210	1.000	.420
.850	228.74	98.91	2916.41	.000	45.33	999.6	.213	1.000	.425
.860	226.73	98.04	2914.55	.000	46.33	1007.3	.215	1.000	.430
.870	224.75	97.19	2912.73	.000	47.34	1015.0	.218	1.000	.435
.880	222.83	96.36	2910.96	.000	48.36	1022.6	.220	1.000	.440
.890	220.94	95.54	2909.23	.000	49.39	1030.1	.223	1.000	.445
.900	219.10	94.74	2907.55	.000	50.42	1037.6	.225	1.000	.450
.910	217.29	93.96	2905.91	.000	51.46	1045.0	.228	1.000	.455
.920	215.53	93.20	2904.31	.000	52.51	1052.4	.230	1.000	.460
.930	213.80	92.45	2902.75	.000	53.57	1059.7	.233	1.000	.465
.940	212.11	91.72	2901.23	.000	54.63	1066.9	.235	1.000	.470
.950	210.45	91.01	2899.75	.000	55.70	1074.1	.238	1.000	.475
.960	208.83	90.30	2898.30	.000	56.78	1081.2	.240	1.000	.480
.970	207.25	89.62	2896.89	.000	57.86	1088.3	.243	1.000	.485
.980	205.69	88.94	2895.51	.000	58.96	1095.3	.245	1.000	.490
.990	204.17	88.29	2894.17	.000	60.05	1102.2	.248	1.000	.495

TEST CASE BASED ON 40HTC3

TIME(MS)	P-BR(MPA)	P-BASE(MPA)	TEMP(K)	YFR(-)	PR. DISP(CM)	PR. VEL(M/S)	ALPHA(-)	BETA(-)	E-FRAC(-)
1.000	202.67	87.64	2892.86	.000	61.16	1109.1	.250	1.000	.500
1.010	201.21	87.01	2891.58	.000	62.27	1116.0	.253	1.000	.505
1.020	199.77	86.39	2890.33	.000	63.39	1122.8	.255	1.000	.510
1.030	198.36	85.78	2889.11	.000	64.52	1129.6	.258	1.000	.515
1.040	196.98	85.18	2887.93	.000	65.65	1136.3	.260	1.000	.520
1.050	195.63	84.59	2886.76	.000	66.79	1143.0	.263	1.000	.525
1.060	194.30	84.02	2885.63	.000	67.94	1149.6	.265	1.000	.530
1.070	192.99	83.45	2884.52	.000	69.09	1156.1	.268	1.000	.535
1.080	191.71	82.90	2883.44	.000	70.25	1162.7	.270	1.000	.540
1.090	190.45	82.36	2882.38	.000	71.42	1169.2	.273	1.000	.545
1.100	189.22	81.82	2881.35	.000	72.59	1175.6	.275	1.000	.550
1.110	188.01	81.30	2880.34	.000	73.77	1182.0	.278	1.000	.555
1.120	186.82	80.78	2879.35	.000	74.95	1188.4	.280	1.000	.560
1.130	185.65	80.28	2878.39	.000	76.14	1194.7	.282	1.000	.565
1.140	184.50	79.78	2877.44	.000	77.34	1201.0	.285	1.000	.570
1.150	183.37	79.29	2876.52	.000	78.55	1207.2	.287	1.000	.575
1.160	182.26	78.81	2875.62	.000	79.76	1213.5	.290	1.000	.580
1.170	181.17	78.34	2874.74	.000	80.97	1219.6	.292	1.000	.585
1.180	180.09	77.88	2873.88	.000	82.20	1225.8	.295	1.000	.590
1.190	179.04	77.42	2873.03	.000	83.42	1231.9	.297	1.000	.595
1.200	178.00	76.97	2872.21	.000	84.66	1237.9	.300	1.000	.600
1.210	176.98	76.53	2871.40	.000	85.90	1244.0	.302	1.000	.605
1.220	175.98	76.10	2870.61	.000	87.15	1249.9	.305	1.000	.610
1.230	174.99	75.67	2869.84	.000	88.40	1255.9	.307	1.000	.615
1.240	174.02	75.25	2869.09	.000	89.66	1261.8	.310	1.000	.620
1.250	173.06	74.84	2868.35	.000	90.92	1267.7	.312	1.000	.625
1.260	172.12	74.43	2867.62	.000	92.19	1273.6	.315	1.000	.630
1.270	171.19	74.03	2866.92	.000	93.47	1279.4	.317	1.000	.635
1.280	170.28	73.63	2866.22	.000	94.75	1285.2	.320	1.000	.640
1.290	169.38	73.24	2865.54	.000	96.04	1291.0	.322	1.000	.645
1.300	168.50	72.86	2864.88	.000	97.33	1296.7	.325	1.000	.650
1.310	167.62	72.48	2864.23	.000	98.63	1302.4	.327	1.000	.655
1.320	166.76	72.11	2863.59	.000	99.94	1308.1	.330	1.000	.660
1.330	165.92	71.75	2862.97	.000	101.25	1313.8	.332	1.000	.665
1.340	165.08	71.39	2862.35	.000	102.57	1319.4	.335	1.000	.670
1.350	164.26	71.03	2861.76	.000	103.89	1325.0	.337	1.000	.675
1.360	163.45	70.68	2861.17	.000	105.22	1330.5	.340	1.000	.680
1.370	162.65	70.34	2860.59	.000	106.55	1336.1	.342	1.000	.685
1.380	161.87	69.99	2860.03	.000	107.89	1341.6	.345	1.000	.690
1.390	161.09	69.66	2859.48	.000	109.23	1347.1	.347	1.000	.695
1.400	160.33	69.33	2858.94	.000	110.58	1352.5	.350	1.000	.700
1.410	159.57	69.00	2858.41	.000	111.94	1358.0	.352	1.000	.705
1.420	158.83	68.68	2857.89	.000	113.30	1363.4	.355	1.000	.710
1.430	158.09	68.36	2857.38	.000	114.67	1368.7	.357	1.000	.715
1.440	157.37	68.05	2856.88	.000	116.04	1374.1	.360	1.000	.720
1.450	156.65	67.74	2856.39	.000	117.41	1379.4	.362	1.000	.725
1.460	155.95	67.44	2855.91	.000	118.80	1384.7	.365	1.000	.730
1.470	155.25	67.13	2855.44	.000	120.18	1390.0	.367	1.000	.735
1.480	154.57	66.84	2854.98	.000	121.58	1395.3	.370	1.000	.740
1.490	153.89	66.54	2854.53	.000	122.97	1400.5	.372	1.000	.745

TEST CASE BASED ON 40MTC)

TIME(MS)	P-BR(MPA)	P-BASE(MPA)	TEMP(K)	YFR(-)	PR. DISP(CM)	PR. VEL(M/S)	ALPHA(-)	BETA(-)	E-FRAC(-)
1.500	153.22	66.26	2854.08	.000	124.38	1405.7	.375	1.000	.750
1.510	152.56	65.97	2853.65	.000	125.78	1410.9	.377	1.000	.755
1.520	151.91	65.69	2853.22	.000	127.20	1416.1	.380	1.000	.760
1.530	151.26	65.41	2852.80	.000	128.62	1421.3	.382	1.000	.765
1.540	150.63	65.14	2852.39	.000	130.04	1426.4	.385	1.000	.770
1.550	150.00	64.86	2851.99	.000	131.47	1431.5	.387	1.000	.775
1.560	149.38	64.60	2851.59	.000	132.90	1436.6	.390	1.000	.780
1.570	148.77	64.33	2851.20	.000	134.34	1441.6	.392	1.000	.785
1.580	148.16	64.07	2850.82	.000	135.79	1446.7	.395	1.000	.790
1.590	147.57	63.81	2850.45	.000	137.24	1451.7	.397	1.000	.795
1.600	146.97	63.56	2850.08	.000	138.69	1456.7	.400	1.000	.800
1.610	146.39	63.30	2849.72	.000	140.15	1461.7	.402	1.000	.805
1.620	145.81	63.05	2849.37	.000	141.61	1466.6	.405	1.000	.810
1.630	145.24	62.81	2849.02	.000	143.08	1471.6	.407	1.000	.815
1.640	144.68	62.56	2848.68	.000	144.56	1476.5	.410	1.000	.820
1.650	144.12	62.32	2848.34	.000	146.04	1481.4	.412	1.000	.825
1.660	143.57	62.08	2848.02	.000	147.52	1486.3	.415	1.000	.830
1.670	143.03	61.85	2847.69	.000	149.01	1491.2	.417	1.000	.835
1.680	142.49	61.62	2847.38	.000	150.50	1496.0	.420	1.000	.840
1.690	141.96	61.39	2847.07	.000	152.00	1500.8	.422	1.000	.845
1.700	141.43	61.16	2846.76	.000	153.50	1505.7	.425	1.000	.850
1.710	140.91	60.93	2846.46	.000	155.01	1510.4	.427	1.000	.855
1.720	140.40	60.71	2846.17	.000	156.52	1515.2	.430	1.000	.860
1.730	139.89	60.49	2845.88	.000	158.04	1520.0	.432	1.000	.865
1.740	139.39	60.27	2845.59	.000	159.56	1524.7	.435	1.000	.870
1.750	138.89	60.06	2845.31	.000	161.09	1529.5	.437	1.000	.875
1.760	138.40	59.85	2845.04	.000	162.62	1534.2	.440	1.000	.880
1.770	137.91	59.64	2844.77	.000	164.16	1538.9	.442	1.000	.885
1.780	137.43	59.43	2844.50	.000	165.70	1543.5	.445	1.000	.890
1.790	136.95	59.22	2844.24	.000	167.25	1548.2	.447	1.000	.895
1.800	136.48	59.02	2843.99	.000	168.80	1552.8	.450	1.000	.900
1.810	136.01	58.81	2843.74	.000	170.35	1557.5	.452	1.000	.905
1.820	135.55	58.62	2843.49	.000	171.91	1562.1	.455	1.000	.910
1.830	135.09	58.42	2843.25	.000	173.48	1566.7	.457	1.000	.915
1.840	134.64	58.22	2843.01	.000	175.05	1571.2	.460	1.000	.920
1.850	134.19	58.03	2842.77	.000	176.62	1575.8	.462	1.000	.925
1.860	133.75	57.84	2842.54	.000	178.20	1580.4	.465	1.000	.930
1.870	133.31	57.65	2842.32	.000	179.78	1584.9	.467	1.000	.935
1.880	132.87	57.46	2842.09	.000	181.37	1589.4	.470	1.000	.940
1.890	132.44	57.27	2841.88	.000	182.96	1593.9	.472	1.000	.945
1.900	132.02	57.09	2841.66	.000	184.56	1598.4	.475	1.000	.950
1.910	131.59	56.90	2841.45	.000	186.16	1602.9	.477	1.000	.955
1.920	131.18	56.72	2841.24	.000	187.76	1607.4	.480	1.000	.960
1.930	130.76	56.54	2841.04	.000	189.37	1611.8	.482	1.000	.965
1.940	130.35	56.37	2840.83	.000	190.98	1616.2	.485	1.000	.970
1.950	129.95	56.19	2840.64	.000	192.60	1620.7	.487	1.000	.975
1.960	129.54	56.02	2840.44	.000	194.23	1625.1	.490	1.000	.980
1.970	129.14	55.84	2 [illegible]5	.000	195.85	1629.5	.492	1.000	.985
1.980	128.75	55.67	2840.06	.000	197.48	1633.8	.495	1.000	.990
1.990	128.36	55.51	2839.88	.000	199.12	1638.2	.497	1.000	.995

TEST CASE BASED ON 40MTC3

TIME(MS)	P-BR(MPA)	P-BASE(MPA)	TEMP(K)	YFR(-)	PR. DISP(CM)	PR. VEL(M/S)	ALPHA(-)	BETA(-)	E-FRAC(-)
2.000	127.97	55.34	2839.70	.000	200.76	1642.6	.500	1.000	1.000
2.010	126.82	54.84	2823.76	.000	202.41	1646.9	.502	1.000	1.000
2.020	125.67	54.34	2807.85	.000	204.05	1651.2	.505	1.000	1.000
2.030	124.54	53.85	2791.96	.000	205.71	1655.4	.507	1.000	1.000
2.040	123.42	53.37	2776.11	.000	207.37	1659.6	.510	1.000	1.000
2.050	122.30	52.89	2760.28	.000	209.03	1663.8	.512	1.000	1.000
2.060	121.20	52.41	2744.49	.000	210.69	1667.9	.515	1.000	1.000
2.070	120.11	51.94	2728.74	.000	212.36	1672.0	.517	1.000	1.000
2.080	119.03	51.47	2713.02	.000	214.04	1676.1	.520	1.000	1.000
2.090	117.96	51.01	2697.34	.000	215.72	1680.1	.522	1.000	1.000
2.100	116.90	50.55	2681.71	.000	217.40	1684.1	.525	1.000	1.000
2.110	115.85	50.10	2666.11	.000	219.08	1688.1	.527	1.000	1.000
2.120	114.81	49.65	2650.57	.000	220.77	1692.0	.530	1.000	1.000
2.130	113.78	49.20	2635.06	.000	222.47	1695.9	.532	1.000	1.000
2.140	112.83	48.79	2621.32	.000	224.17	1699.7	.535	1.000	1.000
2.150	111.91	48.39	2608.26	.000	225.87	1703.5	.537	1.000	1.000
2.160	111.01	48.00	2595.14	.000	227.57	1707.3	.540	1.000	1.000
2.170	110.10	47.61	2581.97	.000	229.28	1711.1	.542	1.000	1.000
2.180	109.20	47.22	2568.74	.000	230.99	1714.8	.545	1.000	1.000
2.190	108.31	46.83	2555.47	.000	232.71	1718.5	.547	1.000	1.000
2.200	107.42	46.45	2542.15	.000	234.43	1722.1	.550	1.000	1.000
2.210	106.53	46.07	2528.80	.000	236.16	1725.8	.552	1.000	1.000
2.220	105.65	45.69	2515.40	.000	237.88	1729.4	.555	1.000	1.000
2.230	104.78	45.31	2501.98	.000	239.61	1732.9	.557	1.000	1.000
2.240	103.91	44.93	2488.53	.000	241.35	1736.5	.560	1.000	1.000
2.250	103.05	44.56	2475.05	.000	243.09	1740.0	.562	1.000	1.000
2.260	102.19	44.19	2461.54	.000	244.83	1743.5	.565	1.000	1.000
2.270	101.33	43.82	2448.02	.000	246.57	1746.9	.567	1.000	1.000
2.280	100.49	43.45	2434.48	.000	248.32	1750.4	.570	1.000	1.000
2.290	99.64	43.09	2420.92	.000	250.07	1753.8	.572	1.000	1.000
2.300	98.81	42.73	2407.36	.000	251.83	1757.1	.575	1.000	1.000
2.310	97.97	42.37	2393.78	.000	253.59	1760.5	.577	1.000	1.000
2.320	97.15	42.01	2380.20	.000	255.35	1763.8	.580	1.000	1.000
2.330	96.33	41.65	2366.61	.000	257.12	1767.1	.582	1.000	1.000
2.340	95.51	41.30	2353.02	.000	258.89	1770.3	.585	1.000	1.000
2.350	94.70	40.95	2339.44	.000	260.66	1773.6	.587	1.000	1.000
2.360	93.90	40.60	2325.85	.000	262.43	1776.8	.590	1.000	1.000
2.370	93.10	40.26	2312.27	.000	264.21	1780.0	.592	1.000	1.000
2.380	92.31	39.92	2298.70	.000	265.99	1783.1	.595	1.000	1.000
2.390	91.52	39.58	2285.13	.000	267.78	1786.2	.597	1.000	1.000
2.400	90.74	39.24	2271.58	.000	269.56	1789.3	.600	1.000	1.000
2.410	89.97	38.91	2258.25	.000	271.36	1792.4	.603	1.000	1.000
2.420	89.36	38.64	2248.95	.000	273.15	1795.4	.605	1.000	1.000
2.430	88.74	38.37	2239.52	.000	274.95	1798.5	.608	1.000	1.000
2.440	88.13	38.11	2229.96	.000	276.75	1801.5	.610	1.000	1.000
2.450	87.51	37.84	2220.27	.000	278.55	1804.4	.613	1.000	1.000
2.460	86.89	37.57	2210.47	.000	280.36	1807.4	.615	1.000	1.000
2.470	86.28	37.31	2200.56	.000	282.16	1810.3	.618	1.000	1.000
2.480	85.66	37.04	2190.54	.000	283.98	1813.3	.620	1.000	1.000
2.490	85.04	36.77	2180.41	.000	285.79	1816.2	.623	1.000	1.000

TEST CASE BASED ON 40MTC3

TIME(MS)	P-BR(MPA)	P-BASE(MPA)	TEMP(K)	YFR(-)	PR. DISP(CM)	PR. VEL(M/S)	ALPHA(-)	BETA(-)	E-FRAC(-)
2.500	84.42	36.51	2170.18	.000	287.61	1819.0	.625	1.000	1.000
2.510	83.81	36.24	2159.86	.000	289.43	1821.9	.628	1.000	1.000
2.520	83.19	35.97	2149.45	.000	291.25	1824.7	.630	1.000	1.000
2.530	82.58	35.71	2138.95	.000	293.08	1827.5	.633	1.000	1.000
2.540	81.96	35.44	2128.37	.000	294.91	1830.3	.635	1.000	1.000
2.550	81.35	35.18	2117.71	.000	296.74	1833.1	.638	1.000	1.000
2.560	80.74	34.91	2106.97	.000	298.57	1835.9	.640	1.000	1.000
2.570	80.13	34.65	2096.15	.000	300.41	1838.6	.643	1.000	1.000
2.580	79.52	34.38	2085.27	.000	302.25	1841.3	.645	1.000	1.000
2.590	78.91	34.12	2074.33	.000	304.09	1844.0	.648	1.000	1.000
2.600	78.30	33.86	2063.32	.000	305.94	1846.7	.650	1.000	1.000
2.610	77.69	33.60	2052.25	.000	307.79	1849.3	.653	1.000	1.000
2.620	77.09	33.34	2041.13	.000	309.64	1851.9	.655	1.000	1.000
2.630	76.49	33.07	2029.95	.000	311.49	1854.6	.658	1.000	1.000
2.640	75.89	32.82	2018.72	.000	313.35	1857.1	.660	1.000	1.000
2.650	75.29	32.56	2007.45	.000	315.20	1859.7	.663	1.000	1.000
2.660	74.69	32.30	1996.13	.000	317.07	1862.3	.665	1.000	1.000
2.670	74.10	32.04	1984.77	.000	318.93	1864.8	.668	1.000	1.000
2.680	73.50	31.78	1973.37	.000	320.80	1867.3	.670	1.000	1.000
2.690	72.91	31.53	1961.93	.000	322.66	1869.8	.673	1.000	1.000
2.700	72.32	31.27	1950.46	.000	324.53	1872.2	.675	1.000	1.000
2.710	71.73	31.02	1938.96	.000	326.41	1874.7	.678	1.000	1.000
2.720	71.15	30.77	1927.43	.000	328.28	1877.1	.680	1.000	1.000
2.730	70.57	30.52	1915.87	.000	330.16	1879.5	.683	1.000	1.000
2.740	69.99	30.26	1904.29	.000	332.04	1881.9	.685	1.000	1.000
2.750	69.41	30.01	1892.68	.000	333.93	1884.3	.688	1.000	1.000
2.760	68.83	29.77	1881.05	.000	335.81	1886.6	.690	1.000	1.000
2.770	68.26	29.52	1869.40	.000	337.70	1888.9	.693	1.000	1.000
2.780	67.69	29.27	1857.74	.000	339.59	1891.3	.695	1.000	1.000
2.790	67.23	29.07	1849.32	.000	341.48	1893.5	.698	1.000	1.000
2.800	66.93	28.94	1845.34	.000	343.38	1895.8	.700	1.000	1.000
2.810	66.62	28.81	1841.12	.000	345.27	1898.1	.703	1.000	1.000
2.820	66.30	28.67	1836.67	.000	347.17	1900.4	.705	1.000	1.000
2.830	65.97	28.53	1832.01	.000	349.07	1902.6	.708	1.000	1.000
2.840	65.64	28.39	1827.13	.000	350.98	1904.8	.710	1.000	1.000
2.850	65.31	28.24	1822.04	.000	352.88	1907.1	.713	1.000	1.000
2.860	64.97	28.09	1816.74	.000	354.79	1909.3	.715	1.000	1.000
2.870	64.62	27.94	1811.25	.000	356.70	1911.5	.718	1.000	1.000
2.880	64.28	27.79	1805.56	.000	358.62	1913.7	.720	1.000	1.000
2.890	63.92	27.64	1799.69	.000	360.53	1915.8	.723	1.000	1.000
2.900	63.56	27.49	1793.63	.000	362.45	1918.0	.725	1.000	1.000
2.910	63.20	27.33	1787.40	.000	364.37	1920.2	.728	1.000	1.000
2.920	62.84	27.17	1780.98	.000	366.29	1922.3	.730	1.000	1.000
2.930	62.47	27.01	1774.41	.000	368.21	1924.4	.733	1.000	1.000
2.940	62.09	26.85	1767.66	.000	370.14	1926.5	.735	1.000	1.000
2.950	61.72	26.69	1760.76	.000	372.06	1928.6	.738	1.000	1.000
2.960	61.34	26.52	1753.70	.000	373.99	1930.7	.740	1.000	1.000
2.970	60.95	26.36	1746.49	.000	375.93	1932.8	.743	1.000	1.000
2.980	60.57	26.19	1739.14	.000	377.86	1934.9	.745	1.000	1.000
2.990	60.18	26.02	1731.64	.000	379.79	1936.9	.748	1.000	1.000

TEST CASE BASED ON 40HTC3

TIME(MS)	P-BR(MPA)	P-BASE(MPA)	TEMP(K)	YFR(-)	PR. DISP(CM)	PR. VEL(M/S)	ALPHA(-)	BETA(-)	E-FRAC(-)
3.000	59.79	25.85	1724.01	.000	381.73	1939.0	.750	1.000	1.000
3.010	59.40	25.68	1716.24	.000	383.67	1941.0	.753	1.000	1.000
3.020	59.00	25.51	1708.34	.000	385.61	1943.0	.755	1.000	1.000
3.030	58.60	25.34	1700.31	.000	387.56	1945.0	.758	1.000	1.000
3.040	58.20	25.17	1692.17	.000	389.50	1947.0	.760	1.000	1.000
3.050	57.80	24.99	1683.90	.000	391.45	1948.9	.763	1.000	1.000
3.060	57.40	24.82	1675.52	.000	393.40	1950.9	.765	1.000	1.000
3.070	56.99	24.64	1667.03	.000	395.35	1952.8	.768	1.000	1.000
3.080	56.59	24.47	1658.43	.000	397.31	1954.8	.770	1.000	1.000
3.090	56.18	24.29	1649.72	.000	399.26	1956.7	.773	1.000	1.000
3.094	56.02	24.23	1646.42	.000	400.00	1957.4	.773	1.000	1.000

MAXIMUM PRESSURE(MPA): 491.9

RATE	XBET	MVDAT	PMAX	MV
.000	1.000	22	491.9	1957.4

APPENDIX E

Nominal Data Base for XKTC Simulation of ETG

INTENTIONALLY LEFT BLANK.

ETG8(.0361/1/.20): 14MM ETG, WATER AS MONOLITHIC CHARGE

XNOVAKTC VERSION NUMBER 1.018

CONTROL DATA

LOGICAL VARIABLES:
PRINT T PLOT F DISK WRITE T DISK READ F
I.B. TABLE T FLAME TABLE F PRESSURE TABLE(S) F
EROSIVE EFFECT 0 WALL TEMPERATURE CALCULATION 0
BED PRECOMPRESSED 0
HEAT LOSS CALCULATION 0

BORE RESISTANCE FUNCTION 2
1: LINEAR INTERPOLATION OF ENGRAVING RESISTANCE DATA
2: LIKE 1 TIMES EXPONENTIAL VELOCITY FUNCTION
3: LIKE 1 TIMES RATIONAL VELOCITY FUNCTION
4: LIKE 1 PLUS AIR SHOCK
5: LIKE 1 PLUS PROJECTILE SETBACK
6: LIKE 1 PLUS AIR SHOCK AND PROJECTILE SETBACK

SOLID TRAVELING CHARGE OPTION (0=NO,1=YES) 0
EXPLICIT COMPACTION WAVE(0=NO;1=YES) 0
CONSERVATIVE SCHEME TO INTEGRATE SOLID-PHASE CONTINUITY EQUATION (0=NO,OLD; 1=YES,NEW) 0
KINETICS MODE (0=NONE;1=GAS-PHASE ONLY;2=BOTH PHASES) 0
TANK GUN OPTION (0=NO,1=YES) 0
INPUT ECHO OPTION 0
FORWARD BOUNDARY CONDITION (0=CLOSED;1=OPEN;2=ROCKET) 0
LIQUID TRAVELING CHARGE OPTION(0=NO,1=YES) 0
GRAIN FRACTURE OPTION(0=NO;1=YES) 0
GRAIN FRACTURE DATA BASED ON INTRINSIC AVERAGE STRESS
(0=NO;1=YES) 0
ELECTROTHERMAL GUN OPTION(0=NO;1=YES) 1

INTEGRATION PARAMETERS

NUMBER OF STATIONS AT WHICH DATA ARE STORED	99
NUMBER OF STEPS BEFORE LOGOUT	4
TIME STEP FOR DISK START	0
NUMBER OF STEPS FOR TERMINATION	99000
TIME INTERVAL BEFORE LOGOUT(SEC)	0.5000E-04
TIME FOR TERMINATION (SEC)	1.000
PROJECTILE TRAVEL FOR TERMINATION (INS)	57.09
MAXIMUM TIME STEP (SEC)	0.1000E-02
STABILITY SAFETY FACTOR	2.00
SOURCE STABILITY FACTOR	0.0500
SPATIAL RESOLUTION FACTOR	0.0100
TIME INTERVAL FOR I.B. TABLE STORAGE(SEC)	0.2000E-04
TIME INTERVAL FOR PRESSURE TABLE STORAGE (SEC)	0.2000E-04

FILE COUNTERS

NUMBER OF STATIONS TO SPECIFY TUBE RADIUS	4		
NUMBER OF TIMES TO SPECIFY PRIMER DISCHARGE	0		
NUMBER OF POSITIONS TO SPECIFY PRIMER DISCHARGE	0		
NUMBER OF ENTRIES IN BORE RESISTANCE TABLE	0		
NUMBER OF ENTRIES IN WALL TEMPERATURE TABLE	0		
NUMBER OF ENTRIES IN FORWARD FILLER ELEMENT TABLE	0		
NUMBER OF TYPES OF PROPELLANTS	1		
NUMBER OF BURN RATE DATA SETS	1		
NUMBER OF ENTRIES IN VOID FRACTION TABLE(S)	0	0	0
NUMBER OF ENTRIES IN PRESSURE HISTORY TABLES	0		
NUMBER OF ENTRIES IN REAR FILLER ELEMENT TABLE	0		

GENERAL PROPERTIES OF INITIAL AMBIENT GAS

INITIAL TEMPERATURE (DEG.R)	550.0
INITIAL PRESSURE (PSI)	14.7
MOLECULAR WEIGHT (LBM/LBMOL)	28.896
RATIO OF SPECIFIC HEATS	1.4000

GENERAL PROPERTIES OF PROPELLANT BED

INITIAL TEMPERATURE (DEG.R)	550.0
MINIMUM IMPACT VELOCITY FOR EXPLICIT COMPACTION WAVE (IN/SEC)	100000000.

PROPERTIES OF PROPELLANT 1

PROPELLANT TYPE		WORKING FLUID WATER
MASS OF PROPELLANT (LBM)		0.0987
DENSITY OF PROPELLANT (LBM/IN**3)		0.0361
FORM FUNCTION INDICATOR		16
OUTSIDE DIAMETER (INS)		0.8106
INSIDE DIAMETER (INS)		0.8106
LENGTH (INS)		5.0690
NUMBER OF PERFORATIONS		1.
SLOT WIDTH (NFORM=11) OR SCROLL DIA. (NFORM=13)	(INS)	0.0000
PROPELLANT STACKED (0=NO,1=YES)		0
ATTACHMENT CONDITION (0=FREE,1=ATTACHED TO TUBE, 2=ATTACHED TO PROJECTILE)		1
BOND STRENGTH (LBF) (N.B. ZERO DEFAULTS TO INFINITY)		0.000000
DRAG RELAXATION EXPONENT (STACKED GRANULAR ONLY)		1.000
GRAIN INHIBITED ON OUTER SURFACE (0=NO,1=YES)	0	

GRAIN IS MONOLITHIC WITH EXTERIOR CONFORMING TO TUBE
PERFORATION IS DESCRIBED BY FOLLOWING DATA

POSITION (IN)	DIAMETER (IN)
0.000	0.8106
5.069	0.8106

RHEOLOGICAL PROPERTIES

SPEED OF COMPRESSION WAVE IN SETTLED BED (IN/SEC)	17400.
SETTLING POROSITY	1.0000
SPEED OF EXPANSION WAVE (IN/SEC)	50000.
POISSON RATIO (-)	0.0000

SOLID PHASE THERMOCHEMISTRY

MAXIMUM PRESSURE FOR BURN RATE DATA (LBF/IN**2)	100000.
BURNING RATE PRE-EXPONENTIAL FACTOR (IN/SEC/PSI**BN)	1.000
BURNING RATE EXPONENT	1.0000
BURNING RATE CONSTANT (IN/SEC)	0.0000
IGNITION TEMPERATURE (DEG.R)	549.0
THERMAL CONDUCTIVITY (LBF/SEC/DEG.R)	0.2770E-01
THERMAL DIFFUSIVITY (IN**2/SEC)	0.1345E-03
EMISSIVITY FACTOR	0.600

GAS PHASE THERMOCHEMISTRY

CHEMICAL ENERGY RELEASED IN BURNING(LBF-IN/LBM)	.00000
MOLECULAR WEIGHT (LBM/LBMOL)	17.6000
RATIO OF SPECIFIC HEATS	1.2035
COVOLUME	16.8570

LOCATION OF PACKAGE(S)

PACKAGE	LEFT BDDY(INS)	RIGHT BDDY(INS)	MASS(LBM)	INNER RADIUS(IN)	OUTER RADIUS(IN)
1	0.000	5.069	0.099	0.000	0.000

PARAMETERS TO SPECIFY TUBE GEOMETRY

DISTANCE(IN)	RADIUS(IN)
0.000	0.579
5.069	0.579
6.250	0.276
63.340	0.276

THERMAL PROPERTIES OF TUBE

THERMAL CONDUCTIVITY (LBF/SEC/DEG.R)	0.0000
THERMAL DIFFUSIVITY (IN**2/SEC)	0.0000
EMISSIVITY FACTOR	0.000
INITIAL TEMPERATURE (DEG.R)	550.00

PROJECTILE AND RIFLING DATA

INITIAL POSITION OF BASE OF PROJECTILE(INS)	6.250
MASS OF PROJECTILE (LBM)	0.040
POLAR MOMENT OF INERTIA (LBM-IN**2)	0.000
ANGLE OF RIFLING (DEG)	0.000

DATA FOR SIMULATION OF ELECTROTHERMAL GUN

PLASMA DISCHARGE IN INTEGRATED(0) OR DETAILED(1) FORMAT	0
NUMBER OF SETS OF DATA TO CHARACTERIZE DISCHARGE	2
TOTAL PLASMA ENERGY(LBF-IN)	0.326150E+07
TOTAL PLASMA MASS(LBM)	0.220000E-02
AVERAGE DIAMETER OF CAPILLARY(IN)	0.0394
AVERAGE RATIO OF SPECIFIC HEATS OF PLASMA(-)	1.2035
AVERAGE MOLECULAR WEIGHT OF PLASMA(LBM/LBMOL)	16.8570
PLASMA MIXING LENGTH(IN)	1.000
COEFFICIENT FOR MIXING OF GAS WITH WORKING FLUID(-)	0.200000

INTEGRATED DESCRIPTION OF PLASMA DISCHARGE

TIME(MSEC)	ENERGY FRACT.(-)	MASS FRACT.(-)	VELOCITY(IN/SEC)
0.000000	0.000000	0.000000	0.000000
0.800000	1.00000	1.00000	0.000000

No. of Copies	Organization
2	Administrator Defense Technical Info Center ATTN: DTIC-DDA Cameron Station Alexandria, VA 22304-6145
1	Commander U.S. Army Materiel Command ATTN: AMCAM 5001 Eisenhower Ave. Alexandria, VA 22333-0001
1	Director U.S. Army Research Laboratory ATTN: AMSRL-OP-CI-AD, Tech Publishing 2800 Powder Mill Rd. Adelphi, MD 20783-1145
1	Director U.S. Army Research Laboratory ATTN: AMSRL-OP-CI-AD, Records Management 2800 Powder Mill Rd. Adelphi, MD 20783-1145
2	Commander U.S. Army Armament Research, Development, and Engineering Center ATTN: SMCAR-IMI-I Picatinny Arsenal, NJ 07806-5000
2	Commander U.S. Army Armament Research, Development, and Engineering Center ATTN: SMCAR-TDC Picatinny Arsenal, NJ 07806-5000
1	Director Benet Weapons Laboratory U.S. Army Armament Research, Development, and Engineering Center ATTN: SMCAR-CCB-TL Watervliet, NY 12189-4050
1	Director U.S. Army Aviation Research and Technology Activity ATTN: SAVRT-R (Library) M/S 219-3 Ames Research Center Moffett Field, CA 94035-1000

No. of Copies	Organization
1	Commander U.S. Army Missile Command ATTN: AMSMI-RD-CS-R (DOC) Redstone Arsenal, AL 35898-5010
1	Commander U.S. Army Tank-Automotive Command ATTN: AMSTA-JSK (Armor Eng. Br.) Warren, MI 48397-5000
1	Director U.S. Army TRADOC Analysis Command ATTN: ATRC-WSR White Sands Missile Range, NM 88002-5502
1	Commandant U.S. Army Field Artillery School ATTN: ATSF-CSI Ft. Sill, OK 73503-5000
(Class. only) 1	Commandant U.S. Army Infantry School ATTN: ATSH-CD (Security Mgr.) Fort Benning, GA 31905-5660
(Unclass. only) 1	Commandant U.S. Army Infantry School ATTN: ATSH-CD-CSO-OR Fort Benning, GA 31905-5660
1	WL/MNOI Eglin AFB, FL 32542-5000
	Aberdeen Proving Ground
2	Dir, USAMSAA ATTN: AMXSY-D AMXSY-MP, H. Cohen
1	Cdr, USATECOM ATTN: AMSTE-TC
1	Dir, ERDEC ATTN: SCBRD-RT
1	Cdr, CBDA ATTN: AMSCB-CII
1	Dir, USARL ATTN: AMSRL-SL-I
10	Dir, USARL ATTN: AMSRL-OP-CI-B (Tech Lib)

No. of Copies	Organization
1	Director U.S. Army BMD Advanced Technology Center P. O. Box 1500 Huntsville, AL 35807
1	Chairman DOD Explosives Safety Board Room 856-C Hoffman Bldg. 1 2461 Eisenhower Ave. Alexandria, VA 22331-0600
1	Department of the Army Office of the Product Manager 155 mm Howitzer, M109A6, Paladin ATTN: SFAE-AR-HIP-IP, Mr. R. De Kleine Picatinny Arsenal, NJ 07806-5000
3	Project Manager Advanced Field Artillery System ATTN: SFAE-ASM-AF-E, LTC A. Ellis T. Kuriata J. Shields Picatinny Arsenal, NJ 07801-5000
1	Project Manager Advanced Field Artillery System ATTN: SFAE-ASM-AF-Q, W. Warren Picatinny Arsenal, NJ 07801-5000
1	Commander Production Base Modernization Agency U.S. Army Armament Research, Development, and Engineering Center ATTN: AMSMC-PBM-E, L. Laibson Picatinny Arsenal, NJ 07806-5000
3	PEO-Armaments Project Manager Tank Main Armament Systems ATTN: AMCPM-TMA, K. Russell AMCPM-TMA-105 AMCPM-TMA-120 Picatinny Arsenal, NJ 07806-5000

No. of Copies	Organization
5	Director Benet Laboratories U.S. Army Watervliet Arsenal ATTN: SARWV-RD, L. Johnson G. Carafano R. Thierry R. Hasoenbein P. Votis Watervliet, NY 12189
3	Commander U.S. Army AMCCOM ATTN: AMSMC-IRC, G. Cowan SMCAR-ESM(R), W. Fortune R. Zastrow Rock Island, IL 61299-7300
1	Commander, USACECOM R&D Technical Library ATTN: ASQNC-ELC-IS-L-R, Myer Center Fort Monmouth, NJ 07703-5301
1	Commandant U.S. Army Aviation School ATTN: Aviation Agency Fort Rucker, AL 36360
1	President U.S. Army Armor and Engineering Board ATTN: ATZK-AD-S Fort Knox, KY 40121
1	Director HQ, TRAC RPD ATTN: ATCD-MA, MAJ Williams Fort Monroe, VA 23651-5143
1	Headquarters U.S. Army Materiel Command ATTN: AMCICP-AD, Michael F. Fisette 5001 Eisenhower Ave. Alexandria, VA 22333-0001

No. of Copies	Organization
7	Commander U.S. Army Armament Research, Development, and Engineering Center ATTN: SMCAR-AE, J. Picard SMCAR-AEE-B, D. Downs S. Einstein A. Bracuti D. Chiu SMCAR-AEE, J. Lannon SMCAR-AES, S. Kaplowitz Picatinny Arsenal, NJ 07806-5000
4	Commander U.S. Army Armament Research, Development, and Engineering Center ATTN: SMCAR-CCH-V, C. Mandala E. Fennell SMCAR-CCH-T, L. Rosendorf SMCAR-CCS Picatinny Arsenal, NJ 07806-5000
3	Director Benet Weapons Laboratories ATTN: SMCAR-CCB-RA, G. P. O'Hara G. A. Pflegl SMCAR-CCB-S, F. Heiser Watervliet, NY 12189-4050
6	Commander U.S. Army Armament Research, Development, and Engineering Center ATTN: SMCAR-FSE, R. Zimmany T. Gora B. Knutelsky L. Harris A. Graf H. Naber-Lebby Picatinny Arsenal, NJ 07806-5000
2	Commander U.S. Army Research Office ATTN: Technical Library D. Mann P.O. Box 12211 Research Triangle Park, NC 27709-2211

No. of Copies	Organization
1	ODDR&E (AT) ATTN: Mr. R. Menz The Pentagon, Room 3D1089 Washington, DC 20301-3080
1	Commander U.S. Army Belvoir R&D Center ATTN: STRBE-WC, Technical Library (Vault) Bldg. 315 Fort Belvoir, VA 22060-5606
1	Office of Naval Research ATTN: Code 473, R S. Miller 800 N. Quincy St. Arlington, VA 22217
2	Commander Naval Sea Systems Command ATTN: SEA 62R SEA 64 Washington, DC 20362-5101
1	Commander Naval Air Systems Command ATTN: AIR-954-Technical Library Washington, DC 20360
1	Naval Research Laboratory Technical Library Washington, DC 20375
2	Commander Naval Surface Warfare Center ATTN: Code G33, T. Doran Code DX-21, Technical Library Dahlgren, VA 22448-5000
2	Commander Naval Underwater Systems Center Energy Conversion Dept. ATTN: Code 5B331, R. S. Lazar Technical Library Newport, RI 02840
1	Commander Naval Weapons Center ATTN: Code 388, C. F. Price Info Science Div China Lake, CA 93555-6001

No. of
Copies Organization

3 Director
Sandia National Laboratories
ATTN: R. Woodfin
D. Benson
S. Kempka
Advanced Projects Div 14
Organization 9123
Albuquerque, NM 87185

1 Director
Sandia National Laboratories
Combustion Research Facility
Division 8357
ATTN: S. Vosen
Livermore, CA 94551-0469

1 The Johns Hopkins University/CPIA
ATTN: T. Christian
10630 Little Patuxent Parkway, Suite 202
Columbia, MD 21044-3200

2 Pennsylvania State University
Dept. of Mechanical Engr.
ATTN: Dr. K. Kuo
Dr. F. Cheung
312 Mechanical Engineering Bldg.
University Park, PA 16802

1 North Carolina State University
ATTN: John G. Gilligan
Box 7909
1110 Burlington Engineering Labs
Raleigh, NC 27695-7909

1 SRI International
Propulsion Sciences Division
ATTN: Technical Library
333 Ravenswood Ave.
Menlo Park, CA 94025

3 FMC Corporation
ATTN: Dr. A. Giovanetti
Mr. J. Dyvik
Dr. D. Cook
4800 East River Road
Minneapolis, MN 55421-1498

No. of
Copies Organization

3 GT Devices
ATTN: Dr. S. Goldstein
Dr. R. J. Greig
Dr. N. Winsor
5705A General Washington Dr.
Alexandria, VA 22312

2 General Dynamics Land Systems
ATTN: Dr. B. VanDeusen
Dr. M. Weidner
P. O. Box 2074
Warren, MI 48090-2074

2 Olin Ordnance
ATTN: V. McDonald, Library
Hugh McElroy
P. O. Box 222
St. Marks, FL 32355

1 Paul Gough Associates, Inc.
ATTN: P. S. Gough
1048 South St.
Portsmouth, NH 03801-5423

1 Physics International Library
ATTN: H. Wayne Wampler
P.O. Box 5010
San Leandro, CA 94577-0599

2 Princeton Combustion Research
Laboratories, Inc.
ATTN: M. Summerfield
N. Messina
Princeton Corporate Plaza
11 Deerpark Dr., Bldg. IV, Suite 119
Monmouth Junction, NJ 08852

2 Science Applications, Inc.
ATTN: J. Batteh
L. Thornhill
1519 Johnson Ferry Rd.
Suite 300
Marietta, GA 30062-6438

1 Eli Freedman & Associates
ATTN: E. Freedman
2411 Diana Rd.
Baltimore, MD 21209

No. of
Copies Organization

3 Deputy Commander
Strategic Defense Command
ATTN: SFAE-SD-HVA,
S. Smith
LTC Kee
T. Aden
P. O. Box 1500
Huntsville, AL 35887-3801

1 Veritay Technology, Inc.
4845 Millersport Hwy.
P. O. Box 305
East Amherst, NY 14051-0305

1 Battelle
ATTN: TACTEC Library, J. N. Huggins
505 King Ave.
Columbus, OH 43201-2693

1 Martin Marietta
Defense Systems Division
ATTN: Dr. J. Mandzy
Mail Drop 43-220
100 Plastics Ave.
Pittsfield, MA 01201

1 Naval Sea System Command
Department of the Navy
ATTN: CSEA/CDR Dampier
06KR12
Washington, DC 20362-5101

3 SAIC
ATTN: Mr. N. Sinha
Dr. S. Dash
Dr. A. Hosanadi
501 Office Center Drive
Suite 420
Fort Washington, PA 19034-3211

1 Dr. W. J. Sargeant
James Clark Maxwell Professor
Department of Electrical Engineering
Bonner Hall—Room 312
Buffalo, NY 14260

No. of
Copies Organization

Aberdeen Proving Ground

23 Dir, USARL
ATTN: AMSRL-WT-P, I. May
AMSRL-WT-PA,
G. Wren (10 cps)
W. Oberle
P. Tran
T. Coffee
S. Richardson
AMSRL-WT-PC, B. Filer
AMSRL-WT-PD, B. Burns
AMSRL-WT-PE,
P. Conroy
A. Horst
T. Minor
F. Robbins
D. Kooker
G. Keller

INTENTIONALLY LEFT BLANK.

USER EVALUATION SHEET/CHANGE OF ADDRESS

This Laboratory undertakes a continuing effort to improve the quality of the reports it publishes. Your comments/answers to the items/questions below will aid us in our efforts.

1. ARL Report Number ARL-CR-47 Date of Report July 1993

2. Date Report Received _____

3. Does this report satisfy a need? (Comment on purpose, related project, or other area of interest for which the report will be used.) _____

4. Specifically, how is the report being used? (Information source, design data, procedure, source of ideas, etc.) _____

5. Has the information in this report led to any quantitative savings as far as man-hours or dollars saved, operating costs avoided, or efficiencies achieved, etc? If so, please elaborate. _____

6. General Comments. What do you think should be changed to improve future reports? (Indicate changes to organization, technical content, format, etc.) _____

CURRENT ADDRESS

_____
Organization

_____
Name

_____
Street or P.O. Box No.

_____
City, State, Zip Code

7. If indicating a Change of Address or Address Correction, please provide the Current or Correct address above and the Old or Incorrect address below.

OLD ADDRESS

_____
Organization

_____
Name

_____
Street or P.O. Box No.

_____
City, State, Zip Code

(Remove this sheet, fold as indicated, tape closed, and mail.)

(DO NOT STAPLE)

DEPARTMENT OF THE ARMY

OFFICIAL BUSINESS

BUSINESS REPLY MAIL
FIRST CLASS PERMIT No 0001, APG, MD

Postage will be paid by addressee.

Director
U.S. Army Research Laboratory
ATTN: AMSRL-OP-CI-B (Tech Lib)
Aberdeen Proving Ground, MD 21005-5066

NO POSTAGE
NECESSARY
IF MAILED
IN THE
UNITED STATES